

GUIDE TO NAVAGATING THIS DOCUMENT

Key words in this document are linked to other pages, tables, figures, or plates. Clicking on blue highlighted words in the body of the document with the mouse cursor will cause the screen to automatically go to a linked page. For example, if you click on the word [CONTENTS](#) the screen will go to the start of the table of contents of this document. To get back to where you started, click on the right mouse button and then click on “Go Back” (try it). Alternately, clicking on any heading in the body of the document will bring you back to the place in the table of contents were the heading is listed. Clicking on red text in the body of the document will take you to a related table, figure, or plate. For example, clicking on [Figure 1](#) will take you to Figure 1. Clicking on the right button and then clicking on “Go Back” will take you back. Use the “Help” menu of Acrobat Reader for more information, such as searching for specific words in the text or changing the scale of the figures and plates.

Good Luck.

**GENESIS OF CAVE OF THE WINDS,
MANITOU SPRINGS, COLORADO**

By

Fredrick George Luiszer

B.A., University of Colorado, 1987

A thesis submitted to the
Faculty of the Graduate School of the
University of Colorado in partial fulfillment
of the requirements for the degree of
Doctor of Philosophy
Department of Geological Sciences

1997

This Thesis entitled:
Genesis of Cave of the Winds, Manitou Springs, Colorado
written by
Fredrick George Luiszer
has been approved for the Department of Geological Sciences

Chair of Committee

Committee member

Date _____

The final copy of this thesis has been examined by the signators, and we find that both content and the form meet acceptable presentation standards of scholarly work in the above mentioned discipline.

ABSTRACT

Luiszer, Fredrick George (Ph.D., Geology)

Genesis of Cave of the Winds, Manitou Springs, Colorado

Thesis directed by Professor Edwin E. Larson

Cave of the Winds is located 1.5 km north of Manitou Springs, Colorado. The cave is a phreatic feature that has developed along joints associated with the Laramide Orogeny and bedding planes of the Manitou, Williams Canyon, and Leadville Formations. Aminostratigraphy and magnetostratigraphy, along with geomorphologic features, were used to determine that cave dissolution and sedimentation started ~4.5 Ma. At that time, springs similar to those in present-day Manitou Springs were located just south of and above the Cave of the Winds. Beneath these springs, ascending deep-seated water, mixing with southward flowing dilute near-surface water, formed a corrosive mixture that dissolved limestone, thus producing cave passages up to 20-m high and 10-m wide. Other chemical changes taking place in the zone where these two waters were mixing resulted in the precipitation of manganese and iron oxides. In the northern part of the mixing zone streams transported detrital sediments into the mixing zone. With subsequent regional uplift and stream downcutting, the springs and the underlying mixing zone moved down and to the south. Because different parts of the mixing zone were associated with different types of sedimentation, the movement of the mixing zone is recorded in the cave sediments as a distinct sequence. From the oldest to the youngest, the sediment sequence include: solution debris, iron oxide, manganese oxide, clay, silty sand, and gravel.

A paleoclimate history of the Manitou Springs area was constructed from environmental information associated with both the clay mineralogy of cave sediments and mollusks collected from local alluvia. In general, the climate before 2 Ma was wetter than present. A more detailed climate record that spans the interval from ~1.9 to 1.7 Ma is preserved as variations in the magnetic susceptibility of the cave sediments. These variations may record local glaciation.

ACKNOWLEDGMENTS

I express gratitude to John Drexler for the use of his laboratory and his feedback on the waters of Manitou Springs and related cave sediments. I thank Peter Birkeland for the use of his laboratory and his input on the cave clays and soils. I am grateful to Gifford Miller and his staff for determining amino acid ratios, to Lang Farmer for the strontium isotope analysis and to James White for the carbon and oxygen analyses. I would especially like to thank Ed Larson, not only for the use of his laboratory, but also for editing this manuscript and for the many years of encouragement and prodding. Grant Carey and his employees must also be recognized for graciously giving me access to Cave of the Winds throughout the study. I also appreciate the access giving to me by all of the owners of the springs in Manitou Springs. The employees of the city of Manitou Springs should also be complimented for happily answering many questions related to this study. The assistance of many cavers is gratefully acknowledged, especially Donald G. Davis and Mark Maslyn, for their thought-provoking discussions and Randy Reck for his field assistance. Without the help of the graduate students, professors, and the staff at the Department of Geological Sciences this study would not have been possible. A few of the many that helped are Eric Hiatt, Paul Boni, and Emmett Evanoff. I am particularly thankful to my family and friends who gave me the encouragement needed to accomplish this seemingly endless endeavor.

CONTENTS

ABSTRACT

ACKNOWLEDGMENT

LIST OF TABLES

LIST OF FIGURES

LIST OF PLATES

INTRODUCTION

History Of Manitou Springs And Previous Work

History Of Cave Of The Winds And Previous Work

Purpose Of Present Study

Geology Of Manitou Springs Region

Climate And Vegetation

FIELD AND LABORATORY PROCEDURES

Water Analysis In The Field

Water Analysis In The Laboratory

Isotope Study

Clay Mineralogy

Amino Acid Dating

Paleomagnetism

Magnetic Susceptibility

Other Analysis

RESULTS AND DISCUSSION

Water Chemistry

Correlation Of Modern And Ancient Processes

Source Of The H₂O

Source Of The CO₂

Spring And Stream Chemistry

Genesis Of Spring End Members

Genesis Of Williams Canyon Creek Water

Genesis Of Iron Geyser Water

Genesis Of The 7-minute East Water

Genesis Of The Cave Of The Winds Water

Four Source Mixing Model

The Mixing Zone

Chemistry Of Water In The Mixing Zone

Position And Geometry Of Mixing Zone

Movement Of The Mixing Zone

Cave Sedimentation Model

Correlation of Cave-Of-The-Winds Sediments With Spring Sediments

Source Of Cave Infill

Importance Of Provenance

Red Clay

Detrital Sediments And Speleothems

Chronology Of Speleogenesis

Age Of Cave Passages

Age Of Cave Fill

Aminostratigraphy

Mollusks

Discussion Of A-I Ratios

Age Of The Alluvia

Parabolic Curve Fitting

Magnetostratigraphy

Paleomagnetic Results

Criteria For Reversal Assignment

Effects Of Post-Depositional Remanent Magnetization On Sediments

Paleomagnetic Correlation

PLIOCENE-PLEISTOCENE CLIMATE

Climate Record In Cave Sediments

Large-Scale Sediment Changes As Climate Indicators

Magnetic Susceptibility

Periodicity Of Susceptibility

Potential of Correlating Susceptibility with Climate

Pliocene-Pleistocene Mollusk Record

CONCLUSIONS

REFERENCES

APPENDIX

Location And Description Of Springs And Other Sampling Sites

TABLES

Table

1. Analytical uncertainty of selected ions in water samples
2. Isotopic data
3. Analytical data of springs and related waters
4. Oxide and elemental composition of rocks in contact with spring water
- 5A. Analyses of sediments being deposited by modern springs
- 5B. Analyses of stratigraphic column at south end of Thieves Canyon
6. Mollusk species identified, their location, and amount of shells counted
- 7A. Alloisoleucine and isoleucine ratios (A/I) of snails
- 7B. Average values and standard deviation of A/I of snails
8. Uranium-thorium and ¹⁴C dates
9. Complete paleomagnetic results of Hole 6, Grand Concert Hall
10. Chemical analysis of the magnetic grains from cave sediments and rock samples

FIGURES

Figure

1. Location map of study area
2. Location map of springs, wells, streams, and other sampling sites
3. Schematic cross-section of Manitou Springs system
4. Piper diagram of spring and related waters
5. Plot of sodium versus chloride of selected springs and related waters
6. Plot of calcium carbonate versus the PCO_2 of surface and mineral waters
7. Plot of PCO_2 and SIs for calcite and ferrihydrite versus pH of the Iron Geyser water
8. Schematic cross section of mixing zone
9. Plot of potassium versus relative distance between springs
10. Photograph of outcrop at south end of Thieves Canyon
11. Photomicrographs of fossilized bacteria at south end of Thieves Canyon
- 12A. Plot of calcite, clay, silt, and sand content of limestone
- 12B. Plot of mineralogy of clay in limestone
- 12C. Plot of sand, silt, and clay content of cave sediment
- 12D. Plot of mineralogy of cave clay
- 12E. Plot of sand, silt, and clay content of surface soils and sediment from the Nussbaum Alluvium
- 12F. Plot of mineralogy of surface soil clays and clay from the Nussbaum Alluvium

13. Plot of D-alloisoleucine/L-isoleucine from snails versus age
14. Paleomagnetic correlation with stratigraphy of Grand Concert Hall
Hole 5
15. Drawing of postulated geomorphological changes at Cave of the Winds
over the last 2 Ma
16. Plot of magnetic susceptibility of samples from Holes 1 and 5
17. Chart comparing insolation, magnetic susceptibility, and ocean record
versus time
18. Partial record of the Pliocene-Pleistocene climate of the Manitou
Springs area

PLATES

Plate

1. Geology map of Cave of the Winds, Manitou Springs, and vicinity
2. Map of Cave of the Winds showing sampling locations
3. Geology map of Colorado Springs and Manitou Springs area with locations of snail and clay study collection sites
4. Stratigraphic descriptions of alluvial sites
5. Mass balance spreadsheet
6. Paleomagnetic cross-section of sampled pits and cored holes from Grand Concert Hall and Heavenly Hall

INTRODUCTION

History Of Manitou Springs And Previous Work

Manitou Springs, which is located 10 km west of Colorado Springs (Figure 1), is well known for the mineral springs that issue from several locations within the city (Figure 2). Before Europeans came to Colorado, members of several different Indian tribes revered the springs and used the water for medicinal purposes (Daniels and McConnell, 1964). Dr. Edwin James, a member of Major Long's expedition, examined the springs in 1820 (James, 1823). He noted that one spring was highly carbonated, had a high calcium content and discharged ~50 gallons per minute. When John C. Fremont visited the springs in 1843, he studied some of the calcite deposited by the springs and measured a water temperature of ~15° C (Fremont, 1845). Beginning almost 25 years later, the springs were studied in some detail by members of the Hayden expeditions (Hayden, 1869, 1872, 1873, 1874). The glowing reports generated by these expeditions, which favorably compared the springs to the great spas of Europe, helped attract thousands of people to the area in just a few years.

In 1872 the city of Manitou Springs was born when entrepreneurs developed the mineral springs into Colorado's first health resort, which by 1874, had become as famous as the spas of Europe (Daniels and McConnell, 1964). Oscar Loew of the Wheeler Expedition was the first to accurately analyze the chemistry of the springs (Wheeler, 1875). His analyses were quoted by many doctors, who prescribed the waters for hydrotherapy, thus guaranteeing the continuing growth of the town as a health resort (Solly, 1875; Denison, 1880; Peale, 1886; Crook, 1899). In the

early part of this century, because of the notion that radioactivity could cure various diseases, interest in the springs was revitalized when it was discovered that several of the springs were slightly radioactive (George, 1920; Shedd, 1912; Schlundt, 1914). By 1920, as hydrotherapy fell into disuse, the springs became not much more than a curious tourist attraction. In the last 20 years, because of the fashionable use of mineral water, the bottling of mineral water at Manitou Springs has been somewhat successful. In the last ten years, the citizens of Manitou Springs have recognized the need to preserve their colorful past and have begun to restore and rebuild the springhouses and fountains (Judith L. Hamilton, per. comm., 1993).

History Of Cave Of The Winds And Previous Work

Cave of the Winds, which is 1.5 km north of Manitou Springs, was first discovered by Arthur B. Love in the early 1870's (Snider, 1916). He reported that there was no trail to the cave and there was no evidence that anyone had ever been to the cave before he found it. This report makes Charles Cross's claim of discovering the cave in 1874 somewhat dubious (Snider, 1916). To further complicate the story, the Pickett brothers claimed to have discovered the cave in 1880 (Snider, 1916), in spite of the fact that the cave was pictured and labeled as Cave of the Winds in an 1875 issue of Harper's Weekly (Randolph, 1875). In 1880 and 1881 large portions of the cave became known from efforts of George W. Snider, who dug open many of the sediment-filled passages; soon thereafter the cave was commercialized (Davis, 1985). Geologist H. C. Hovey visited the cave in 1881. His subsequent report throws little light on the genesis of the cave. In his report of 1887, however, he proposed that decomposed Pikes Peak Granite was the

source for the red clay present in the cave and that it was brought into the cave by streams (Hovey, 1887).

Strieby (1893) was the first to suggest that Cave of the Winds and the springs of Manitou Springs were genetically related. He correlated red clay found in limestone cavities near the springs to the red clay in Cave of the Winds. He also presented hypotheses regarding the origin of the CO₂ and mineral water that were remarkably sound considering the paucity of available data. Finlay (1906) put forth the hypothesis that Cave of the Winds was dissolved by meteoric water and soil-derived CO₂. He proposed that the clay in the cave was mostly a residue from dissolved limestone. He concluded that the cave was a vadose feature and gave a partially correct explanation for stalagmite, stalactite, and flowstone deposition.

In his famous paper, "Features of Limestone Caverns", Bretz (1942) states that Cave of the Winds is phreatic with no evidence of vadose activity. Morgan (1950) suggested that the Cave of the Winds was associated with the Laramide Orogeny and was dissolved by CO₂-rich groundwater. Bianchi (1967) indicated that the Cave of the Winds was exposed during an erosional event related to oscillating climatic conditions during the Pleistocene.

Purpose Of Present Study

The purpose of this study is to investigate the genesis of the Cave of the Winds. Pertinent questions concerning the formation of the cave include: What is the chemical process responsible for the dissolution of limestone?, What is the composition of the sediments in the cave?, How were cave sediments transported into the cave?, What is the timing of cave formation and sedimentation?, and Can paleoclimate be gleaned from the cave-sediment record?.

The chemistry of cave dissolution was evaluated by analysis of hydrogeologic and geochemical data from springs, streams, and other associated water sources as well as analysis of sediments found at the springs and similar sediments at Cave of the Winds. The results of these analyses in conjunction with local geology can be used to elucidate the process of dissolution taking place at the springs today as well as the formation of Cave of the Winds millions of years ago. Cave sediments and possible sediment sources were analyzed to determine the source of cave sediments. Paleomagnetism of cave sediments and amino-acid ratios of snails in alluvium correlated with the cave sediments were studied and used to ascertain the timing of cave sediment deposition. Finally, the magnetic and amino-acid investigations led to the construction of a hypothesized climate record of the Manitou Springs area during the last ~3.7 my.

Geology Of Manitou Springs Region

A large block of Paleozoic sediments (**Plate 1**) hosts the springs of Manitou and the Cave of the Winds. The Ute Pass Fault, a reverse fault that is the southwest boundary of the block, places Precambrian crystalline rocks against Paleozoic sediments. The northwest boundary between the Precambrian crystalline rocks and Paleozoic sediments is an erosional surface. The eastern boundary is the Rampart Range Fault. The Paleozoic sediments in the block generally dip gently to the southeast (Bianchi, 1967). The Pikes Peak Granite and migmatites crop out to the south, west, and north of the block and underlie the block. The sediments in the Paleozoic block consist of limestone, siltstone, sandstone, conglomerate, and shale (**Plate 1**).

The geology in the Manitou Springs area has been studied in detail by various authors. Selected publications that have extensive references to early works are listed here. Morgan (1950) described in detail the stratigraphy of Williams Canyon. Bianchi's (1967) thesis covered a larger area and included a geologic map with detailed structure of the Manitou Springs area and an extensive bibliography. A petrographic study of the Manitou Formation by Dinkmeyer (1977) is comprehensive and also includes an extensive reference list.

Climate And Vegetation

The climate in the Manitou Springs area is semiarid (Bianchi, 1967). The mean annual temperature of nearby Colorado Springs is 9.3° C. The mean annual temperature of Manitou Springs is probably slightly lower because it is ~100 m higher in elevation and has lower insolation because of its location in a deep valley. The mean annual precipitation at Colorado Springs is 40.0 cm, most of which falls between April and September in the form of rain (Blair, 1975). At higher elevations, especially on the Pike Peak Massif, temperatures are lower and precipitation is greater.

The vegetation in the study area is highly variable, comprising several vegetation zones. The following descriptions are adapted from Netoff (1977). The eastern part of the study area can be classified as mostly grasslands. However, urban development, which started in the 1870's and continues unabated to this day, has covered most of the area with housing developments and industrial parks. Manitou Springs and Cave of the Winds are in the lower montane forest zone. Upper montane forest and subalpine forest zones can be found ~10 km west of Manitou Springs at higher elevations. The summit of Pikes Pike, which is ~12 km west of Manitou

Springs, is in the alpine tundra zone.

FIELD AND LABORATORY PROCEDURES

Water Analysis In The Field

Figure 2 shows the general locations of the sampling sites. Detailed descriptions and specific locations of the springs and samplings sites are compiled in the [appendix](#). Immediately after collection, the samples were vacuum-filtered by means of 0.45 μm membrane filters. The filtered water samples were placed into two 500-ml polyethylene bottles. Those analyzed for anions were stored in bottles cleaned in RBS-PF, a phosphate-free cleanser. These samples, which were transported to the lab in an ice-filled cooler, were transferred to a refrigerator that was maintained at $\sim 4.5^\circ\text{C}$. Anion analysis was performed within two days following collection. The samples analyzed for cations were stored in bottles that were previously soaked overnight in 2% nitric acid to remove any possible metal contamination. The cation samples were acidified with 4 ml of 8 M double-distilled nitric acid. Cations were determined within 2 months of collection.

The spring waters were collected as close to their sources as possible to preclude the possibility of contamination from spring basins, piping, or surface waters. At springs where the water was flowing into the bottom of basins, conductivity, temperature, pH and Eh were measured in the basin. In these springs the ampules used to measure dissolved oxygen (DOX) were filled well below the water surface to prevent contamination from atmospheric oxygen. In the springs where the water fell from pipes into basins, a flexible Nalgene™ hose was attached to the piping. The hose was used to fill a clean glass beaker, in which conductivity, temperature, pH and Eh were

measured. At these springs the water was allowed to flow into the bottom of the beaker for several minutes before sampling the bottom of the beaker for DOX measurement. This procedure helped prevent contamination from atmospheric oxygen.

Water collected for the measurement of dissolved CO₂ (DCO₂) and alkalinity was collected in the same manner as the DOX samples. This helped prevent the outgassing of CO₂. The alkalinity was measured within minutes of collection. CO₂ was measured within seconds of collection to minimize CO₂ loss.

An Orion 290A temperature-compensated pH/voltmeter was used to determine pH, Eh, and CO₂ in the field. To maintain an accuracy of ± 0.05 pH units, the pH probe was calibrated at the beginning of each day with pH 4.00 and pH 7.00 buffers. The thermocouple on the pH meter was used to record the temperature of the spring waters. This thermocouple was checked for accuracy in an ice bath (0.0° C) and was found to be within $\pm 0.1^\circ$ C. A platinum-strip electrode and Corning calomel electrode were used to measure the Eh. The conductivity was measured in the field with a temperature-compensated Hach Conductivity/Total Dissolved Solids (TDS) meter. To maintain an accuracy of $\pm 1\%$, a 1000-ppm NaCl solution was used at the beginning of each day to calibrate the conductivity meter. CO₂ was measured with a Fisher ion-selective probe. Laboratory calibration of the CO₂ probe indicated that it had an accuracy of $\sim 10\%$. However, because the spring waters are outgassing CO₂, the measured DCO₂ of the springs may be much lower than the actual value. Total alkalinity was determined by titration with sulfuric acid. DOX was measured with a Hach DR-100 colorimeter. Both the total alkalinity and DOX measurements have a $\pm 5\%$ accuracy.

Water Analysis In The Laboratory

The anion contents—fluoride (F^-), chloride (Cl^-), bromide (Br^-), nitrite (NO_2^-), nitrate (NO_3^-), phosphate (PO_4^{3-}), and sulfate (SO_4^{2-})—were determined by means of a 4500i ion chromatograph with an AS-9 column (see **Table 1** for error). The cation contents—lithium (Li^+), sodium (Na^+), potassium (K^+), magnesium (Mg^{++}), and calcium (Ca^{++})—were determined on the same chromatograph equipped with a Dionex CS-3 column (see **Table 1** for error). A set of standards was run before and after each batch of unknowns for the purpose of calibration and quality control. The silica (SiO_2), total iron (Fe^{3+}), manganese (Mn^{2+}), and boron (B) contents were analyzed by means of a Hach DR-3000 Spectrophotometer (see **Table 1** for error).

Isotope Study

Water for strontium-isotope analysis was collected in two-liter polyethylene bottles from the Ute Magnetic Spring, Cheyenne Spring, Western 7-Minute Spring, Iron Geyser (see **Figure 2** for spring locations) and the J. A. McCullough Water tunnel (see Appendix for Pikes Peak Granite water sample location). Additionally, for Sr-, C-, and O-isotope analysis, fresh limestone of the Manitou Formation was collected from Ordovician Avenue in Cave of the Winds (see **Plate 2** for location of sampling site). Gases for carbon- and oxygen-isotope analyses were collected in evacuated, one-liter steel tanks from the Ute Magnetic, Cheyenne, Iron Geyser, and Eastern 7-Minute Springs. $^{87}Sr/^{86}Sr$ was determined on a Finnigan-MAT6-collector solid-source mass spectrometer utilizing the four-collector static mode. $\delta^{13}C$ and $\delta^{18}O$ were determined on a SIRA Series II mass spectrometer.

Clay Mineralogy

To ascertain the mineralogy of the clay in cave sediments, eight samples were collected at one-meter intervals from Core #5 in the Grand Concert Hall ([Plate 2](#)). To help identify the source of the cave clay, five unweathered samples of the Manitou Formation were collected at 15-m intervals from the stratigraphic section near the entrance of Hucacove Cave ([Figure 2](#)). These bulk samples were washed with a 1 M HCl solution to remove any soil or other clay contamination. Additionally, three soils were sampled: a mixed A and B horizon from above the cave, a B horizon from the Nussbaum Alluvium, and a B horizon from the Rocky Flats Alluvium ([Plate 3](#)).

The Cave of the Winds soil sample was collected from the top of the ridge above the cave. The ~15-cm-thick soil at this sampling site mantled a slightly weathered fractured bedrock, which was either the Leadville or Williams Canyon Formation. The ~5-cm-thick, brownish-black A horizon was mostly composed of pine needles in various stages of decomposition. The ~10-cm-thick, brown B horizon was a pebbly loam. Because of the poorly defined contact between the two horizons, both were sampled together as a combined sample. This site was devoid of granite and metamorphic clasts, which were abundant at the alluvial sites. Microscopic examination of this sample revealed that the sand and silt sized fractions consist of ~80% quartz, ~10% biotite, and ~10% feldspar. This mineral assemblage, which is similar to the main components of the Pikes Peak Granite, indicate that the soil at this site is mainly developed from weathered Pikes Peak Granite that has been transported to the site by wind.

A soil sample was collected from a ~46-cm pit at a site that has been mapped as Nussbaum Alluvium (Trimble and Machette, 1979). The ~15-cm-

thick A horizon consisted of a dark brown, sandy-gravelly loam. The >30-cm-thick B horizon consisted of reddish-brown, sandy-gravelly clay. The gravel in the A and B horizon consisted of lithic clasts of granite and metamorphic rocks. At the site that has been mapped as Rocky Flats Alluvium (Trimble and Machette, 1979), a soil sample was collected from a reddish brown B horizon that was overlain by a ~15-cm-thick, brown A horizon. In addition to the soil samples, a silt sample, which was assumed to contain clays similar to those that could have been carried into Cave of the Winds by streams, was collected from the Nussbaum Alluvium at the Black Canyon site (Plate 3). The silt sample was collected from a snail-rich bed located ~2.5 m below the top of the outcrop (Plate 4). The snail shells in this bed are very well preserved, as evidenced by their aragonite tests, which would have been dissolved or altered to calcite if there had been any significant diagenesis. The shells and silt in this bed are probably unaltered because of the overlying, nonporous calcrete, which would have prevented any appreciable water/rock interaction.

Prior to grain-size and powder X-ray diffraction analysis of the sediments the >2-mm fraction was removed from the soil samples by means of a 2-mm sieve. Hydrogen peroxide was used to remove organic material according to Jackson (1973). A pH 5 buffered acetic acid-sodium acetate solution was used to remove the carbonate from the cave and soil samples (Jackson, 1973). A rapid carbonate-removal method using a similar solution adjusted to pH 2.5 was used on the limestone samples to prevent the alteration of the clays and to reduce extraction time (Rabenhorst and Wilding, 1984). Samples were centrifuged and decanted followed by the addition of distilled water, centrifuging, and decanting to remove the dissolved carbonate and acetic acid-sodium acetate solution. The calcite content of the limestone

samples was determined by weighing the dried residue remaining after the dissolution of the limestone and subtracting that from the starting weight. All samples were then treated with hydrogen peroxide heated to 70° C to remove organic material. The samples were then wet sieved to remove and measure the >53 µm sand fraction.

The silt and clay size fractions were measured by applying Stokes Law (Jackson, 1973). This was achieved by suspending the samples in water, in which sodium pyrophosphate was added to prevent flocculation, and allowing the sediment to settle. Then a pipette was used to remove aliquots of the water and sediment from specified depths at specified times according to the temperature of the sediment-water mixture (Jackson, 1973).

The clay fraction from the grain-size analysis was deposited on ceramic tiles (Jackson, 1973) and analyzed on a Scintag PAD 5, automated diffractometer equipped with Cu K α radiation (1.54059 Å) and a single crystal, graphite monochromator. Clay minerals were identified according to Moore and Reynolds (1989). Semi-quantification of the clay types was adapted from Netoff (1977). Because of the inherent difficulties in quantifying clay species (Moore and Reynolds, 1989), the reported values in this study are only relative amounts. These values are used for the comparison of samples within this study and for making generalizations.

Amino Acid Dating

Snails were collected from outcrops of the Nussbaum Alluvium, and from younger radiometrically dated alluvia (**Plate 3**), for the purpose of dating the Nussbaum Alluvium by means of amino-acid racemization. Stratigraphic descriptions of the six older alluvial sites are on **Plate 4**. The modern floodplain site is ~20 m north of the Louviers site and is ~1 m above and 10

m south of the nearby stream. The snails were collected from newly deposited flood debris that was less than a month old and from the top few centimeters of soil. The vegetation at this site consists of thick grass and weeds along with sparse prickly pear and yucca .

Approximately 50 kg of sandy silt was collected at each site. To minimize sample contamination, washed plastic buckets and fresh plastic bags were used. The samples were loaded into containers with a clean metal shovel and with minimal hand contact. In the lab, the samples were disaggregated by putting them in buckets filled with tap water and letting them soak overnight.

The samples were then washed with tap water through 0.5-mm mesh screen. Following air drying, the mollusks were hand picked from the remaining matrix by means of a small paintbrush dipped in tap water. The mollusks were then identified. Only shells that were free of sediment and discoloration were selected for further processing. These shells were washed at least five times in distilled water while being sonically agitated. The amino-acid ratios were determined on a high-performance liquid chromatograph (HPLC) at the Institute of Arctic and Alpine Research (University of Colorado, Boulder).

Paleomagnetism

A coring device was used to sample the cave sediments at six cored holes in the Grand Concert Hall ([Plate 2](#)). The core samples were obtained by means of a coring device in which a hand-powered hydraulic cylinder drives a stainless steel, knife-edged barrel down into the sediments. Up to 40 cm of sediment could be cored each trip into the hole without sediment distortion. Samples were also collected from hand-dug pits at Mummys

Alcove and Sniders Hall (Plate 2). Additionally, samples were collected from a vertical outcrop in Heavenly Hall (Plate 2). The pits and outcrops were sampled for paleomagnetic study by carving flat vertical surfaces and pushing plastic sampling cubes into the sediment at stratigraphic intervals ranging from 3.0 to 10.0 cm. The samples were oriented by means of a Brunton compass.

The core barrel and all pieces of drill rod that attached to the barrel were engraved with a vertical line so that the orientation of the core barrel could be measured with a Brunton compass within $\pm 2^\circ$. A hand-operated hydraulic device was used to extract the sediment core from the barrels. As the core was extruded, a fixed thin wire sliced it in half, lengthwise. Plastic sampling cubes were then pushed into the soft sediment along the center line of the flat surface of the core half at regular intervals (generally ~ 5.0 cm). The samples at Sniders Hall, Mummys Alcove, and Hole 1 were taken with 3.2 cm^3 sampling cubes; all other samples were taken with 13.5 cm^3 cubes.

In the lab, the NRM (Natural Remanent Magnetization) of all samples was initially measured. Subsequently, the samples were subjected to alternating-field (A. F.) demagnetization and remeasured. All samples were first demagnetized at 10, and then at 15 millitesla (mT). Some samples at the bottom of Hole 5 that displayed aberrant inclinations and declinations were additionally demagnetized at fields up to 30 mT. All remanence measurements were made on a Schonstedt SSM 1A spinner magnetometer with a sensitivity of 1×10^{-4} A/m. Repeat measurements indicate an angular reproducibility of $\sim 2^\circ$ at an intensity of 1×10^{-6} A/m².

Magnetic Susceptibility

After the samples taken from the cores were measured for NRM, their low-field bulk volume susceptibility was measured on a Sapphire Model 1A susceptibility meter. Two measurements were made of each sample. Noise levels for all measurements were less than $\pm 1\%$. All measurements were significant to at least three figures.

Other Analysis

Two charcoal samples were collected and sent to Krueger Enterprises, Inc. for radiocarbon age determination. One sample was a composite sample collected from the walls and ceilings of Manitou Cave ([Figure 2](#)). The source of charcoal sample appears to be wood charcoal brought into the cave by a flood. Another sample was a composite sample collected from the Centennial site (location on [Plate 3](#) and description on [Plate 4](#)). This sample also appears to be wood charcoal. Both samples appear to have been deposited by streams. These samples were collected with a stainless-steel teaspoon and then put into plastic bags. Extreme care was taken to eliminate any possible contamination from extraneous carbon sources, such as bare hands or modern organic matter.

To establish the relationship between spring waters and cave sediments, Mn- and Fe-rich sediments were collected from the south end of Thieves Canyon ([Plate 2](#)), and from the Ouray, Little Chief, and Iron Geyser Springs ([Figure 2](#)). These samples were dried, ground to a fine powder and analyzed for Mn, Fe, Co, Ni, As, Sb, Ba, W, and Pb on a Kevex 0700 X-ray fluorescence unit (EDSXRF).

Rock and sediment samples were collected for the purpose of determining the mineralogy and provenance of the magnetic minerals in the

cave sediments. A sample of red clay was collected 50 m inside Narrows Cave, which is located ~150 m west of Huccacove Cave ([Figure 2](#)). The Cave-of-the-Winds sample, a clayey silt, was collected in Silent Splendor ([Plate 2](#)). A sample of the Pikes Pike granite was taken from an outcrop and a migmatite stream cobble was collected along Williams Canyon Creek ~ 0.5 km upstream from Cave Of The Winds. Both samples appeared to be unweathered. About 250 g of each sediment sample was disaggregated in a mixture of 500 ml water and 10 ml Joy® soap. About 250 g of each rock sample was crushed and pulverized. A strong magnet was used to carefully extract the magnetic particles from each sample. Four polished grain mounts were made of these magnetic particles. The polished grain mounts were analyzed by means of both a petrographic microscope by the author and a JOEL microprobe by John Drexler.

To ascertain the elemental composition of the limestone, five unweathered samples of the Manitou Formation were collected at 15-m intervals from the stratigraphic section near the entrance of Hucacove Cave ([Figure 2](#)). These samples were collected from essentially the same location as the samples that were used for clay analysis. Two additional samples were collected for limestone analysis. The base of the Leadville Formation was sampled near Hucacove Cave. The Williams Canyon Formation was sampled ~50 m south of the entrance to Cave of the Winds. Most of the outer weathered portions of the samples were chipped off by means of a rock hammer. The samples were then cleaned in a 2% nitric bath with a plastic brush. After drying, the samples were crushed and then pulverized. Iron particles that were introduced into the sample during crushing and pulverizing were removed by means of a strong magnet. The pulverized samples were then ground to a very fine powder by means of a motorized agate mortar and

pestle. Four grams of each powdered sample was mixed with 1 gram of
®Argo cornstarch. The mixture was pressed into 32 mm diameter pucks,
which were analyzed with a Phillips PW 1400 wavelength XRF.

RESULTS AND DISCUSSION

Water Chemistry

Correlation Of Modern And Ancient Processes

The water that dissolved limestone and deposited sediments at the Cave of the Winds has long since disappeared. However, by comparing sediments being deposited at the springs of Manitou Springs with those that were deposited at the Cave of the Wind, and by studying the water chemistry of the modern springs, it can be shown that limestone dissolution and sediment deposition that is taking place under the modern springs are similar to processes that occurred at the Cave of the Winds. Because the composition of ascending deep-seated and near-surface waters control the dissolution of limestone and precipitation of minerals, the sources of the water and their dissolved solids and gasses require discussion.

Source Of The H₂O

Evans and others (1986) determined that the $\delta^{18}\text{O}$ and δD of the H₂O of the Iron Geyser is -12.11‰ and -84.5 ‰, respectively, and that of the 7-Minute Spring is -11.91‰ and -84.6 ‰, respectively, indicating that the H₂O of these two springs is of meteoric origin. This suggests that the H₂O of the other mineral springs is also of meteoric origin. The northeastern flanks of the Pikes Peak massif, which is located southwest of Manitou Springs, and the southern end of the Rampart Range, which is located northwest of Manitou Springs, are the probable recharge areas for the springs (Figure 3).

Source Of The CO₂

The Manitou waters contain large amounts of dissolved CO₂. Some springs emit large volumes of CO₂ gas (Evans and others, 1986). The carbon dioxide has several possible sources: atmospheric, metamorphic, biogenic, and outgassing from the mantle. The high concentration of CO₂ in the springs, about 1000 times that of water in equilibrium with atmospheric CO₂, precludes atmospheric CO₂ as a primary source. An alternate interpretation is that the CO₂ is produced from contact metamorphism by local plutons (Evans and others, 1986). Because there is no evidence of modern plutonism in the area, this hypothesis is unsupported. The $\delta^{13}\text{C}$ of biogenic CO₂ is between -25 ‰ and -15‰ (Perrodon, 1983); therefore, a biogenic source for the CO₂ must also be excluded because the $\delta^{13}\text{C}$ of free CO₂ from representative springs at Manitou ranges from -5.05 ‰ to -4.03 ‰ (Table 2). Several studies have shown that CO₂ issuing from springs along deep-seated faults have $\delta^{13}\text{C}$ values (-10‰ to -2 ‰, Batard and others, 1982; -4‰ to -8 ‰, Blavoux and others, 1982) comparable to those at Manitou Springs (Table 2). These studies suggest that outgassed CO₂ from the upper mantle ascends along major faults and mixes with meteoric water. This appears to be the same process taking place at Manitou Springs (Figure 3).

Spring And Stream Chemistry

The waters that are part of the Manitou Springs system can be grouped into five categories according to their location and general chemistry (Figure 2 and Figure 4). The 7-minute East, and West Springs, which have the highest chloride, sulfate and TDS content of any of the springs in Manitou, are located east of the downtown area. They are grouped together

as the Eastern Springs (Figure 2 and Figure 4). The Iron Geyser, Ouray, and Chief Springs are located southwest of the downtown area along Ruxton Creek (Figure 2). Because of their very high iron content, these springs are grouped together as the Iron Springs. Additionally, the Iron Springs contain higher concentrations of arsenic, lead, sodium and potassium than any of the other springs in Manitou.

The Shoshone, Cheyenne, Soda, Navajo, Wheeler, and Stratton Springs are located in the downtown area and therefore are grouped as the Downtown Springs (Figure 2). They are similar to the Eastern Springs, except they have lower chloride and sulfate concentrations (Figure 4). The Ute Magnetic, Twin, Ute Chief, Gusher, and Creighton Springs are northwest of the downtown area and, even though they are not as far west as the Iron Springs, they are grouped as the Western Springs for simplicity (Figure 2 and Figure 4). In general, these springs have the lowest chloride, sulfate, and TDS contents and the highest nitrate concentrations of any of the springs in Manitou. The exception to the correlation of location and chemistry is Twin Spring, which is located between the Downtown and Iron Springs, but is grouped with the Western Springs (Figure 2 and Figure 4). This anomaly will be discussed later.

The Cave of the Winds spring is grouped by itself (Figure 4). It is located ~0.4 km west of Cave of the Winds (Figure 2). The chemistry of this spring is similar to many of the other springs, however, its TDS content is much lower (Table 3). This spring is the water supply for the tourist facilities at Cave of the Winds. The samples collected along Williams Canyon Creek and the Blue Ice Spring, which flows into Williams Canyon Creek, are grouped together (Figure 4). This creek is located north of Manitou Springs

(Figure 2). The Downstream sample and the Blue Ice Spring contain more nitrate than any of the other surface waters analyzed in this study (Table 3).

A careful attempt was made during spring and site selection, sampling, and analyses to obtain data that were indicative of the source conditions. For this reason the partial results from the two springs, Little Chief and Hiawatha (see appendix for descriptions), were not included in Table 3. Their conductivity or temperature indicated that they had been altered by soil conditions or were mixed with very near-surface sources.

Genesis Of Spring End Members

Subsequent discussion will show that four different water sources consisting of the Williams Canyon Creek downstream water and waters with compositions very similar to the Iron Geyser, 7-minute East Spring, and Cave of the Winds Spring are mixing beneath Manitou Springs to form the variable water compositions of the Downtown Springs, Western Springs, and 7-minute West Spring (Figure 5). The chemistry of the Iron Geyser appears to be controlled by rock-water interaction with the Pikes Peak Granite. The chemistry of the 7-minute East Spring is similar to the Iron Geyser water, but appears to have been modified by rock-water interaction with marine sediments. The Williams Canyon Creek downstream water is a low-TDS near-surface water that has been modified by input from the Blue Ice Spring. The Cave of the Winds Spring is somewhat similar to many of the other springs, but has a much lower TDS content. The genesis of these waters will be discussed in detail, because the compositional differences of these waters will be important in understanding the chemical reactions taking place beneath Manitou Springs.

Genesis Of Williams Canyon Creek Water

Figure 5 indicates that downstream Williams Canyon Creek, which is high in nitrate (Table 3), is one of the end members of the Manitou Springs waters. Because I use the nitrate content of the springs to show that waters of different composition are mixing beneath Manitou Springs, I will discuss the source of the nitrate in some detail. Nitrate is normally associated with anthropogenic sources such as sewage treatment facilities or ammonium nitrate from fertilizers and explosives. Because there is no farming in the Manitou Springs area, nitrate input from fertilizers can be discounted. Another possible source of nitrate is from the Castle Concrete limestone quarry, which is located about 1 km east of Cave of the Winds. At the quarry a mixture of ammonium nitrate and diesel fuel was used as an explosive to break up the limestone. Because about 10% of the ammonium nitrate (Walt Rubeck, 1995, per. comm.) remains after the explosion, it is possible that residue from the explosive could be carried by runoff into the quarry pit (which is located in the Manitou Formation) and eventually emerge at the springs in Manitou. The quarry-nitrate input, however, must be very small, because even though the quarry was permanently shut down about the same time the springs were originally sampled by me, subsequent periodic spot checks of the high-nitrate springs indicated no change in their nitrate content.

The most probable nitrate source is from the breakdown of human waste. Subsurface nitrate input from septic systems can be excluded because Manitou Springs is connected to a sewer system (Johnny Price, per. comm. 1995). Ruxton and Fountain Creeks have slightly elevated nitrate concentrations (Table 3), which are probably associated with upstream human activity. These two streams, however, can also be excluded as

principal nitrate sources, because some of the springs, especially the Gusher Spring, contain more nitrate than either of the two creeks.

The high nitrate content of the downstream Williams Canyon Creek, which infiltrates into the limestone in lower Williams Canyon, indicates that it is probably the major nitrate source for the springs. Furthermore, the nitrate must originate on the Cave of the Winds property, because both the Cave of the Winds Spring, which is the water supply for the facilities at the cave, and upstream Williams Canyon Creek have low nitrate contents. The Blue Ice Spring, which drains into the creek, however, has a very high nitrate concentration. The most likely source of the nitrate in the Blue Ice Spring is the break down of human waste in the Cave of the Winds' septic field, which is located about 100 m uphill from the spring. The Blue Ice Spring is so named because in the wintertime, as the water freezes, it excludes many of the ions present in the water. The remaining water, which starts out fairly concentrated to begin with ([Table 3](#)), increases in concentration until the solubility of the contained dissolved solids is exceeded, at which time, minerals precipitate. The resultant microscopic mineral crystals, which are suspended in the ice, scatter light, giving the ice a light-blue hue. The Blue Ice Spring along with many smaller seeps located near it, are the most obvious point source of the nitrate present in downstream Williams Canyon Creek.

Except for the nitrate, most of the dissolved content of downstream Williams Canyon Creek water is from rock-water interaction with the Pikes Peak Granite, which crops out in the head waters of Williams Canyon Creek and to a lesser extent limestone, which rims Williams Canyon. The water is much more dilute than the Iron Geyser water, because the rock-water reaction takes place at much lower temperatures and during a much shorter

time interval. The nitrate content of downstream Williams Canyon Creek identifies it as one of the low TDS source that is mixing with other waters beneath Manitou Springs.

Genesis Of Iron Geyser Water

There are several lines of evidence that indicate that the Iron Geyser represents water that has been modified solely by contact with the Pikes Peak Granite. The elements that are relatively abundant in the granite are sodium (Na), potassium (K), lithium (Li), iron (Fe), and silicon (Si) (Table 4). Accordingly, the water of the Iron Geyser contains elevated amounts of all of these elements (Table 3). The high concentrations are probably related to the elevated temperature at which the water-rock interaction took place and the extended period of time that the water was in contact with the rock. The quartz-with-no-steam-loss geothermometer (temperature in °C=[1309/[5.19-log SiO₂]]-273.15 where SiO₂ = mg/kg, Henley and others, 1984) indicates a temperature of 126° C. Assuming an average geothermal gradient of 30° C/km (Leet, Judson, and Kauffman, 1982), the calculated temperature is equivalent to a depth of ~4 km. Several of the spring waters in Manitou Springs have been C¹⁴ dated (Maslyn and Blomquist, 1985). The dates indicate that the water issuing from the springs can be up to ~30 Ka. The Iron Geyser may be much older, because the springs are actually a mixture of near-surface modern water and water similar to the Iron Geyser.

Apparently, the solubility of certain minerals in the Pikes Peak Granite controls the composition of the Iron Geyser. Major minerals that occur in the Pikes Peaks Granite include quartz, biotite, potassium feldspar, and sodic feldspar (Hawley and Wobus, 1977). Accessory minerals include fluorite, zircon, magnetite, apatite, and topaz (Hawley and Wobus, 1977). The

saturation index (SI) of albite indicates that it is a likely source of the sodium in the Iron Geyser (Table 3). The very low SI of anorthite suggests that it is the source of calcium (Table 3). The potassium most likely comes from the K-feldspar and biotite. The abundance of K-feldspar in the Pikes Peak Granite alone would suggest that it is the source for the potassium. Additionally, the calculated SI of K-feldspar (microcline, SI = -0.69) in the Iron Geyser water also suggests that it controls the potassium content of the water (Table 3).

The near-equilibrium SI (-0.26) of biotite indicates another potential source of silica, potassium, and iron to the Iron Geyser water. Certainly the high SI (13.09) of magnetite excludes it as a control on the iron content (Table 3). Additionally, the manganese and lithium content of the Iron Geyser is probably controlled by biotite, which contains appreciable amounts of manganese and lithium (Table 4).

Given the high fluorine content of biotite in the Pikes Peak Granite (Table 4), it is probably also the source of the fluoride in the Iron Geyser. The SI (1.25) of fluorite is slightly supersaturated, which suggests that it does not control the fluoride or calcium content of the water (Table 3). Other possible sources of fluoride are apatite ($\text{Ca}_5(\text{PO}_4)_3(\text{F},\text{Cl},\text{OH})$) and topaz ($\text{Al}_2\text{SiO}_4(\text{F},\text{OH})_2$). The low phosphate content of the Iron Springs would negate the possibility that the dissolution of apatite contributes to its fluoride content (Table 3). The insolubility of topaz (Hurlbut and Klein, 1977) would exclude it as a source of fluoride.

The $^{87}\text{Sr}/^{86}\text{Sr}$ of minerals in the Pikes Peak Granite can also be used to shed some light on the source of the elements in the Iron Geyser water. The low $^{87}\text{Sr}/^{86}\text{Sr}$ of the Iron Geyser relative to that of K-feldspar and biotite suggests that plagioclase has a larger influence on the $^{87}\text{Sr}/^{86}\text{Sr}$ of the spring

water than does K-feldspar (Table 2). The strontium is probably in the anorthite component of the plagioclase, where it replaces calcium. Although biotite has a high $^{87}\text{Sr}/^{86}\text{Sr}$ and a low SI, the small amount of strontium contained in the biotite probably limits its affect on the $^{87}\text{Sr}/^{86}\text{Sr}$ of the Iron Geyser (Table 4). Some of the strontium in the springs that are a mixture of Iron-Geyser-type water and low TDS water (such as the Ute Magnetic and Cheyenne springs) apparently comes from the dissolution of limestone. This is evidenced by the Ute Magnetic and Cheyenne Spring $^{87}\text{Sr}/^{86}\text{Sr}$ values, which are between those of the Manitou Limestone and Iron Geyser (Table 2). The $^{87}\text{Sr}/^{86}\text{Sr}$ values of these springs are related to the amount of dissolved limestone contained in each. The high TDS Cheyenne Spring, which is a mixture of mostly Iron-Geyser-like water and a small amount of a low-TDS water, does not contain as much dissolved limestone as the Ute Magnetic Spring, which contains larger amounts of a low TDS water. The dissolution of limestone will be discussed in detail later in this study.

Identifying the source of the sulfate and chloride in the Iron Geyser water is problematic. Although analysis of the spring for H_2S was negative, the spring has a very slight H_2S smell. This coupled with the high iron content of the spring suggests that pyrite (FeS_2) could be the source of sulfate in the water. Pyrite, however, has not been identified as a mineral present in the Pikes Peak Granite (Hawley and Wobus, 1977). Chloride is probably from the alteration of biotite, although the high fluorine/chlorine ratio of the biotite (Table 4) does not agree with the high fluorine/chlorine ratio of the Iron Geyser water (Table 3). This suggests that either there are other sources for the chloride or the fluoride is being taken out of solution by precipitation of a mineral (such as fluorite). Further study is necessary to clear up the problem associated with sulfate and chloride.

Genesis Of The 7-minute East Water

One of the four mixing end members appears to have a composition similar to the 7-minute East Spring. The elevated amounts of sulfate, chloride, and boron (Table 3), suggest that the 7-minute East Spring has a different hydrochemical evolution than the other end members. Sulfate, chloride and boron are anions that are commonly associated with marine sediments, suggesting that the Eastern Springs may have been modified by rock-water interaction with marine sediments. The low sulfur and chlorine content of the marine limestone of the Manitou and Leadville Formations (Table 4) removes these formations from consideration. Another rock with which water could be interacting is the Gleneyrie Member of the Fountain Formation (Plate 1), a marine shale that overlays the limestone beds. Another possibility is the Pierre Formation, a marine shale that abuts the Rampart Range Fault east of Manitou Springs (Plate 3). More study would be needed to enable the assignment of the marine influence to either of these marine shales or other marine sediments.

Genesis Of The Cave Of The Winds Water

One of the four mixing end members appears to have a composition similar to the Cave of the Winds Spring water. Because this spring issues from the Pikes Peak Granite, the water probably has a genesis very similar to the Iron Geyser. The main difference between the two waters is that the Cave of the Winds water has a lower TDS content. The quartz-with-no-steam-loss geothermometer (Henley and others, 1984) indicates that the Cave of the Winds Spring water obtained a temperature of 77° C. The temperature at which the rock-water interaction took place is much lower for the Cave of the Winds Spring water than the Iron Geyser water (126°). The

lower temperature indicates that the Cave of the Winds water has not reached the same depth as the Iron Geyser. This would suggest that the Cave of the Winds Spring water has been in contact with the granite for a shorter period of time. The lower rock-water interaction temperature and the shorter interaction time are the most probable reasons why the Cave of the Winds Spring has a much lower TDS content than the Iron Geyser.

The low-TDS near surface water, which is modeled as being similar to the Cave of the Winds Spring water, is apparently entering the mixing zone beneath Manitou Springs along a fault that is sub-parallel to the Ute Pass Fault (Plate 1). This fault, which lines up with and ends not far from the Cave of the Winds Spring, can be traced back under Manitou Springs (Plate 1), suggesting that water similar to the Cave of the Winds Spring could also be ascending this fault and entering the mixing zone. The low TDS and fairly low nitrate content of the Creighton Spring (Table 3) and the spring's location near the fault suggests that that the low-TDS near-surface end member may be entering the mixing zone from a point source along the fault southeast of the Creighton Spring.

Four Source Mixing Model

The Williams Canyon Creek downstream water has been identified as one of the sources entering the mixing zone beneath Manitou Springs. The Iron Geyser, 7-minute East Spring, and Cave of the Winds Spring are assumed to closely approximate the water chemistry of the other three sources. To support this interpretation, mass balance calculations were made by equating the potassium, sodium, sulfate, chloride and fluoride output of the Downtown Springs and the Western Springs to the known and modeled inputs. These five ions were chosen because they were assumed

to be very conservative in the water beneath Manitou Springs. Once in the mixing zone (Plate 1), these ions should not increase in concentration, because the rock-water interaction that is taking place in the mixing zone is the dissolution of limestone, which has very low concentrations of potassium, sodium, sulfur, and chlorine (Table 4). Fluoride was also included, because the fluorine content of most limestone is very low (Hem, 1992). Moreover, these five ions are not lost in the mixing zone from the precipitation of minerals containing these ions. This is born out in subsequent sections of this study that show that the sediments in Cave of the Winds, which were deposited a mixing zone thought to be very similar to the one present beneath Manitou Springs, do not contain sodium-, sulfur-, fluorine-, or chlorine-bearing phreatically formed authigenic minerals. Only potassium is present in minor amounts in a rare manganese-oxide mineral in the sediments at Cave of the Winds. Subsequent mass balance calculations indicate that the potassium loss from the precipitation of this mineral is vanishingly small.

Mass balance was achieved by equating the ion input of the spring system to the ion output. The flow rates and ion content of the Downtown and Western springs were used to calculate the ion output of the spring system (Plate 5, A). The flow rate and ion content of the Williams Canyon Creek downstream water was used to calculate part of the ion input (Plate 5, A). The ion contents of the Iron Geyser, 7-minute East Spring, and the Cave of the Winds Spring were used as models for the sources that enter the spring system at depth (Plate 5, A). The unknown flow rates of the three modeled sources could then be calculated by constructing at least three independent equations and solving for the unknowns (Plate 5, B).

Five unique mass balance equations were constructed for each of the selected ions (Plate 5, C). Only three equations were necessary to solve for the three unknowns. However, in an attempt to ameliorate some of the problems associated with modeling and analytical error, ten matrices containing ten unique combinations of the five equations were solved (Plate 5, D). Summing of the resultant flow rates showed that eight of the ten results agreed fairly well with the measured output of the springs (Plate 5, E). The two results that were anomalous were excluded from further consideration. The eight remaining results were averaged.

The calculated total input to the spring system was ~10% greater than the measured total discharge. To compensate for this, the calculated input flow rates were normalized to equal the total discharge (Plate 5, F). These flow rates were then added back into the mass balance equation (Plate 5, F). The average relative percent difference (RPD) between the spring system input and discharge for the conservative ions was 8.5% (Plate 5, G), which, considering the use of the modeled inputs and the analytical uncertainty (Table 1), is acceptable. The mass balances of the ions, lithium, bromide and nitrate were also calculated as a check to see if the ion content of the modeled inputs and calculated input flow rates were reasonable.

Lithium was not included in the equations for determining the input flow rates because the lithium content of the limestone was not measured. Carbonates in general, however, contain very little lithium (~5 ppm, Hem, 1992). The biotite of the Pikes Peak Granite, however, contains a fairly large amount of lithium (Table 4) and is the most likely source of the lithium in the spring waters. Therefore, lithium should also be conservative in the mixing zone. Bromide was not included in the equations for determining the input flow rates because the bromide content of the limestone was not measured.

Carbonates, however, normally contain very little bromide (~7 ppm, Hem, 1992). The bromide content of the deep-seated source (Iron Geyser) is fairly high at 1.0 mg/L. The bromide is probably from the breakdown of biotite, which has a high halogen content (Table 4). A main contributor of bromide to the spring system is most likely the marine modified source (7-minute East), which contains 2.1 mg/L bromide (Table 3). This suggests that the bromide is unrelated to the dissolution of limestone. It should be another conservative ion in the mixing zone.

The nitrogen content of the limestone was also not analyzed. Carbonates, however, normally contain no nitrogen (Hem, 1992). Nitrogen, which would more than likely be leached out as nitrate, is, however, normally present in shale (Hem, 1992). This could explain the slightly elevated nitrate content of the Marine Modified source (7-minute East, Table 3). Williams Canyon Creek with its very high nitrate content has already been shown to be the main source of the nitrate in the mixing zone. Nitrate, therefore, also appears to be a conservative ion in the mixing zone. The low RPD's (~9%, Plate 5, G) between the lithium, bromide and nitrate input and output suggests that the composition of the modeled sources and their calculated input flow rates are appropriate. The high RPD's of calcium, magnesium, iron, and manganese suggest that they are not conserved in the mixing zone (Plate 5, H).

The Mixing Zone

Chemistry Of Water In The Mixing Zone

The large differences between the input and discharge of the non-conservation ions (calcium, magnesium, iron, and manganese) at the

Manitou Springs system indicate that chemical reactions are taking place beneath Manitou Springs. The increase in the calcium and magnesium strongly suggests that the dolomitic limestone, which is present beneath Manitou Springs, is dissolving. The decrease in the iron and manganese suggests that these ions are lost by precipitation. I propose that the dissolution of dolomitic limestone and the precipitation of iron and manganese are from the mixing of two general types of water in a mixing zone located beneath Manitou Springs. One type is a deep-seated water moving upward and mixing with a near-surface water (Figure 3).

The reactions, dissolution and precipitation, which are taking place in the mixing zone, are a function of the chemical composition of these two water types and the host rock of the mixing zone. The relatively high iron and manganese contents and very high CO₂ content are the reactants that the deep-seated water delivers to the mixing zone. Dissolved oxygen is the reactant that the low-TDS source delivers to the mixing zone. Calcite and dolomite, contained in the dolomitic limestone, which hosts the mixing zone, are also reactants.

From a speleological point of view the most important reaction taking place in the mixing zone is the dissolution of the limestone. Bögli (1964) pointed out that this reaction, which he named "Mischugskorrosion" (mixing corrosion), occurs by mixing two different waters in the presence of limestone. One of these waters contains relatively small amounts of dissolved CaCO₃ and CO₂ and the other, relatively large amounts. Both waters, however, may be saturated with respect to calcite. Because the solubility of calcite in a CO₂ system is not linear (Figure 6), the mixing of these two waters forms a corrosive mixture, or, as the proposed case in the

Manitou Springs system, a mixture that can dissolve more limestone than either of the end members.

The Manitou Springs system is somewhat more complex in that it has at least four distinct waters that feed into the mixing zone. These waters, however, can be combined into the two main water types, which are normally present in a corrosive mixing system. The modeled low-TDS sources (Cave of the Winds spring) and downstream Williams Canyon Creek can be combined to form the low-content dissolved-CaCO₃-CO₂ mixing end member (Figure 6). The modeled marine modified source (7-minute East Spring) and the deep-seated source (Iron Geyser) can be combined to form the high-content dissolved-CaCO₃-CO₂ mixing end member (Figure 6). The shaded polygon drawn on Figure 6, which has these end members as its vertices, should contain all of the compositions of the springs that issue from the mixing zone. Water in the shaded area is undersaturated with calcite and therefore would dissolve the limestone. Many of the measured values, however, do not coincide with the shaded area. This apparent anomaly will be discussed in more detail.

PHREEQC (Parkhurst, 1995) was used to calculate saturation indices and determine speciation of the spring waters. It was useful in determining the saturation indices for silicates and rough values for carbonate and oxide saturation indices and species (Table 3). PHREEQC, however, cannot be used to accurately calculate carbonate and oxide chemistry, because the Manitou Springs system is not in equilibrium. Additionally, obtaining accurate pH and meaningful DCO₂ measurements necessary for calculating aqueous speciation was difficult, because these parameters change rapidly as the water nears the surface and as it issues from the springs. The biologically mediated precipitation of iron and probably manganese oxides is another

factor that negates some of the usefulness of PHREEQC in predicting the geochemistry of the Manitou Springs system.

The relatively high degree of undersaturation of the Creighton, Gusher, and Twin Springs suggests that these waters are not in equilibrium with respect to calcite (Table 3). The calculated saturation indices for these springs indicate that the springs are also not in equilibrium with dolomite (Table 3). This suggests the water ascends to the surface fairly quickly, before it has a chance to dissolve sufficient calcite or dolomite to be in equilibrium with either of these minerals. The geometry of the conduits that feed the springs plays a role in this. Many of the springs are actually drilled wells, which probably have small diameters (~10 cm); thus, even at low flow rates the water will ascend to the surface at a relatively high velocity. Other springs that drain the mixing zone are natural and most likely issue from fractures in the Fountain Formation (Plate 1). Similar to the drilled wells, these fractures will have small cross sectional areas and the water will ascend along them at fairly high velocities.

The lack of meaningful DCO_2 measurements adversely affects speciation calculations. The DCO_2 measurements of the springs at Manitou do not take into account the large amounts of emitted CO_2 gas, which is probably in solution at depth. For example, at a depth of only ~30 m the hydrostatic head would be sufficient to permit a PCO_2 of ~3.0, which is higher than any of the springs in Manitou (Figure 6). At this pressure all of the CO_2 would be in solution. As the water nears the surface and the hydrostatic pressure is decreased, the CO_2 begins to outgas from the water. The DCO_2 content and pH of the water at depth could be calculated if the CO_2 emitted from the springs could be measured. The physical layout and plumbing of most of the springs prevents accurate measurement of the amount of emitted

CO₂ gas, except for the Iron Geyser, for which it was estimated that the CO₂ gas emitted was at least equal in volume to the water flow. Knowing that the measured DCO₂ of the springs is a minimum and that it is likely greater at depth, the true DCO₂ contents of the springs in the shaded area on [Figure 6](#) were estimated using the difference between the measured (1.43) and the at-depth calculated PCO₂ (~2.5) of the Iron Geyser.

Other adjustments of the estimated PCO₂ and calcium values were made according to the flow rate and PCO₂ magnitude of each spring. The difference between the estimated and measured PCO₂ of springs such as the Creighton and Gusher was expected to be less ([Figure 6](#)). The smaller difference is because they are roughly 50/50 mixtures of the two main end members, so that their initial PCO₂ should be about half of the more concentrated end members and, accordingly, they are plotted as having half as much difference between the measured and estimated PCO₂. Additionally, springs with a high flow rate, like the Creighton and Gusher, were expected to have even smaller differences, because their waters ascend at higher velocities, giving the water less time to outgas CO₂. This approach was applied in estimating the PCO₂ of the more concentrated, low flow rate springs, like the Cheyenne and Shoshone. The calcium content of all of the spring waters, except the Iron Geyser and 7-minute East, which are fixed as end members, was estimated to be slightly lower in the mixing zone, because these reactive waters probably pass through and dissolve some limestone as they ascend to the surface.

Another parameter that is essential for calculating SI's and speciation is pH, which is directly related to PCO₂ ([Figure 7](#)). Outgassing CO₂ makes the accurate measurement of the pH of the springs very difficult. The data from the Iron Geyser can be used to show this problem ([Figure 7](#)). The

measured pH of the Iron Geyser (6.27) can not be the actual pH because the calculated SI's of ferrihydrite and calcite suggest that they would precipitate (Table 3). Both of these minerals, however, do not precipitate until after the water issues from the spring, where continued CO₂ outgassing increases the pH. The minimum pH of the spring water has to be less than ~6.12 for these minerals to stay in solution (Figure 7). It should be noted that, as the water flows away from the Iron Geyser, ferrihydrite precipitates first and then calcite, as indicated in Figure 7. The measured PCO₂ correlates with a pH of ~5.88 (Figure 7). If the outgassed CO₂ is added back into the water as DCO₂, the pH at depth would have to be ~5.62 (Figure 7).

The difference between the measured pH and the pH calculated from the measured DCO₂ is probably related to the differences in analytical techniques. The pH was measured directly from water flowing from the springs. Bubbles of CO₂ were seen effervescing from the probe tip and sides of the beaker that contained the pH probe, suggesting that the pH of the water was increasing even as it was being measured. The CO₂ was measured with a CO₂ probe. The CO₂ content of the water was much greater than the CO₂ probe was designed to measure. To compensate for this, the spring waters were diluted to a 10% concentration with deionized water. The deionized water was gently poured into the spring water and mixed by lightly swirling to further minimize the loss of CO₂. The diluted mixture effervesced very little CO₂ during the DCO₂ measurement. As shown in Figure 7, the true pH of the water, as it issues from the ground, can be more accurately determined by calculating it from the DCO₂. Moreover, the outgassed CO₂ of each spring would also have to be accounted for before the true pH of the water at depth in the mixing zone could be calculated. To circumvent this problem, future study of the springs should include opening some of the

springs, which in many cases are drilled and cased wells, and performing down-hole measurements.

Other limitations associated with using programs like PHREEQC to calculate SI's and speciation accurately are that thermodynamic data is lacking for some minerals and biologically mediated precipitation is not addressed. The inability of PHREEQC to properly predict the precipitation of iron and manganese oxides in the Manitou Springs system is a good example of these problems. The ionic mass balance of the spring system shows that iron and manganese are lost in the mixing zone. The SI's, however, of almost all of the springs indicate that ferrihydrite, the most likely iron mineral to precipitate first, is not supersaturated ([Table 3](#)). Subsequent discussion will show that iron oxide in Cave of the Winds was probably precipitated by bacteria. The precipitation of iron oxide in the mixing zone is probably also being mediated by bacteria, thus the calculation of the SI's is not an appropriate method to assess hydrochemical evolution or mineral paragenesis of these minerals. The SI's of the springs also show that the manganese oxide, manganite, which is the most likely mineral to precipitate in the mixing zone, should be in solution ([Table 3](#)). Subsequent discussion will show that hollandite, which is present in nearby Cave of the Winds, is probably the manganese oxide mineral that is precipitating in the mixing zone. Unfortunately, there are no thermodynamic data available for hollandite.

Position And Geometry Of Mixing Zone

Factors that control the position of the mixing zone are the high permeability and solubility of the limestone, the position of Fountain Creek, and the structure of the limestone beds. The high permeability of the

limestone-bearing rocks in the Manitou Springs area is directly related to the rock's cavernous porosity, which has had a complex history. The earliest permeability and porosity enhancement is associated with development of paleokarst features that are present in the Leadville, Williams Canyon, and Manitou Formations (Forster, 1977). These features, which consist mostly of paleo-caves and -fissures, were filled with detrital sediments soon after the limestone was deposited in the Late Paleozoic. Subsequent dissolution of passages along paleo-caves and -fissures is probably related to the slightly higher permeability of the detrital sediments than the surrounding limestone. Passages developed along paleokarst features, however, make up only a small portion (5%-10%) of the total cave volume in the study area.

Most cave passages are developed along fractures that were formed during Larimide faulting and folding (Blanton, 1973). Incipient Cenozoic dissolution along the paleokarst features and Larimide fractures produced extensive secondary permeability, which made the limestones much more permeable than either the overlying Fountain Formation or the underlying Sawatch Formation and Pikes Peak Granite. Thus, the Paleozoic carbonates became major aquifers for conducting water.

The geometry of the limestone beds also controls the location of the mixing zone. The southern, down-dip end of the limestone beds abuts the Ute Pass Fault, where ascending CO₂-rich mineral water preferentially enters the highly permeable limestone. The eastern, down-dip end of the limestone beds abuts the Rampart Range Fault, where additional CO₂-rich mineral water may be ascending and entering the limestone. As discussed earlier, this water may have been modified by contact with marine shale, such as the Pierre Formation. The up-dip side of the limestone crops out on the southeastern flank of the Rampart Range where dilute meteoric water enters

the limestone. The position of Fountain Creek also controls the location of the mixing zone, because the springs, which are a drainage focal point for both the deep-seated waters and the near-surface waters, are located near the creek where the hydraulic head is the highest. If Fountain Creek were to erode down to a lower level, the increased head at the lower level would soon force the spring water to utilize fractures and conduits nearer the new, lower creek level. Thus, the springs and the mixing zone will continue to maintain their general positions relative to Fountain Creek.

The approximate areal extent of the mixing zone ($\sim 1.2 \text{ km}^2$) is shown on [Plate 1](#). The boundaries on the west and north correspond to the approximated intersection of the limestone beds and the water table. The boundary on the south coincides with the Ute Pass Fault. The boundary on the east extends the Eastern Springs, because the high TDS of these springs suggest that very little mixing with low TDS water is occurring east of these springs.

The mixing zone can be modeled as a large underground tank that is $\sim 1 \text{ km}$ in diameter and $\sim 107 \text{ m}$ thick ([Figure 8](#)). It is confined by impermeable rocks (Glen Eyrie Member of the Fountain Formation on the top and Sawatch Formation on the bottom, [Figure 8](#)) and is tilted $\sim 12^\circ$ to the southeast. The ceiling (upper impermeable bed) of this tank is held up by pillars (cave walls) that probably occupy 90 to 95% of the tank volume. Water enters the mixing zone at several points ([Figure 8](#)). Deep-seated and marine-modified water enters at the bottom of the mixing zone on the southeast end ([Figure 8](#)). The low TDS waters enter at the top on the northwest end ([Figure 8](#)). The density contrast between the two waters is large enough that the water in the mixing zone is vertically stratified ([Figure 9](#)). This stratification explains several phenomena.

To construct a stratification model, three assumptions are made. The first assumption is that each spring taps one specific level in the mixing zone and is not a mixture of two levels. The second assumption is that the potassium content of each spring is proportional to the spring's depth (Figure 9). Potassium was chosen because it is conservative in the mixing zone, relatively concentrated in the deep-seated water (~94 mg/L), and virtually absent from the low-TDS waters (~1 mg/L). A third assumption is that the potassium concentration increases linearly with increasing depth (Figure 9). The relationship of a spring's location to its chemistry can now be easily explained. The chemistry of the each spring is determined not only by its location but also by its depth. For example, the Twin Spring, which is located near the Downtown Springs, has the chemistry of the Western Springs because it taps a higher level of the mixing zone (Figure 9). Conversely, the Ute Magnetic Spring, which is located with the Western Springs, has a chemistry somewhat similar to the Downtown Springs, because it taps a level intermediate between the Downtown and Western Springs (Figure 9).

The phenomenon of the relatively higher manganese content of the Downtown Springs as compared to either of the inputs—the modeled deep-seated input (Iron Geyser, Table 3) or the modeled marine modified input (7-minute East, Table 3)—can also be explained by a vertically stratified mixing zone. Unlike the potassium content, the manganese content does not vary linearly with depth (Figure 9). This is apparently related to the dissolution and precipitation dynamics of a manganese-bearing solid phase (hollandite?), which is partially removing manganese from solution as indicated from the mass balance calculations (Plate 5, I). As shown at Lake Biwa, Japan (Kawashima and others, 1988) manganese released from the reaction of anoxic bottom waters with lake sediments precipitates as it ascends into the

more oxygenated lower epilimnion. The precipitated manganese particles drop back in the anoxic hypolimnion where they re-dissolve, thus maintaining an equilibrium that preserves a ~0.5-m-thick manganese-rich layer at the thermocline.

The manganese peak in the Manitou Springs mixing zone ([Figure 9](#)) is probably related to precipitation of a manganese oxide resulting from an increase either in DOX or pH. As the manganese precipitates some of the particles are able to drift downward in open cave passage where they re-dissolve at lower levels. The only time that manganese is retained in the system is when the falling particles land on horizontal surfaces in the upper part of the manganese zone, where the solution chemistry prevents the manganese particles from re-dissolving. Earthy, horizontal layers of hollandite in Cave of the Winds support this hypothesis ([Figure 10](#)). The dissolved manganese content of the manganese zone is controlled not only by the concentration of the input waters, but also by the placement and flow rates of the springs and the presence of horizontal sediment traps. The location of the springs is probably the most important control. If the Downtown Springs did not exist, all of the manganese would probably precipitate in the mixing zone long before reaching the oxygenated waters of the Western Springs. Also, if the Downtown Springs had higher flow rates, much more of the dissolved manganese would be drawn out of the system and there would be less available for precipitation. Horizontal sediment traps are also important. Manganese would not be lost as a solid if the manganese zone, which is estimated to be ~24 m thick, was hosted in a cave passage of larger dimensions. In this case, precipitated manganese would not reach the bottom of the cave passage. A spring tapping such a passage would be able to draw off most of the manganese in the dissolved form.

The above examples also show the importance of the plumbing configuration of the mixing zone on controlling mineral dissolution and precipitation. Mass-balance calculations on the present system indicate that the manganese-oxide beds should be only $\sim 1/16$ as thick as the iron-oxide beds (Plate 5, J). The equally thick beds of iron and manganese deposits in Cave of the Winds (Figure 10), therefore, suggest that the plumbing of the system may have been different in the past. The thicker manganese beds at Cave of the Winds imply that the plumbing was such that all of the available manganese was precipitated and deposited in the cave. Alternately, in the past the chemistry of the water feeding the mixing zone may have been different than today.

Evidence at Cave of the Winds also suggests that in the past, unlike the present system, the low-TDS near-surface input and deep-seated input mixed at depth. This is evidenced by the large subaqueous calcite crystals (1 to 5 cm in length) at the south end of Thieves Canyon (calcite nodule, Figure 10) and the Guides Rest (Plate 2). These large crystals are associated with iron- and manganese-oxides, suggesting that the deep-seated and low TDS waters mixed at a sufficient depth to permit all of the CO_2 to stay in solution, thus creating a very corrosive mixture capable of dissolving large amounts of limestone. Then, as this mixture ascended to shallower depths, the pressure would have decreased, allowing CO_2 to outgas and pH to increase. This would have allowed the precipitation of manganese-oxides, iron-oxides, and calcite. The outgassing of CO_2 is evidenced by the bubble trails present at the Guides Rest and the southern end of Cave of the Winds (Plate 2). Apparently, bubble trails are formed when ascending CO_2 -rich water reaches a shallow-enough depth that the CO_2 outgasses and bubbles up against overhanging features, where it etches vertically oriented channels.

Movement Of The Mixing Zone

The mixing zone, which in the past was located near Cave of the Winds, has steadily moved laterally and down to its present position beneath Manitou Springs. The cave itself is probably the best evidence that a mixing zone existed at Cave of the Winds. Other evidence includes an alluvium-filled sinkhole above the cave and an alluvium capped ridge ~0.5 km east of the cave (Plate 3)—both deposits apparently associated with ancient Fountain Creek that flowed just above the Cave of the Winds. Additionally, a ridge ~1.0 km southeast of the cave is capped by a 20-meter-thick strath deposit that is perpendicular to Williams Canyon. This indicates not only that ancient Fountain Creek was located above the cave, but also that it flowed to the east, perpendicular to the present canyon.

Much like the present situation at Manitou Springs, the intersection of the stream valley and the limestone would have been the site where water rose to form paleosprings on the surface. Evidence confirming this is the solution breccia located just south of the cave. The breccia consists of corroded blocks of limestone, chert, and clays in a matrix of earthy dolomite, which in many places still exhibits the original bedding of the Manitou Formation. This is strong evidence that the calcite in the dolomitic Manitou Formation was dissolved by aggressive water in a mixing zone that would have been located below the paleosprings.

If it is assumed that the water chemistry, flow rates, down-cutting rates, and the amount of rock involved at the modern mixing zone is similar to the paleo-mixing zone, the mass-balance calculations can be used to show that extensive solution breccia should be associated with the paleo-mixing zone. Evidence at the modern mixing zone indicates that all of the limestone

present beneath Manitou Springs would be dissolved as the mixing zone moves through the limestone with time (Plate 5, K). This suggests that the central portion of the paleo-mixing zone should consist entirely of solution breccia. Large areas of solution breccia occur south of Cave of the Winds and west of Manitou Springs.

During subsequent erosion, Fountain Creek cut downward as it migrated to the south. The springs, always rising near the point where the creek intersected the Paleozoic carbonates, also moved to the south. The mixing zone, maintaining its position below the springs, moved with the springs. The movement of the mixing zone through the cave system as the creek moved laterally can be deciphered by the superposition of distinctive cave sediments.

Cave Sedimentation Model

As already shown, the present mixing zone beneath Manitou Springs can be divided into different sub-zones. Minerals precipitating in these sub-zones along with sediments in active caves in lower Williams Canyon, can be used to develop a cave sedimentation model. The mass-balance calculations have already shown that iron-oxide precipitates in the mixing zone. The low iron content of the downtown springs is indicative that iron-oxide is precipitating in a sub-zone in the southeastern part of the mixing zone. As discussed earlier, manganese oxide is probably also being deposited beneath the Downtown Springs in a manganese-oxide sub-zone.

The separation of iron and manganese oxides into two distinctive sub-zones is a consequence of differential oxidation and solubility (Krauskopf, 1967). Iron, which reacts with oxygen more readily than does manganese, precipitates in the oxygen-poor southern region of the mixing zone. Further

to the north, the water has a higher oxygen content from the increasing admixture of oxygenated near-surface water. This results in the precipitation of manganese oxide. When the iron oxide precipitates, it is capable of adsorbing large amounts of heavy metals such as arsenic, lead, antimony, and tungsten (Drever, 1988). Sediments at the Iron Springs contain up to 4200 ppm arsenic and 225 ppm lead (Table 5A). The low arsenic and lead content of the iron-poor springs suggests that phreatic iron precipitation has removed most of the arsenic and lead from these springs (Table 3).

The northern boundary of the mixing zone lies between the western springs and Williams Canyon (Plate 1). In the northern area of the mixing zone, the detrital load brought into the system by Williams Canyon Creek is being deposited. The sediment-free nature of the Western Springs indicates that all of the sediment load brought into this area of the system is deposited in water-filled caves.

Continuous southward and downward movement of the mixing zone through the limestone will therefore result in the superposition of cave sediments. Because dissolution of limestone takes place throughout the mixing zone, the residue remaining from the partial dissolution of limestone will be deposited on the cave floors throughout the mixing zone. However, only in the southernmost part of the mixing zone would solution debris be preserved in discrete beds. In the central and northern portions of the mixing zone, the large volume of other sediments being deposited would dilute and mask the solution debris.

With continued movement of the mixing zone to the south, iron oxide would eventually be deposited on the solution debris; subsequently, manganese oxide would be precipitated and deposited on the iron oxide. Continued southward movement of the mixing zone would be recorded in the

northern part of the mixing zone by a coarsening-upward detrital sequence. Williams Canyon Creek, which already has been shown to be the major meteoric-water input for the springs, also transports detrital sediments into the mixing zone. This process is evident in the vadose portion of Manitou Cave, which is located just below the area where Williams Canyon Creek normally infiltrates into its streambed (Figure 2). In Manitou Cave, stream erosion not only prevents sedimentation, but cuts into sediments that were deposited earlier when the cave was water filled.

Introduction of new sediment and the erosion of existing sediment apparently occur only when Williams Canyon Creek is swollen from spring runoff or floods. Active streams in Manitou Cave have been observed during spring runoff. In 1921 a large flood roared down Williams Canyon flooding Manitou Cave, blocking some of the lower passages with sediment (Rhinehart, 1996). Charcoal and snails preserved on many of the ceilings in the upper passageways indicate the occurrence of even older floods, which will be discussed later in more detail. When the stream enters water-filled passages further to the south, the water velocity is greatly reduced, so that within a very short distance (~100 m) cobbles, gravel, sand, and silt are deposited in that order (Bögli, 1980). Clay, because of its ability to stay in suspension longer, is carried greater distances into the cave system. However, because of the long travel time to the springs (estimated to be 2-4 weeks) and the low water velocity, even the finest clay particles settle out of the water before reaching the springs.

Taking all of the above sedimentation regimes into account, the migrating mixing zone, as it moves down and to the south through the limestone, should result in the deposition of the following generalized sediment column from bottom to top: solution debris, iron oxide, manganese

oxide, clay, silt, sand, and gravel. If the sediments at Cave of the Winds were a product of this type of migrating mixing zone, then the average cave sediment column should be very similar to the hypothesized column.

Correlation of Cave-Of-The-Winds Sediments With Spring Sediments

According to the cave sedimentation model, the three lowest stratigraphic units, from base upward, would consist of solution debris, iron oxide and manganese oxide. These beds are normally found throughout the cave in a sequence usually not more than 5-cm thick, making detailed chemical and petrographic analysis very difficult. In the south end of Thieves Canyon ([Plate 2](#)), however, a 30-cm-thick sequence of these beds facilitates detailed analysis ([Figure 10](#), [Table 5B](#)). The basal bed consists predominantly of rounded, frosted quartz grains with smaller amounts of feldspar, illite, and silicified fossil fragments. The insoluble residue from the Manitou Formation has a composition very similar to the basal bed (Morgan, 1950). Overlying this bed are two iron-oxide-rich beds ([Figure 10](#), [Table 5B](#)) that contain variable amounts of hematite and goethite. The micro-morphology of the iron oxide suggests that it was deposited by bacteria ([Figure 11](#)). The rod shaped iron oxide has a morphology that is very similar to the sheathed bacteria *Leptothrix* (Peck, 1986). Apparently, this bacteria precipitates a ferrihydrite-like compound, which, with time, recrystallizes into goethite and hematite ([Figure 11D](#)). These iron-oxide deposits have very high concentrations of arsenic and lead ([Table 5B](#), As = 8900 ppm, Pb = 6200 ppm) and are similar to modern iron-oxide deposits precipitating from the waters of the Iron Springs ([Table 5A](#), As = 4200 ppm, Pb = 225 ppm).

Overlying the iron-oxide layer is a manganese-oxide layer, which consists mostly of the mineral hollandite ([Figure 10](#)). Clay, which in some

parts of the cave can be up to 8-m thick, overlies the manganese-oxide, in agreement with the sedimentation model. The model also predicts that a coarsening-upward sequence of silt, sand, gravel, and cobbles should overlie the clay. This sequence, which is up to 2-m thick, is found throughout the cave.

Source Of Cave Infill

Importance Of Provenance

Proving the provenance of the detrital sediments present at Cave of the Winds is important because it shows that the detrital sediments present in the cave are indeed allochthonous and that the sediment column present at the cave is the result of a sedimentation process similar to the one taking place in the mixing zone beneath Manitou Springs today. The provenance of the clay will be discussed first and in much more detail than the coarser sediments present at Cave of the Winds because of the controversies over the origin of the clay and because of the importance of the origin of the clay for climate modeling.

Red Clay

Bretz (1942) suggested that the red clay commonly present in caves is derived from soil that overlies the surface above the caves. Some authors believed that this clay was derived from the *in situ* dissolution of limestone (Davis, 1930, Warwick, 1953). Modern studies have shown that cave clays are derived from local regoliths and transported into caves by streams (Reams, 1968; Frank, 1965; Milske, 1982; White, 1988). These two schools of thought suggest that the clay at Cave of the Winds can come from either of

two sources; residue from the dissolution of limestone or allochthonous sediment washed into the cave.

The large difference between the amounts of clay minerals present in the red clay and the clay present in the limestone is evidence that the limestone-derived clay contributes little to the total clay fill in the cave. The cave clay contains ~13% smectite (Figures 12C and 12D), whereas the limestone contains only ~1.0% of that type of clay (Figure 12B). Additionally, by looking at the volume of clay-filled passages as compared to the available limestone-derived clay it can be shown that limestone-derived clay can not be a major source of the red clay. The passages at Cave of the Winds are ~50% clay filled, a conservative estimate, in as much as many of the passages have thick clay remnants up to the ceiling. The average clay content of the limestone is ~2% (Figure 12A). Accordingly, if all of the clay released during the dissolution of the limestone was deposited in the same passage where dissolution took place, and the passage is ~50% filled with clay, then only a maximum of ~4% of the clay filling the passage could be from the limestone.

As discussed in the sedimentation model, stream transport of surface-derived sediment is the most likely process for introducing most of the clay into the cave. The two likely sources for these transported clays are clays in weathered Pikes Peak Granite or clays in soils developed from the Pikes Peak Granite. Weathered Pikes Peak Granite contains very little clay (Blair, 1975). However, soils, which develop from grus, loess, and alluvium derived from the granite, do contain abundant clay (Blair, 1975). Comparing the clay content and mineralogy of a clay-rich alluvium and clay-rich B horizons of three local soils (Figures 12E and 12F) with the cave clay (Figures 12C and 12D) indicates that the soil-derived clays contain the same types and

proportions of these clays. Eroded soil, especially the B horizon, therefore, appears to be the main source for the clay transported into the cave.

Detrital Sediments And Speleothems

The top of the coarsening-upward sequence at Cave of the Winds is capped by an up-to-2-m-thick graded bed of silt, sand, and gravel. The silt and sand contain feldspars, quartz, and biotite, which are the main mineral components of the Pikes Peak Granite. Furthermore, some of the gravel clasts are rounded, lithic fragments of the Pikes Peak Granite. This indicates that the coarse, upper sediments in the cave were deposited by surface streams, in agreement with the sedimentation model.

According to the previously presented sedimentation model, coarse sediments are being deposited near the phreatic-vadose interface, which is ~0.5 km north of Manitou Springs. This suggests that when the coarse sediments were being deposited at Cave of the Winds the springs were south of the cave. At this time Fountain Creek was just beginning to erode the Nussbaum Alluvium.

After deposition of the coarse detrital sediments at Cave of the Winds, there has been continued minor deposition. For example, at Holes 3 and 4 in the Grand Concert Hall (**Plate 2**) there are four distinct layers of calcite travertine (flowstone), which is banded and can be up to 5 cm thick. The NRM of the uppermost calcite layer has reversed polarity, suggesting that the calcite is at least 780 ka. Throughout the cave, there are other calcite and aragonite deposits (speleothems) in the form of stalactites, stalagmites, and flowstone that post-date stream sedimentation (Modreski, 1987). Also, in cave passages that intersect the surface (entrances), the floors are commonly covered with small angular rock fragments (breakdown). This type

of breakdown is normally the result of frost splitting (congelifraction) of the ceiling and walls. Additionally, detritus washed into the cave by hillside flooding and organic debris brought into the cave by animals is present near the cave entrances.

Chronology Of Speleogenesis

Age Of Cave Passages

Because Cave of the Winds is an erosional feature, its exact age cannot be determined. However, geologic and geomorphic features related to the cave can be used to bracket the age of incipient and major cave development. Solution breccia in the Manitou Formation indicate that there may have been some Middle Ordovician to Devonian cave development (Forster, 1977). Sediment-filled paleo-caves and -sinkholes at Cave of the Winds indicate Devonian to Late Mississippian karst development (Hose and Esch, 1992). Subsequent Cenozoic dissolution along some of these paleokarst features has resulted in the formation of cave passages (Fish, 1988). Between the Pennsylvanian and Late Cretaceous, about 3000 m of sediments, which contain abundant shale beds, were deposited on top of the initial cave. Very little, if any, cave development could take place during this period of deep burial under the thick blanket of the nearly impervious sediments and rock.

The Laramide Orogeny, beginning in the Late Cretaceous (~75 Ma, Mutschler and others, 1987), was associated with the uplift of the Rocky Mountains. The uplift, which included the Rampart Range and Pikes Peak, caused the activation of the Ute Pass and Rampart Range Faults (Morgan, 1950; Bianchi, 1967). In the Manitou Springs area, movement on the Ute

Pass Fault resulted in the folding, jointing and minor faulting of the rocks (Hamil, 1965; Blanton, 1973). The subsequent flow of corrosive water along the fractures related to the folding and faulting would produce most of the passages in Cave of the Winds and nearby caves. Uplift during the early Laramide Orogeny increased the topographic relief in the Manitou Springs area, resulting in the initiation of erosion of the overlying sediments and also increased the local hydraulic head. The erosion of some of the impervious shale along with the increased hydraulic head may have initiated some minor water flow through the joints and faults, causing incipient dissolution. However, in the first 25 m. y. of the Laramide Orogeny, erosional stripping almost equaled uplift (Tweto, 1975) resulting in a subdued topography with a maximum elevation of about 1000 m (Epis and Chapin, 1975). It was unlikely, therefore, that a large hydraulic head existed. A large hydraulic head is necessary to force large volumes of water through the rock needed for development of a large cave system.

A Late Miocene-Early Pliocene alluvial deposit on the Rampart Range, 18 km northwest of Manitou Springs, indicates renewed Miocene-Pliocene uplift, which in some places was up to 3000 m (Epis and Chapin, 1975). At the same time, movement along the Ute Pass Fault caused redirection of Fountain Creek from its former position near the above-mentioned alluvial deposit to its present position (Scott, 1975). Valley entrenchment along the Ute Pass Fault by Fountain Creek, in conjunction with uplift, created the hydraulic head needed to drive the mineral springs and the mixing zone. It is likely, therefore, that the age for the onset of major dissolution at Cave of the Winds is probably Late Miocene-Early Pliocene (7 Ma to 4 Ma).

Age Of Cave Fill

Sedimentation in the cave appears to have been contemporaneous with passage development. There are a few problems in proving this chronology. One is the lack of datable materials in the sediments, such as fossils or volcanic ashes. Preliminary study of the sediments indicated that magnetic reversal stratigraphy (magnetostratigraphy) might be useful in dating the sediments. The use of this method, however, presents another problem: it requires that the polarity sequence be constrained by at least one independent date.

The Nussbaum Alluvium, which crops out east of the cave and is ~20 m higher in elevation, is apparently related to coarse sediments present at the top of sediment sequences in Cave of the Winds. If an age is assigned to the Nussbaum Alluvium and the relationship of the Nussbaum Alluvium to the coarse sediments in the cave deciphered, then an independent date can be assigned to at least one polarity reversal in the cave. The age of the Nussbaum Alluvium will be dealt with first, because the age of the Nussbaum Alluvium is poorly constrained. Various authors have assigned that range from Late Pliocene to early Pleistocene (Scott, 1963; Soister, 1967; Scott, 1975). For the purpose of correlating the Nussbaum Alluvium with a paleomagnetic reversal, a more accurate date for the Nussbaum Alluvium was needed. This problem was solved by aminostratigraphy.

Aminostratigraphy

Most amino acids exist as two forms: L- and D-isomers (Miller and Brigham-Grette, 1989). In a living organism, the amino acids are L-isomers. After the death of an organism, the amino acids racemize, which is the natural conversion of the L-isomers into D-isomers. Eventually the amino

acids in the dead organism equilibrate to a 50/50 mixture of L- and D-isomers. The amino acids used in the present study are D-alloisoleucine and L-isoleucine (A/I). These amino acids are somewhat more complex, because L-isoleucine actually changes to a different molecule, D-alloisoleucine. This reaction, similar to racemization, is called epimerization (Miller and Brigham-Grette, 1989).

The rate at which this reaction takes place is a function of temperature. For example, if the burial-temperature history for a group of mollusks of different ages has been the same, the ratio of the two amino acids – alloisoleucine and isoleucine (A/I) – in the mollusk shells can be used for relative dating and in some cases, absolute dating (Miller and Brigham-Grette, 1989). Because temperature controls the rate of racemization, the temperature history of buried fossils must be considered before using A/I to derive ages.

Solar insolation, fire, altitude, and climate can effect the burial temperature of fossils. Diurnal or seasonal solar heating of fossils buried at shallow depths may accelerate racemization and increase the apparent age of the samples (Goodfriend, 1987; Miller and Brigham-Grette, 1989). Therefore, samples should be obtained from depths that exceed 2 m (Miller and Brigham-Grette, 1989). During the intense heat associated with a fire, racemization can also be greatly accelerated. For example, charcoal, which has a ^{14}C age of ~1500 years, found with snails at Manitou Cave suggests that the snails were exposed to a forest fire before being transported into the cave. If so, the A/I of the snails may be anomalously high for their age.

The altitude of the collection site can also affect racemization rates. For example, snails in this study were collected at altitudes between 1890 and 2195 m above sea level. Because of the normal adiabatic effect, the

highest site averages about 1.7° C less than the lowest site. Another temperature variable is long-term climate change. For example, the Nussbaum Alluvium has probably been exposed to episodes of higher or lower temperatures for much longer periods of time than the younger alluvia. Because post-depositional thermal histories are impossible to ascertain, the burial temperature for all alluvia in this study are assumed to be the same.

Mollusks

In all, over 10,000 mollusks, which included one species of slug, one species of clam, and 24 species of snail, were identified and counted. The tabulated number for each species is the number of shells that could be identified. For example, the Chesnut site had ~3,000 snails that could not be identified because they were too small (juvenile) or broken. Because of the small weight of the individual snails (0.3 to 5.0 mg) in relation to the 30 mg necessary for testing, only abundant species could be used for the amino-acid study. The most abundant species from the Black Canyon site were Vallonia cyclophorella and Pupilla muscorum and from the Fillmore, Starlight, and Colorado City sites, Vallonia cyclophorella and Gastrocopta armifera (Table 6). All of the alloisoleucine and isoleucine (A/I) ratios of the snails along with laboratory identification numbers are tabulated in Table 7A. Table 7B contains the average and standard deviation of the A/I of selected snails from each site.

Discussion Of A-I Ratios

The epimerization rates of the four species used in this study are very similar. This is indicated in Table 7A by the comparable A/I values of different snail species at the same sample location. Moreover, shell size did

not appear to greatly effect the A/I. For example, the average Gastrocopta Armifera shell weighs 5 mg; the Vallonia cyclophorella 1 mg; yet, the A/I for these shells from Manitou Cave are similar (Table 7A).

The snails from the Verdos Alluvium, which include the Starlight, Fillmore, and Colorado City sites (locations on Plate 3), were used to test the A/I reproducibility of samples from one site and to compare the A/I from the different sites. Extra effort was put into assuring that the amino acid ratios of snails from Verdos Alluvium were as reliable as possible, because any errors in their A/I determination would greatly amplify the inaccuracies of the extrapolated age of the Nussbaum Alluvium (Figure 13). Therefore, the Starlight site was sampled three times and the Fillmore site, twice. Although each of the two sub-sites at Colorado City were sampled twice, the scarcity of Vallonia cyclophorella and Gastrocopta armifera necessitated combining all snail shells of similar species from the entire site and from both sampling trips. One Starlight-site sample (Table 7A, Lab # AAL-5768) was excluded from the final curve fitting because it had an anomalously high ratio as compared to the others from that site. The snails that made up this sample (AAL-5768) may have been from an older reworked alluvium or there may have been a problem with their preparation or analysis.

The data from the Colorado City site were also excluded from the final curve fitting, primarily because the A/I's of the two species were very different from each other and both A/I's were much lower than those from the Starlight and Fillmore sites. Their low A/I's would indicate that the Colorado City site may actually be either the Slocum or Louviers Alluvium. The anomalously low ratios could also be the result of contamination from modern shells or organic material.

Determination of anomalously high or low ratios would be impossible without multiple sampling. Taking one sample per site would have been insufficient. Two samples per site were acceptable when the A/I ratios were about the same for both species. With 12 samples from the Verdos Alluvium, it was quite appropriate to discard the highest and lowest ratios.

The A/I ratios of land snails determined from this study and other studies of nearby areas (Dethier and Harrington, 1987; Allen Nelson, 1989, oral and written commun.) indicate that racemization rates are slow. The slow epimerization rate may not make this technique useful for dating Holocene deposits. The technique, however, should be very useful for dating Pleistocene and Pliocene deposits, and may even be useful for relative dating of Late Miocene deposits.

Age Of The Alluvia

The higher A/I of the snails from Black Canyon site, which is mapped as Nussbaum Alluvium, indicates that it is older than the other alluvia (Table 7A). Furthermore, by ascertaining the ages of the younger alluvia, plotting those against their relative A/I ratio, and fitting a curve to the resultant plot, an equation can be derived that can be used to calculate the approximate age of the Nussbaum Alluvium.

Snails from the modern flood plain (Plate 3) were used to ascertain the A/I ratio of modern snails. About 50% of the snails at this site were alive when collected. The live snails were not analyzed because the flesh, which may have different amino-acid ratios than the shells, might have contaminated the shell A/I ratios. Empty shells were used for analysis and assumed to be about one year old. There is a possibility that the modern shells were reworked from older sediments such as the Piney Creek

Alluvium. However, the abundant live snails mixed with the dead snails of the same species suggests that all snail specimens were contemporaneous.

The Centennial site ([Plate 3](#)) has been mapped as Piney Creek and Post-Piney Creek (Trimble and Machette, 1979). Charcoal collected from the Centennial site (location on [Plate 3](#) and description on [Plate 4](#)) was ^{14}C dated at 1542 ± 130 years old ([Table 8](#)) indicating that the site should be mapped as Post-Piney Creek Alluvium. The snails collected at Manitou Cave, which have relatively high A/I ratios, were initially thought to be about the same age as dated deposits at Narrows Cave. Narrows Cave is located ~0.4 km north of Manitou Cave and contains flood deposits intercalated with flowstone that has been dated and found to have a maximum uranium-thorium age of 32 ± 2 Ka ([Table 8](#)). They are thought to be the same age because the snails at Manitou Cave and the deposits at were both deposited by paleo-floods and both had similar heights above Williams Canyon Creek. However, charcoal associated with the snails in Manitou Cave was ^{14}C dated with an age of 1552 ± 75 years ([Table 8](#)). Apparently, either young charcoal mixed with old snails during the paleo-flood or the snails were affected by a forest fire that induced anomalously high A/I ratios. This conflicting evidence made it necessary to exclude the Manitou Cave data from the curve fitting.

The Chesnut site was mapped by Trimble and Machette (1979). Elsewhere in Colorado the Louviers has been dated at 115 Ka by Machette (1975). Szabo (1980) gave a minimum age of 102 Ka and inferred that the maximum age was ~150 Ka. The Fillmore, Colorado City, and Starlight sites are all mapped as Verdos Alluvium (Trimble and Machette, 1979), which, in the Denver area, contains the 640-Ka Lava Creek B ash near its base (Sawyer and others, 1995; Izett and others, 1989; Machette, 1975). Because

the Lava Creek B ash gives the maximum age for the Verdos Alluvium, the inferred maximum age of ~150 Ka was assigned to the Louviers Alluvium. The interpolated age of the Nussbaum Alluvium, therefore, represents its maximum age.

Parabolic Curve Fitting

Ages and A/I data (Table 7B) from four of the younger alluvia, together with A/I data from the Nussbaum, were used to extrapolate the age of the Nussbaum. Various authors have applied linear and parabolic curve fitting to amino acid data for both interpolation and extrapolation of age (Miller and Brigham-Grette, 1989). Mitterer and Kriausakul (1989) have employed the parabolic function ($y=x^2$) with good results. Applying the generalized parabolic equation ($y=A+Bx+Cx^2$) to my data resulted in a better curve fit than the specialized parabolic function ($y=x^2$). Use of the specialized parabolic function assumes that the A/I ratio starts at 0.0 and that at an initial age near zero, the racemization rate is infinitely large. The data from my study area suggest that both of these assumptions are invalid (Table 7B and Figure 13).

Ignoring the A+Bx terms appears to have little effect on curve fitting of relatively young snails (<100 Ka). The generalized parabolic function, however, was used in this study because the age of the Nussbaum Alluvium is extrapolated 3 to 4 times beyond the oldest calibration point. Parabolic-curve fits for the average ratio with error bars of one standard deviation indicate an extrapolated age for the Nussbaum Alluvium of 1.9 +0.4/-0.2 Ma (Figure 13).

Extrapolating a date that is 3 to 4 times more than the maximum calibration date is a practice generally frowned upon. I believe that by carefully collecting and handling samples, obtaining precise analysis of the

amino acids, acquiring the best age determinations of the younger deposits, and curve fitting with the generalized parabolic function, I have minimized problems usually associated with such extrapolation. The 1.9-Ma date for the Nussbaum Alluvium is appropriate only for the unit mapped in the Manitou Springs area; it may not be correlative with the type section in Pueblo, Colorado. The date, $1.9 \pm 0.4/-0.2$ Ma, which is the most accurate date available for the Nussbaum Alluvium, was used to calibrate the magnetostratigraphy of the sediments in Cave of the Winds.

Magnetostratigraphy

Unconsolidated sediments can be magnetized by the magnetic field of the earth (Tarling 1983), acquiring natural remanent magnetization (NRM). A type of NRM in sediments is detrital remanent magnetization (DRM), which is formed when the magnetic grains of a sediment, such as magnetite or hematite, are aligned with the earth's magnetic field during or soon after deposition (Verosub, 1977). The DRM of a sediment has the same orientation the earth's magnetic field (Verosub, 1977).

The magnetic field of the earth has reversed many times in the past at an average rate of ~ 1 reversal/0.5 m.y. (Tarling, 1983). Polarity time scales have been constructed by compiling a succession of the reversals from radiometrically dated rocks (generally volcanic) and the established marine linear magnetic anomaly pattern (Mankinen and Dalrymple, 1979; Harland and others, 1982; Hailwood, 1989; Cande and Kent, 1992).

There are several ways to use this time scale to date sediments. By assuming that the top of a sediment section starts at the present and sedimentation has been uninterrupted, such as in deep ocean basins, it is a simple matter of counting the reversals and correlating them with the polarity

time scale. Normally, because of erosion or a hiatus in deposition, however, the top of a sediment section will have a non-zero age that must be ascertained by some other technique before reversals in the section can be correlated with the polarity time scale.

Another way of dating sediments is by pattern matching. If the sedimentation rate of an undated section can be assumed to be constant or is known and there are sufficient reversals (5-10), the polarity record can be matched to the pattern of the polarity time scale to provide dating. This is possible because the timing of reversals is apparently random (Tarling, 1983), therefore, a sequence of reversals is seldom repeated. Both of these techniques were used to refine the age of the sediments at Cave of the Winds.

Paleomagnetic Results

All the paleomagnetic data from Hole 6 are presented to provide a typical example of NRM results and how the samples responded to demagnetization ([Table 9](#)). The complete data set of sites included in this study are available from the author on computer storage disks. Sample depth and magnetic declination after 15-mT AF demagnetization from each site were used to correlate the magnetic polarity sequence within and between the Grand Concert Hall and nearby Heavenly Hall ([Plate 6](#)). An exception to the use of this demagnetization level is Hole 5, from which samples from 6.5 to 10.0 m in depth were subjected to step wise 20-, 25-, and 30-mT-AF demagnetization. The higher fields were applied in an attempt to remove secondary overprints. Even with the increasing demagnetization,

however, the declination of the deeper samples at Hole 5 have greater variability than those from shallower depths (Figure 14). Additionally, the polarity results from Hole 5 are shown in Figure 14, which also shows the correlation with the known polarity record and stratigraphy of the cave sediments.

Criteria For Reversal Assignment

Sequences of samples that had an average declination of $\sim 0.0^\circ$ and an average inclination of $\sim 35.0^\circ$ were assigned to normal polarity. The ideal inclination for DRM in the Manitou Springs area (latitude $\sim N39^\circ$) should be $\sim 60^\circ$. The low values recorded at Cave of the Winds are considered to be the result of inclination error resulting from sediment compaction (Verosub, 1977), a common occurrence among clay-rich sediments. Sequences of samples that had an average declination of $\sim 180^\circ$ were assigned a reversed polarity (Plate 6). In most cases, inclinations of these samples were variable, ranging mostly between -35° and $+10^\circ$. Some of the low, upward inclinations can also be attributed to inclination error; some, however, appear to be related to post-depositional acquisition of remanent magnetization.

Effects Of Post-Depositional Remanent Magnetization On Sediments

Most post-depositional remanent magnetization (PDRM) is the result of realignment of the magnetic particles during compaction and especially dewatering, both of which can take place thousands to millions of years after deposition (Verosub, 1977). A possible explanation of the variability of the inclination of the reversed samples is that these samples were compacted and dewatered during a normal polarity interval, overprinting a normal component. The dewatering and compaction may have occurred rather

quickly following rapid draining of the water in the cave passages related to downcutting by Fountain Creek. Mud cracks present in the top two meters of the sediments at the Grand Concert Hall combined with their mostly normal polarity (Figure 14) indicate that this is a plausible explanation. Further micro-sampling and precision analysis would be necessary to ascertain the mechanism responsible for the difference in the inclinations.

Chemical remanent magnetization (CRM) may also be a contributing factor to anomalous inclination. Alteration and oxidation of iron-bearing minerals in the sediments after deposition could conceivably contribute to CRM. This could only be a factor in the top two meters of coarse sediments (Figure 14), which contain unaltered minerals. The general oxidizing conditions and neutral to slightly alkaline pH of waters percolating through these sediments, however, would preclude mobilization or precipitation of iron oxides. The underlying soil-derived clays, which have already undergone prolonged oxidation before being deposited in the cave, are chemically stable and would not be vulnerable to CRM.

Other evidence that suggests that there is little to no effect from CRM is the presence of magnetite in the sediments at Cave of the Winds. Chemical analysis indicates that the magnetite in the cave sediments is derived from the Pikes Peak Granite and is not authigenic (Table 10). Petrographic examination verified that all samples, rock and cave sediments, contained grains of magnetite that have partially altered to hematite. This indicates that much of the hematite present in the cave sediment is allogenic. Petrographic examination of the cave sediments also confirmed the presence of blood-red beads of microcrystalline hematite. This evidence suggests that some of the hematite was formed after the sediments were deposited in the

cave. However, a ~40% decrease of the NRM intensity with 10-mT-AF demagnetization (Table 9) indicates that the main carrier of the NRM in the cave sediments is magnetite. If the main carrier of the NRM was hematite, a much higher field (>1000 mT) would have been necessary to achieve a similar decrease in NRM (Tarling, 1983). Magnetite, being >100 times more magnetic than hematite, overwhelms any CRM from the formation of authigenic hematite.

Paleomagnetic Correlation

Because there are no independent dates on the cave sediments, correlation of the magnetic polarity record of the Cave of the Winds sediments with the accepted polarity time scale poses a difficult problem. The solution requires matching a part of the sequence of known polarity events with the Cave of the Winds record. The age of the Nussbaum Alluvium, which is apparently related in time to the uppermost coarse cave sediments, however, can be used to help constrain the paleomagnetic correlation.

As discussed previously, clay is deposited in the cave below the phreatic-vadose interface where sediment-laden streams enter water-filled passages. The Nussbaum Alluvium was being deposited on a stream-cut surface at the same time that clay was being deposited in the Grand Concert Hall (Figure 15A). As Fountain Creek downcut and moved to the south, the water table dropped (Figure 15B). The drop in the water table coincided with drop in the water depth in rooms like the Grand Concert. As the water depth dropped, the velocity of the water passing through the room increased. The increased stream energy changed the sedimentation regime from clay deposition, in time, to silt, sand, and gravel deposition (Figure 15B). Fluvial

sedimentation at Cave of the Winds stopped as Fountain Creek moved further to the south and downcut further (Figure 15C). The relationship between the Nussbaum Alluvium and the sediments in the cave indicates that in the Grand Concert Hall the change from silt to clay deposition took place after the Nussbaum was deposited. More specifically, the clay-to-silt interface should be the same age as the Nussbaum Alluvium, minus the time it took for Fountain Creek to cut down and drop the water table to the level of the Grand Concert Hall (Figure 15B).

The sediment floor of the Grand Concert Hall, where the paleomagnetic data was obtained, is about 20 m below the Nussbaum Alluvium. The age of the Nussbaum Alluvium (~1.9 Ma) and its height above modern streams (200 m) provides an estimate of the average down-cutting rate of 10.5 cm/1000 years. Accordingly, accumulation of coarse sediments in the cave 20 m below the Nussbaum Alluvium probably would have begun ~1.7 Ma.

The estimated 1.7 Ma age of the clay-coarse sediment interface correlates well with the onset of the Olduvai Subchron at 1.9 Ma (~2.2 m depth, Figure 14). This is the most probable correlation. Alternatively, one could match the normal-polarity sequence (1.0 to 2.2 m depth, Figure 14) with the Jaramillo Subchron (Harland and others, 1982) or the Gauss Chron (Figure 14). These correlations, however, would result in an age of ~1.0 Ma and ~ 2.6 Ma, respectively, for the clay-coarse-sediment interface—much too young or too old, respectively, for its estimated age.

The complete paleomagnetic correlation shown on Figure 14 follows from correlation of the normal-polarity interval between 1.0 and 2.2 m in depth with the Olduvai Subchron. According to the correlation suggested here, the oldest cave sediment was deposited about 4.3 Ma, a date that

agrees quite well with the previously discussed probable age of the major onset of cave formation (7 Ma to 4 Ma).

PLIOCENE-PLEISTOCENE CLIMATE

Climate Record In Cave Sediments

Studies have shown that the clay mineralogy of soils is related to both the parent material and the climate in which the soils formed (Singer, 1978; Eberl, 1984; Birkeland, 1989). If the soil clays are pedogenic and not inherited from parent material, then soils rich in kaolinite are generally related to moist climates and those rich in smectite, dry climates (Singer, 1978; Eberl, 1984; Birkeland, 1989). For example, along the Front Range of Colorado, smectite is three times more abundant in the dry soils of the plains than in the wetter soils of the mountains (Netoff, 1977). When these soils are eroded they can be transported to, and deposited in caves, such as Cave of the Winds. These deposits, which are protected in the cave from further soil-forming processes or chemical transformations, can be used for interpretation of the climate that existed at the time of soil formation (Frank, 1965; Bögli, 1980). At Cave of the Winds, the oldest clay deposits have relatively less kaolinite and more smectite than the younger clay deposits (**Figure 12D**). This suggests that when clay deposition started the climate was drier and by the time clay deposition ceased, the climate had become wetter. This apparent climate change, however, also could have been related to uplift. As the elevation of the region increased there may have been an increase in precipitation, which would not be related to a global climate change.

Another possible problem with clay/climate correlation is the timing of clay formation and clay deposition. This can be seen in the silty cave deposits, which have a relatively higher smectite content than the underlying clays and about the same amount of kaolinite as the underlying clays (Figure 12D, Samples 1 and 2). The high smectite content suggests a dry climate, whereas, the kaolinite content suggests a wet climate. The chemical properties of the two clays can be used to explain this apparent anomaly. Smectite can transform to kaolinite, but the kaolinite to smectite transformation is much less likely (Singer, 1978). Therefore, kaolinite, which was formed in the soils during a wetter climate, would be stable during a subsequent drier climate, during which time smectite would be forming. Clays eroded from these soils and deposited in the cave would contain kaolinite formed during an earlier, wetter time and smectite forming contemporaneously with soil erosion and cave deposition. The smectite content, therefore, would more accurately record the climate that prevailed at the time of soil erosion and cave deposition.

Large-Scale Sediment Changes As Climate Indicators

Two large-scale sediment changes in the stratigraphic column at Cave of the Winds can be correlated with large-scale climate changes. Morrison has suggested that the Verdos, Rocky Flats, and Nussbaum alluvia were deposited during megacycles (Osterkamp, 1987). He suggests that these megacycles are 400 to 500 k. y. in duration and are associated with large climate changes. The Nussbaum Alluvium, which was deposited during the oldest of these megacycles, is preserved on the ridge above the cave and on the ridge east of the cave. The coarse-grained cave deposit, which can be up to 2-m thick and overlays clay (Figure 14), has been correlated with the

Nussbaum Alluvium. The onset of silt deposition ([Figure 14](#), 2.7 m) suggests that the megacycle associated with the Nussbaum Alluvium started ~2.1 Ma. The cut-off of major sedimentation at Cave of the Winds at ~1.6 Ma has been correlated with the downcutting of the Nussbaum Alluvium as discussed earlier. This downcutting may be associated with the onset of the next megacycle, which Morrison correlates with the Rocky Flats Alluvium.

Magnetic Susceptibility

Magnetic susceptibility is a measure of the ease with which a material becomes magnetized in an applied low-intensity magnetic field (generally, ~0.1 mT). The magnetic susceptibility of a sediment is the combined result of grain size, mineralogy, and amount of magnetic particles in the sediment. Larger particles of the same magnetic mineral display greater magnetic susceptibilities than do smaller ones. In Cave of the Winds sediments, the upper silty and sandy beds have much higher susceptibilities than the lower red-clay beds. The upper beds have a higher susceptibility, because they contain a greater number of larger magnetic particles than the lower clay beds. This was evidenced while attempting to remove magnetic particles from these sediments for mineral identification and elemental determination. Only the upper silty sediments contained enough of the larger magnetic particles for analysis. The lower beds contained only a few small grains (< 1 μm). The minerals magnetite and hematite are the most common magnetic minerals in sediments at Cave of the Winds. Magnetite, however, has a higher susceptibility, so that with other parameters being equal, only a small amount of it relative to hematite can dominate the susceptibility of a sample. The rapid decrease in remanence intensity of samples during A. F. demagnetization, and the identification of abundant magnetite in polished

sections indicate that magnetite is the major carrier of magnetic susceptibility in Cave of the Winds sediments.

Periodicity Of Susceptibility

The plot of magnetic susceptibility of sediments from Holes 1 and 5 versus depth exhibits cyclical patterns of highs and lows (Figure 16). These patterns are especially noticeable in the upper ~3.5 m of Hole 1 (Figure 16), which is a function of higher susceptibility and higher sedimentation rate of these upper beds. The higher susceptibility of these beds has previously been discussed. The higher sedimentation rate of these beds is indicated on Figure 14, which shows that the rate was about twice as great during the Olduvai Polarity Subchron (correlated with the silty-sandy beds) than during the underlying subchrons (correlated with clay beds). Because the samples were collected at regular intervals, more samples were collected per geologic time in the silty-sandy beds than in the clay beds. This results in better resolution of the susceptibility record in the silty-sandy beds. Because of the pronounced susceptibility and better resolution, only the upper beds of Hole 1 will be used in the following climate-susceptibility discussion.

Many studies have shown (Peck and others, 1994; Bloemendal and others 1995) that the cyclical fluctuations in susceptibility can be correlated with climate changes. Bloemendal and others (1995) suggest that variations in susceptibility of Chinese loess reflects episodes of loess dilution, carbonate leaching, and pedogenesis, all of which are related to variations in climate. Peck and others (1994) attribute fluctuating susceptibility of sediments at Lake Baikal, Russia to complex interactions of climate controlled parameters. I propose that the cyclical susceptibility pattern at the Cave of the Winds

records the climate-controlled fluctuation of sediment transport energy of streams that brought sediment into the cave.

Magnetite, the main carrier of susceptibility in the cave sediments, was transported into the cave by surface streams. The size and amount of magnetite grains in the cave sediment is a function of stream transport energy. Because of the high density of magnetite ($\sim 5.18 \text{ g/cm}^3$), it is transported more readily by high-energy streams; therefore, it should be more common in cave sediments that were transported to the cave by high-energy streams. Two major controls of stream transport energy are the stream gradient and discharge.

During the deposition of sediments in Cave of the Winds, the stream gradient in the Manitou Springs area was mainly controlled by epirogenic uplift. The periodicity in the susceptibility record might be explained as the result of periodic rapid uplift along local faults, (such as the Rampart Range and Ute Pass Faults). After uplift local stream gradients would be increased, stream energy would increase and the amount of magnetic particles deposited in the cave would increase. Subsequently, erosion would reduce the stream gradient, stream energy, and the amount of deposition of magnetic particles in the cave. This possibility, however, does not seem plausible because there is no evidence that major earthquakes along the local faults were either common or periodic.

The other possibility is that the cyclic nature of the susceptibility record is the result of climatically induced variation in stream discharge. During episodes of greater precipitation and increased runoff, streams could transport more grains of magnetite of greater size. Sediments, which were transported into and deposited in caves during these episodes of increased

run off, should exhibit higher magnetic susceptibility than those deposited during periods of low runoff.

Potential of Correlating Susceptibility with Climate

The oceanic oxygen-isotope history (ODP 677, Shackleton and others, 1990) records glaciation as variations in the $\delta^{18}\text{O}$ record. If the susceptibility of cave sediments records variations in precipitation related to glaciation there should be a correlation of $\delta^{18}\text{O}$ values in the ocean record with the susceptibility in the cave record. Comparing the cave susceptibility record with $\delta^{18}\text{O}$ record and predicted insolation for the time interval between about 1.7 Ma and 1.9 Ma shows some similarity (Figure 17). Especially noticeable is the cyclic pattern of these three curves. Visual inspection of the insolation curve indicates a periodicity of ~20 k.y, whereas the $\delta^{18}\text{O}$ record has a strong 41 k.y. periodicity with weaker periodicities of 23 k.y. and 19 k.y. (Shackleton and others, 1990). Visual inspection of the magnetic susceptibility record shows a periodicity of ~20 k.y., which agrees with the insolation curve and to a lesser extent with the $\delta^{18}\text{O}$ record. For a more rigorous correlation of the ocean record with the cave-sediment susceptibility record, the cave sediments would have to be dated much more precisely and many more samples would have to be collected.

Pliocene-Pleistocene Mollusk Record

During the course of this study it became apparent that the Pliocene-Pleistocene mollusks used for amino-acid dating and the Pliocene sediments from the Cave of the Winds might be used to reconstruct a partial climate record of the Manitou Springs area. Because different mollusks lived in different environments, the climate that prevailed during mollusk deposition

can be inferred. Most of the species collected during this study were not analyzed for amino acids because they either were not abundant or only occurred at a few sites. All species, however, were identified and counted (Table 6). Because of the large number of species and specimens collected during this study, some level of interpretation of paleo-environment and paleo-climate is possible.

The occurrence of Oxyloma, Derocerus, and Fossaria parva indicates that the Starlight site was moist and at times aquatic (Evanoff, 1983 and 1987). The occurrence of Pupoides inornata and Vallonia cyclophorella indicate that the environment of the Fillmore site was dry, although the presence of Succinea indicates that a water body was nearby (Evanoff, 1983 and 1987). The fossil assemblages from the Starlight and Fillmore sites suggest the presence of perennial streams within a relatively dry environment. The occurrence of Fossaria parva, Oxyloma, and Vertigo at the Louviers site indicates a moist environment near water. Vallonia cyclophorella and Pupilla muscorum indicate that the Nussbaum site, the modern flood plain, and the Piney Creek site were dry habitats with ephemeral streams. Figure 18 was constructed from a combination of snail-environment-inferred climate (0-2 Ma) and clay-mineralogy-inferred climate (2-4 Ma).

CONCLUSIONS

Cave of the Winds is a phreatic cave dissolved from the calcite-rich Manitou, Williams Canyon, and Leadville Formations. Dissolution occurred along joints associated with Laramide faulting and folding. Paleokarst features, such as sediment-filled fissures and caves, indicate that some of the passages at Cave of the Winds are related to cave-forming episodes that started soon after the deposition of the Ordovician Manitou Formation and continued to the beginning of the Cretaceous Laramide Orogeny. Most speleogenesis, however, occurred in the last ~5.0 Ma. Iron and manganese oxide deposits at the cave and at springs in Manitou Springs indicate that the process of limestone dissolution that is taking place today beneath Manitou Springs is the same process that dissolved the Cave of the Winds in the past.

Chemical and isotopic analyses of the spring, well, and surface waters indicate that two principal types of water are mixing below Manitou Springs. One, which is from a deep-seated source and has a high TDS and carbon dioxide content, is ascending along the Ute Pass Fault. The other, which has a low-TDS and carbon dioxide content, is from near-surface sources. Both of these waters are either saturated with respect to calcite or have the capacity to dissolve small amounts of calcite. When mixed, however, mass balance calculations show that these waters are dissolving ~71 tonnes of limestone per year. Mass balance calculations also show that iron and manganese oxides are precipitating in the mixing zone. Iron and manganese oxide bearing sediments preserved in Cave of the Winds show that a mixing zone similar to the one beneath Manitou Springs existed at the cave.

The Nussbaum Alluvium was assigned an age of ~1.9 Ma by means of aminostratigraphy. The age of the Nussbaum Alluvium and its relation to coarse-grained sediments at Cave of the Winds were used to fix an age of ~1.7 Ma for the onset of coarse grained sedimentation in the cave. This enabled the identification of the Olduvai Polarity Subchron in the coarse grained sediments. Correlation of the magnetostratigraphy of cave sediments with the accepted polarity time scale indicates that the mixing zone existed at the cave ~4.2 Ma. The sequence of sediments at the cave and associated model developed from spring and nearby cave sediments indicate that Fountain Creek was flowing over Cave of the Winds until ~2.0 Ma. Subsequently, the creek simultaneously downcut and continually shifted south to its present position in Manitou Springs.

Studies of the clay mineralogy and magnetic susceptibility of sediments at Cave of the Winds indicate that with more work, the information gleaned from the cave sediments could be useful for determining the paleoclimate of the Manitou Springs area. During the aminostratigraphy study, a large assemblage of mollusks were collected and identified. Because many of these mollusks thrive in specific environments, the paleo-environment surrounding each of the alluvial terraces could be determined with some degree of certainty.

REFERENCES

- Adams, C. S., and Swinnerton, A. C., 1937, Solubility of limestone; Transactions, American Geophysical Union, 1937, part 2, p. 504-507
- Batard, F., Baubron, J. C., Bosch, B., Marce, A. and Risler, J. J., 1982, Isotopic identification of gases of a deep origin in French thermomineral waters: Journal of Hydrology, v. 56, p. 1-21.
- Berger, A., and Loutre, M. F., 1991, Insolation values for the climate of the last 10 million years: Quaternary Science Reviews, v. 10, n. 4, p. 297-317
- Bianchi, L., 1967, Geology of the Manitou-Cascade Area, El Paso County, Colorado with a study of the permeability of its crystalline rocks [M.S. Thesis]: Golden, Colorado School of Mines.
- Birkeland, P. W., 1984, Soils and geomorphology: New York, Oxford University Press, 372 p.
- Blair, R. W., 1975, Weathering and geomorphology of the Pikes Peak Granite in the southern Rampart Range, El Paso County, Colorado [Ph.D. thesis]: Golden, Colorado School of Mines, 115 p.
- Blanton, T. L., 1973, The Cavern Gulch Faults and the Fountain Creek Flexure, Manitou Spur, Colorado [M.S. thesis]: Syracuse University, New York, 90 p.
- Blavoux, B., Dazy, L. and Sarrot-Reynaud, J., 1982, Information about the origin of thermomineral waters and gas by means of environmental isotopes in eastern Azerbaijan, Iran, and southeast France: Journal of Hydrology, v. 56, p. 23-38.
- Bloemendal, J., Liu, X. M., and Rolph, T. C., 1995, Correlation of the magnetic susceptibility stratigraphy of Chinese loess and the marine oxygen isotope record; Chronological and palaeoclimatic implications: Earth and Planetary Science Letters, v. 131, p. 371-380.
- Bögli, A., 1964, Mischungskorrosion, - ein Beitrag zum Verkarstungsproblem: Erdkunde 18, 83-92.
- Bögli, A., 1980, Karst hydrology and physical speleology: New York, Springer-Verlag, 284 p.
- Bretz, J. H., 1942, Vadose and phreatic features of limestone Caverns: Journal Geology, v. 50, no. 6, part 2, p. 675-811.
- Cande, S. C., and Kent, D. V., 1992, A new geomagnetic polarity time scale for the Late Cretaceous and Cenozoic: Journal of Geophysical Research, b, v. 97, n. 10, p. 13,917.

- Crook, J. K., 1899, The mineral waters of the United States and their therapeutic Uses: New York and Philadelphia, Lea Brothers and Co., p. 185-187.
- Daniels, B. M. and McConnell, V., 1964, The Springs of Manitou: Denver, Sage Books.
- Davis, D. G., 1985, Cave of the Winds history; New light from forgotten sources: Rocky Mountain Caving, v. 2, no. 1, p. 23-26.
- Davis, W. M., 1930, Origin of limestone caverns: Geological Society of America Bulletin, v. 41, p. 475-628.
- Denison, C., 1880, Rocky Mountain health resorts: Boston, Houghton, Osgood and Company, p. 29, 31, 33, 39-40.
- Dethier, D. P., and Harrington, C. D., 1987, Geologic dating of Late Cenozoic erosion surfaces near Espanola, New Mexico: Friends of the Pleistocene-Rocky Mountain Cell, 1987 Field Trip Guidebook, p. 111-131.
- Dinkmeyer, P. R., 1977, Stratigraphy of Upper Cambrian and Lower Ordovician rocks in the Manitou Park-Manitou Springs-Deadman Canyon Area, Douglas and El Paso Counties, Colorado [M. S. thesis]: Golden, Colorado School of Mines, 218 p.
- Drever, J. I., 1988, The geochemistry of natural waters: Englewood Cliffs, New Jersey, Prentice Hall, p. 342-343.
- Eberl, D. D., 1984, Clay mineral formation and transformation in rocks and soils: Philosophical Transactions Royal Society London, series A, v. 311, p. 241-257.
- Epis, R. C., and Chapin, C. E., 1975, Geomorphic and tectonic implications of the Post-Laramide, Late Eocene Erosion surface in the Southern Rocky Mountains, *in* Curtis, B.F., ed., Cenozoic History of the Southern Rocky Mountains: Geological Society of America Memoir 144, p. 45-74.
- Evanoff, E., 1983, Pleistocene nonmarine mollusks and sediment facies of the Meeker Area, Rio Blanco County, Colorado; University of Colorado master thesis.
- Evanoff, E., 1987, Fossil nonmarine snails from the Horner Site *in* The Horner Site: The Type Site of the Cody Cultural Complex: Academic Press, Inc. p.443-450.
- Evans, W. C., Presser, T. S., and Barnes, I., 1986, Selected soda springs of Colorado and their origins: U.S.G.S. Water-Supply Paper 2310, p.45-52.

- Finlay, G. I., 1906, Colorado springs, A guide book describing the rock formations in the vicinity of Colorado Springs: Colorado Springs, The Out West Company, p. 28-32.
- Fish, L., 1988, The real story of how Cave of the Winds Formed: Rocky Mountain Caving, v. 5, no. 2, p. 16-19.
- Forster, J. R., 1977, Middle Ordovician subaerial exposure and deep weathering of the Lower Ordovician Manitou Formation along the Ute Pass Fault zone: Geological Society of America Abstracts with Programs, v. 9, p. 722.
- Frank, R. M., 1965, Petrologic study of sediments from selected Central Texas caves, [M.A. thesis]: University of Texas, 117 p.
- Fremont, J. C., 1845, Report of the exploring expedition to the Rocky Mountains in the year 1842, and to Oregon and North California in the years 1843-1844: Washington, Gales and Seaton, p. 115-118.
- George, R. D. and others, 1920, Mineral waters of Colorado: Colorado Geological Survey Bulletin, v. 11, p 105-106, 219-222, 353-367.
- Goodfriend, G. A., 1987, Evaluation of amino-acid racemization/epimerization dating using radiocarbon-dated fossil land snails: Geology, v. 15, p. 698-700.
- Hailwood, E. A., 1989, The role of magnetostratigraphy in the development of geological time scales; Paleoceanography, v. 4, no. 1, p. 1-18.
- Hamil, M. M., 1965, Breccias of the Manitou Springs area, Colorado [M.S. thesis]: Louisiana State University, 43 p.
- Harland, W. B., and others, 1982, A geologic time scale: Cambridge, Great Britain, Cambridge University Press, p. 66.
- Hawley, C. C., and Wobus, R. A., 1977, General geology and petrology of the Precambrian crystalline rocks, Park and Jefferson Counties, Colorado: Geological Survey Professional Paper 608-B, 77 p.
- Hayden, F. V., 1869, Preliminary field report of the United States Geological Survey of Colorado and New Mexico: Washington, Government Printing Office, p. 45-46, 118-120.
- Hayden, F. V., 1872, Preliminary report of the United States Geological Survey of Montana and portions of adjacent territories: Washington, Government Printing Office, p. 159-161.
- Hayden, F. V., 1873, Sixth Annual Report of the United State Geological Survey of the Territories: Washington, Government Printing Office, p. 102-103.
- Hayden, F. V., 1874, Seventh Annual Report of the United States Geological and Geographical Survey of the Territories: Washington, Government Printing Office, p. 205-206.

- Hem, J. D., 1992, Study and interpretation of the chemical characteristics of natural water: United States Geological Survey Water-Supply Paper, No. 2254.
- Henley, R. W., Truesdell, A. H., Barton, P. B, and Whitney, J. A., 1984, Fluid-mineral equilibria in hydrothermal systems; Reviews In Economic Geology, Society Of Economic Geologists, v. 1, p. 33.
- Hose, L. D., and Esch, C. J., 1992, Paleo-cavity fills formed by upward injection of clastic sediments to lithostatic load: exposures in Cave of the Winds, Colorado [abs.]: National Speleological Society Convention Program, Salem, Indiana, p.50
- Hovey, H. C., 1881, Pickett's Cave; Scientific American, April 23, 1881, p. 257.
- Hovey, H. C., 1887, Caverns near Manitou, Colorado: Scientific American Supplement, no. 608, p. 9710-9711.
- Hurlbut, C. S., and Klein, C., 1977, Manual of mineralogy (after James D. Dana) 19th edition, John Wiley & Sons, New York,
- Izett, G. A., Obradovich, J. D., and Mehnert, H.H., 1989, The Bishop Ash Bed (Middle Pleistocene) and some older (Pliocene and Pleistocene) chemically and mineralogically similar ash beds in California, Nevada, and Utah: U. S. Geological Survey Bulletin, 1675, 37 p.
- Jackson, M. L., 1973, Soil chemical analysis-advanced course: Published by the Author, Soil Science Department University of Wisconsin, Madison.
- James, E., 1823, Account of an Expedition from Pittsburgh to the Rocky Mountains, *in* Thwaites, R. G., ed., 1905, Early Western Travels 1748-1846: Cleveland, Ohio, The Arthur H. Clark Company, v. 16, p. 11-13.
- Kawashima, M., Takamatsu, T., and Koyama, M, 1988, Mechanisms of precipitation of manganese(II) in Lake Biwa, a fresh water lake: Water Resources, v. 22, no. 5, pp. 613-618.
- Krauskopf, K. B., 1967, Introduction to geochemistry: McGraw-Hill, New York, p. 266-268.
- Leet, L. D., Judson, S., and Kauffman, M. E., 1982, Physical geology, Prentice-Hall, Inc., Englewood Cliffs, N.J. p. 52.
- Luna, R. L., 1971, Forgotten Springs of Manitou: Colorado Springs, Juel Arneson Printing Co., 25 p.
- Machette, M. M., 1975, The Quaternary geology of the Lafayette Quadrangle, Colorado, [M. S. thesis]: Boulder, University of Colorado, 83 p.
- Mankinen, E. A., and Dalrymple, G. B., 1979, Revised geomagnetic polarity time scale for the interval 0-5 m. y. B. P.; Journal of Geophysical Research, v. 84, no. B2, p. 615-626.

- Maslyn, M., and Blomquist, P. K., 1985, Hydrogeology of the mineral springs at Manitou Springs, Colorado [abs.]: Geological Society of America 98th Annual Convention, GSA Abstracts with program, v. 17, # 7, p. 654.
- Milske, J. A., 1982, Stratigraphy and petrology of clastic sediments in Mystery Cave, Fillmore County, Minnesota [M. S. thesis]: University of Minnesota, 111 p.
- Miller, G. H., and Brigham-Grette, J., 1989, Amino acid geochronology: Resolution and precision in carbonate fossils *in* INQUA Quat. Dating Methods, Rutter and Brigham-Grette Eds. Pergamon Press.
- Mitterer, R. M., and Kriausakul, N., 1989, Calculation of amino acid racemization ages based on apparent parabolic kinetics: Quaternary Science Reviews, v. 8, 353-357.
- Modreski, P. J., 1987, Mineralogy of Cave of the Winds, Manitou Springs, Colorado: Geological Society of America Abstracts with Programs, v. 19, no. 5, p. 322.
- Moore, D. M., and Reynolds, R. C., 1989, X-ray diffraction and the identification and analysis of clay minerals: New York, Oxford University Press, 332 p.
- Morgan, G. B., 1950, Geology of Williams Canyon area, north of Manitou Springs, El Paso County, Colorado (Masters thesis): Golden, Colorado School of Mines, 80 p.
- Mutschler, F. E., Larson, E. E., and Bruce, R. M., 1987, Laramide and younger magmatism in Colorado—New petrologic and tectonic variations on old themes: Colorado School of Mines Quarterly, v. 82, no. 4, p. 1-47.
- Netoff, D. I., 1977, Soil clay mineralogy of Quaternary deposits in two Front Range-Piedmont transects, Colorado [Ph. D. thesis]: Boulder, University of Colorado, 169 p.
- Osterkamp, W. R. and others, 1987, Great Plains, *in* Graf, W.L., ed., Geomorphic systems of North America: Boulder, Colorado, Geological Society of America, Centennial Special Volume 2.
- Parkhurst, D. L., 1995, User's guide to Phreeqc—A computer program for speciation, reaction-path, advective-transport, and inverse geochemical Calculations: U. S. Geological Survey, Water-Resources Investigations Report 95-4227.
- Peale, A. C., 1886, Lists and analyses of the mineral springs of the United States: U. S. Geological Survey Bulletin no. 32, p. 188, 189, 192.
- Peck, S. B., 1986, Bacterial deposition of iron and manganese oxides in North American caves: National Speleological Society Bulletin, v.48, no. 1, p.26-30.

- Peck, J. A., King, J. W., Colman, S. M., and Kravchinsky, V. A., 1994, A rock-magnetic record from Lake Baikal, Siberia: Evidence for Late Quaternary climate change: *Earth and Planetary Science Letters*, v. 122, p. 221-238.
- Perrodon, A., 1983, Dynamics of oil and gas accumulations: *Bulletin des Centres de Recherches Exploration-Production Elf-Aquitaine*, Men. 5, p. 57
- Rabenhorst, M. C., and Wilding, L. P., 1984, Rapid method to obtain carbonate free residues from limestone and petrocalcic materials: *Soil Science Society of America Journal*, v. 48, p. 216-219.
- Randolph, J. A., 1875, Scenes in Colorado-Manitou Springs and Vicinity: *Harper's Weekly*, October 2, 1875, p. 797-798.
- Reams, M. W., 1968, Cave Sediments and the geomorphic history of the Ozarks, [Ph. D. thesis]: Saint Louis, Missouri, Washington University, 167 p.
- Rhinehart, R., 1996, Manitou Cave *in* The caves and karst of Colorado, guidebook for the 1996 convention of the National Speleological Society, Edited by Rob Kolstad, 214 p.
- Sawyer, D. A. and others, 1995, New chemical criteria for Quaternary Yellowstone tephra layers in central and western North America: *Geological Society of America Abstracts with Programs*, v. 27, n. 6, p. 109.
- Schlundt, H., 1914, The radioactivity of some Colorado springs: *The Journal of Physical Chemistry*, v. 18, no. 7, p. 662-666.
- Scott, G. R., 1963, Nussbaum Alluvium of Pleistocene(?) age at Pueblo, Colorado. U. S. Geological Survey Professional Paper, 475-C, p. C49-C52
- Scott, G. R., 1975, Cenozoic surfaces and deposits *in* Curtis, B. F., ed., *Cenozoic History of the Southern Rocky Mountains*: Geological Society of America Memoir 144, p. 227-248.
- Shackleton, N. J., Berger, A., and W. R. Peltier, 1990, An alternative astronomical calibration of the lower Pleistocene time scale based on ODP Site 677: *Transactions of the Royal Society of Edinburgh: Earth Sciences*, v.81, p.251-261.
- Shedd, J. C., 1912, Radioactivity of the Mineral Springs of Manitou, Colorado: *The Proceedings of the Colorado Scientific Society*, v. 10, p. 233-263.
- Singer, A., 1978, Clay minerals in sediments as paleoclimatic indicators [abs.]: *Abstracts of lectures presented at the Tenth International Congress On Sedimentology*, Jerusalem, v. 2, p. 614.
- Snider, G. W., 1916, How I found the Cave of the Winds: Denver, Colorado, Carson-Harper.

- Soister, P. E., 1967, Relation of Nussbaum Alluvium (Pleistocene) to the Ogallala Formation (Pliocene) and to the Platte-Arkansas divide, Southern Denver Basin, Colorado. U. S. Geological Survey Professional Paper 575-D, p.D39-D46.
- Solly, S. E., 1875, Manitou, Colorado, U. S. A., Its mineral water and climate: Saint Louis, Jno. McKittrick and Co.
- Strieby, W., 1893, The origin and use of the natural gas at Manitou, Colorado: Colorado College Studies, v. 4, p. 14-36.
- Szabo, B. J., 1980, Results and assessment of uranium-series dating of vertebrate fossils from Quaternary alluviums in Colorado: Arctic and Alpine Research, v. 12, p. 95-100.
- Tarling, D. H., 1983, Palaeomagnetism; principles and applications in geology, geophysics and archaeology: Chapman and Hall Ltd., London, 379 p.
- Trimble, D. E., and Machette, M. M., 1979, Geologic map of the Colorado Springs-Castle Rock Area, Front Range Urban Corridor, Colorado; U. S. Geological Survey, 1:100,000, Map I-857-F
- Tweto, O., 1975, Laramide (Late Cretaceous-Early Tertiary) Orogeny in the Southern Rocky Mountains *in* Curtis, B.F., ed., Cenozoic History of the Southern Rocky Mountains: Geological Society of America Memoir 144, p. 1-44.
- Verosub, K. L., 1977, Depositional and post-depositional processes in the magnetization of sediments: Reviews of Geophysics and Space Physics, v. 15, p. 129-143.
- Warwick, G. T., 1953, Cave formations and deposits, *in* Cullingford, C. H. D., ed., British Caving; an introduction to speleology: London, Routledge & Kegan Paul Limited, p. 77.
- Wheeler, G. M., 1875, Report upon Geographical and Geological Explorations and Surveys West of the One Hundredth Meridian, v. 3, Geology: Washington, Government Printing Office, p. 486-487, 618-619.
- White, W. B., 1988, Geomorphology and hydrology of karst terrains: New York, Oxford University Press, New, 464 p.

APPENDIX

Location And Description Of Springs And Other Sampling Sites

Below is a detailed description of the springs and their exact locations (See **Figure 2** for general locations). When the initial samples were collected the Seven Minute Spring was actually two springs: the eastern spring was next to the road and the other one was ~15 meters to the west. The western spring issued from alluvium into the bottom of a broken cement basin (~80 cm diameter by ~30 cm high). The eastern spring issued from the bottom of a small, natural basin (~20 cm diameter by 10 cm deep) on top of a poorly developed travertine mound. Both of the springs were sampled near their centers where CO₂ was bubbling up, ensuring that the water was not contaminated by air. Since the first sampling, the springs were plugged and a new deeper well was drilled. Partial chemical analysis of the new spring (well) indicates that it is very similar to the old springs.

The Shoshone Spring issues inside of a small circular building. It then drains to the north through an underground plastic pipe into a small basin located on a retaining wall of the parking lot of the General Motors Test Garage parking lot. The Shoshone Spring was sampled at the basin in the parking lot.

The Navajo Spring is located under a small shop on Manitou Avenue and is no longer visible. The spring is piped to a small fountain from which the spring now flows. During the winter the fountain is shut off and the water is diverted into Fountain Creek. The spring drains from a plastic pipe onto a large travertine mound that is located under a bridge. The spring was sampled from the pipe under the bridge.

The Cheyenne Spring is inside of a building similar to the Shoshone. Water and CO₂ issues from the bottom of a circular cement pool. In the center of the pool is a 1.5-m diameter by 2-m high inverted copper cone, which was used to collect CO₂ for bottling. The water then drains to the north through an underground plastic pipe into Fountain Creek. The spring was sampled from the pool inside of the building.

The Manitou Spa building covers the Manitou Soda Spring, which is piped to a fountain inside of the building. Water and CO₂ issue from a plastic pipe on top of a travertine-covered fountain. The spring was sampled from the plastic pipe.

The Wheeler Spring, a drilled spring, is just south of the post office. It issues from piping that is a combination of brass and iron into a ceramic wall-mounted basin that faces Park Avenue. The spring is not a large spring and has been known to run dry in the fall and winter. The spring was sampled directly from the pipe.

The Stratton Spring, a drilled spring, is located in a building about 30 m southeast of the fountain from which it issues. The fountain is on the corner of Ruxton Avenue and Manitou Avenue. The water flows from a pipe (stainless steel or chrome-plated brass?) into a basin, which has a noticeable iron stain. The flow is spasmodic alternating between water and large emissions of CO₂. During the winter the flow is diverted into a nearby storm sewer. The spring was sampled from the pipe.

The Big Indian Spring is 100 m southwest of the cog railway bridge. The spring consists of a group of springs. The main flow issues from a steel standpipe (~25 cm diameter by ~80 cm high) in Ruxton Creek with lesser flows from a large seep next to the pipe and from several nearby small seeps. The water was taken from the large seep to prevent possible iron

contamination from the steel pipe. The standpipe is lined with and the seeps coated with thick iron-oxide deposits.

Ruxton Creek was sampled 5 m upstream from the Big Indian Spring to exclude possible contamination from seeps associated with the spring.

The Ouray Spring is across the creek from the steam engine that is on display in the lower, cog railway parking lot. The spring is under a sealed cement cistern on the east bank of Ruxton Creek. The water flows from a very corroded iron pipe into the creek. Several hundred kilograms of gravel, rocks and debris had to be removed so that the spring could be sampled. The spring was sampled from the pipe. This spring also has associated thick iron-oxide deposits.

The Iron Geyser, a drilled spring, issues from a plastic pipe into a cement and stone fountain, which is under a small pavilion next to Ruxton Avenue. The wetted portions of this fountain are covered with thick iron-oxide deposits. The water sample was collected from a plastic overflow pipe, which is located in the basin about one meter from the spring outlet.

The Twin Springs are two drilled wells that are piped together into one. The spring issues from a galvanized iron pipe into a basin on the front of a building on Ruxton Avenue. The spring was sampled from the galvanized pipe.

The Ute Chief Gusher, a drilled spring, is located on the west side of Manitou Avenue and piped to the east side of the street. The Gusher drains from a 10-cm diameter plastic pipe into Fountain Creek. This spring was sampled from the plastic pipe.

The Ute Chief Spring is on the east side of the street and issues from a copper pipe, which is hidden inside of a jug that is a part of a large Indian

statue. The copper pipe is free of any scale or mineral build up and appears to be dissolving. This spring was sampled from the copper pipe.

The Ute Chief Magnetic Spring is located in a small room under the bottling plant. The spring issues into the bottom of a stainless steel basin that is about 1 m in diameter. A cement basin surrounds the steel basin. This spring emits about 1 m³ of CO₂ every 90 minutes in a very impressive geyser-like eruption. The spring was sampled from the stainless steel basin.

The Creighton Spring is located between two wings of the Shady Del Motel. The spring issues from a cast iron pipe into a cement basin. The spring water is actively corroding iron, steel, and cement.

Fountain Creek was sampled 50 m upstream from the Ute Chief Spring. The creek was turbid and was high because of recent snow and rainfall.

The Williams Canyon upstream sample was collected 30 meters north of the hairpin turn. It had snowed the night before and there was a little snow on the ground. A small leaf-free pool was used for sampling because most of the stream was full of dead leaves.

The Blue Ice Spring is located about 150 m downstream from the hairpin turn. The water issues from a small sediment filled grotto located in red sandstone (Sawatch Formation) on the west wall of the canyon. The water drips over a series of small sandstone ledges and disappears into sediment next to the road. The drips were used for sampling. This spring is called the Blue Ice Spring, because in the winter the water from the spring freezes into a large, light blue mass of ice.

The Williams Canyon downstream sample was taken 10 m south of the Narrows. The sample was taken from a small leaf-free pool 2 m

downstream from a galvanized steel culvert. There was a light rain the night before and conditions were very similar to the week before when the upper stream was sampled. Similar to the upstream sample, the stream at this location also had a large amount of dead leaves in the water.

The entrance to Hucacove Cave is 100 meters above and east of the Narrows. The water was collected from three different pools along a stream at the north end of a large room called God's Country, which is several hundred meters north of the entrance. The water was combined into one sample because of the low volume of the pools. The remote location precluded Eh, DOX, and DCO₂ tests.

The Cave of the Winds water supply are two springs covered by small buildings located on the west side of Cavern Gulch. The upper spring consists of many smaller springs, which run into a trench, then into a plastic collection pipe. The trench was used for sampling. The springs issue from granite. The waterways of this spring contained gelatinous iron oxide coatings up to 1 cm thick.

Two other springs were looked at: the Little Chief and Hiawatha. The Little Chief is supposed to be between Ruxton Creek and the train garage of the cog railway (Luna, 1971). In this area there are actually two springs. One issues from soil and was choked with dead leaves, iron-oxide scum and algae. The other issues from an iron pipe that drains into the creek. The soil spring was not sampled because of its thoroughly disgusting condition and low flow. The iron pipe also was not sampled because its conductivity was

only a bit higher than the creek water. The low conductivity combined with the layout of the cog railway yard suggested that the iron pipe drained surface runoff from the railway yard.

The Hiawatha Spring, which is located in two-meter-deep pit just south of the bottling plant, was only tested from conductivity. The conductivity was only a little greater than Fountain Creek, which is about 5 m west of the pit. The spring appears to be nothing more than ground water with a little mineral water mixed in. This spring was not sampled because of possible ground water dilution and because the spring was stagnant and very polluted with algae, trash, and other unidentifiable objects. Soon after inspecting the Hiawatha Spring a wooden platform was placed over the pit that contains the spring.

The Pikes Peak water sample was collected from a tunnel that was being bored into granite west of the Air Force Academy. This sample was collected 2.6 km inside a tunnel being bored for the J. A. McCullough Water Treatment Center, which is 13 km north of Manitou Springs. The tunnel, which trends due west, is in the Pikes Peak Granite and at the point where the sample was taken is overlain by ~500 m of the same granite. The sample was taken from water that was squirting from a fracture in the rock. This sample was used as an example of relatively young, near-surface groundwater that had only been in contact with Pikes Peak Granite.

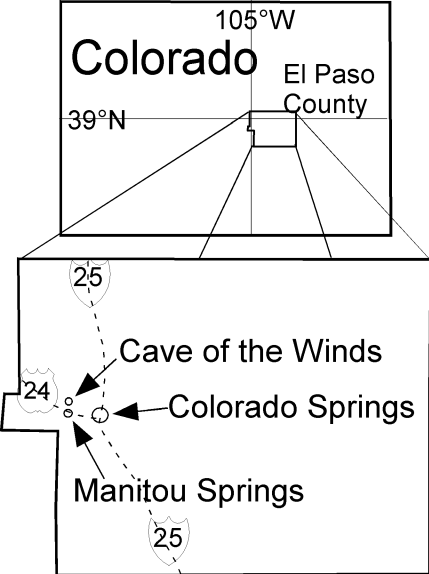


Figure 1. Location map of study area

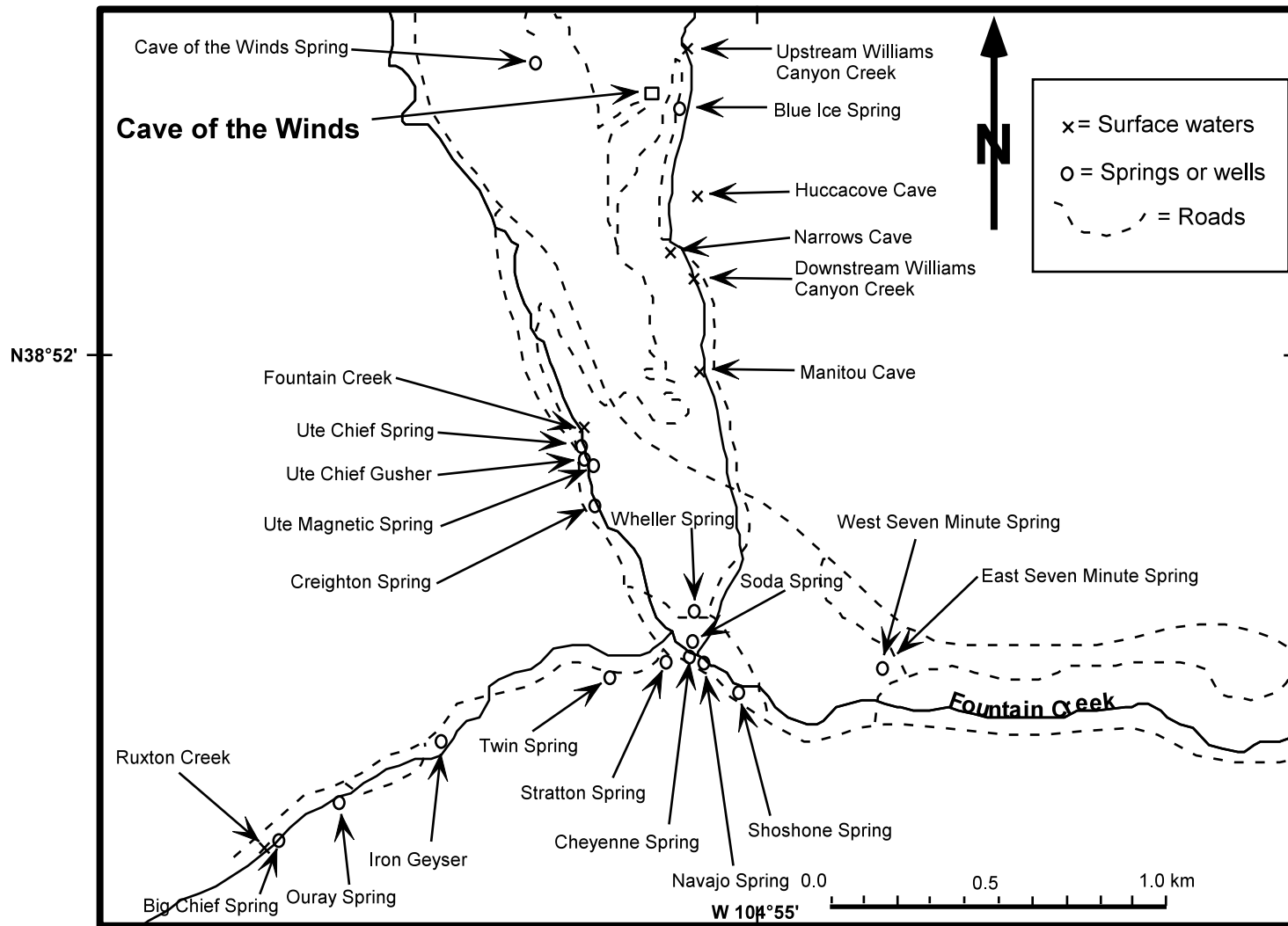


Figure 2. Location map of springs, wells, streams, and other sampling sites.

Table 1. Analytical
uncertainty of selected ions
in water samples

	% error (+/-)
Fluoride (F)	8
Chloride (Cl)	5
Bromide (Br)	10
Nitrate (NO ₃)	8
Sulfate (SO ₄)	4
Phosphate (PO ₄)	20
Boron (B)	10
Iron (Fe total)	5
Manganese (Mn)	5
Lithium (Li)	9
Sodium (Na)	6
Potassium (K)	6
Magnesium (Mg)	6
Calcium (Ca)	10
SiO ₂	5

Plate 1. Geology map of immediate vicinity of Cave of the Winds and Manitou Springs.

By Fred Luiszer, 1996 (Adapted from Luiz Bianchi, 1967)

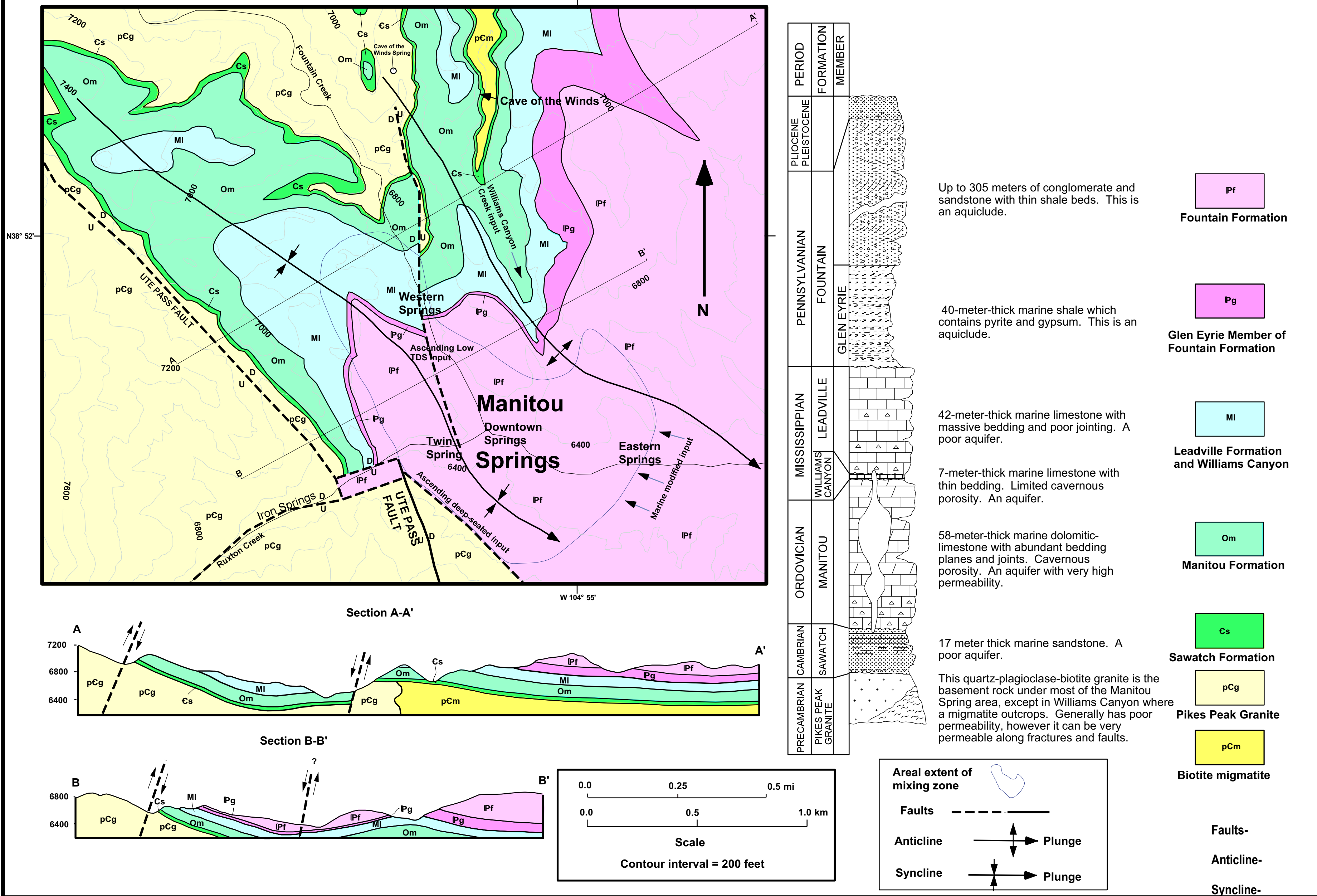


Plate 2. Map Of Cave Of The Winds, Manitou Springs, Colorado showing locations of samplings sites.

Modified from Paul Burger, 1996

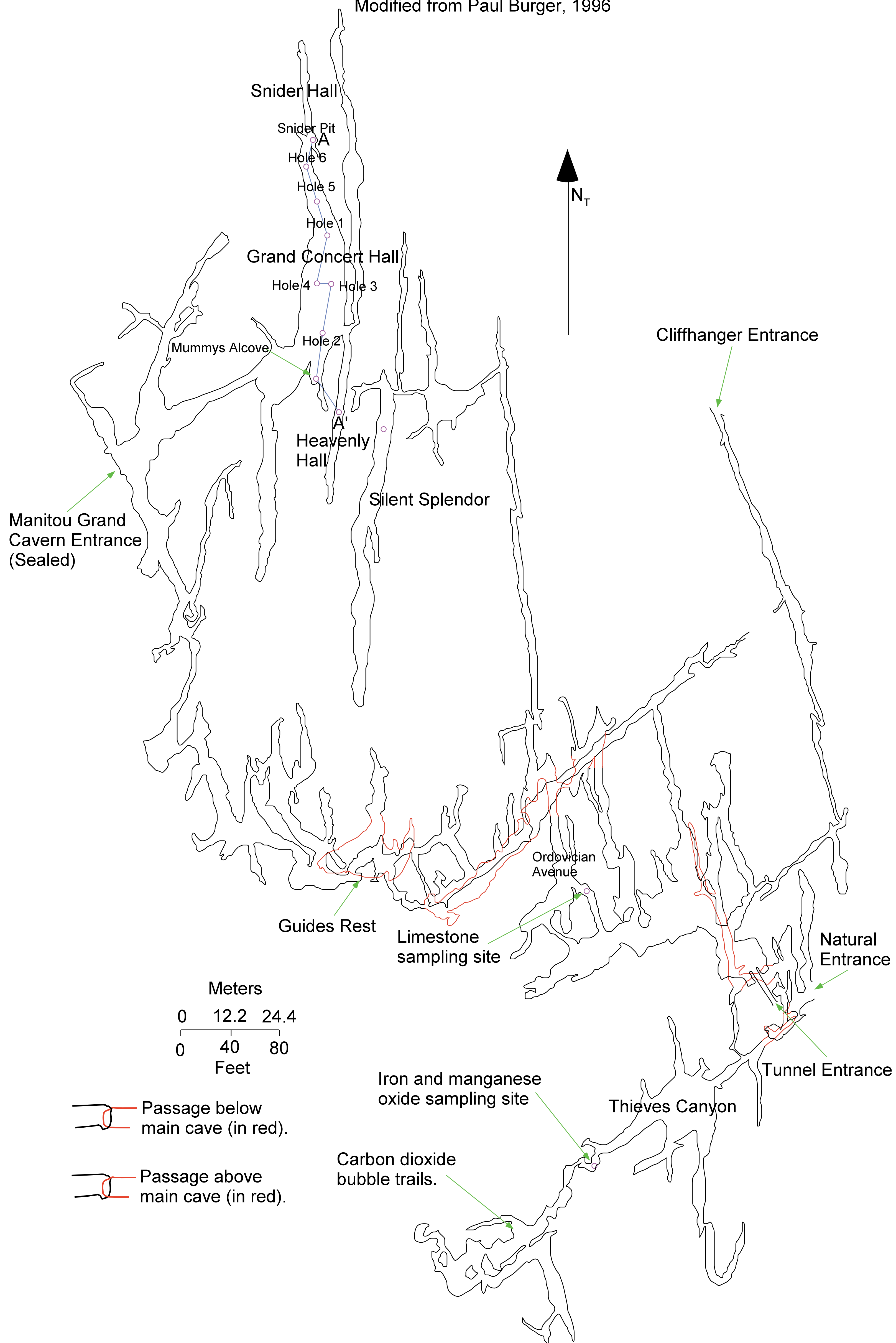
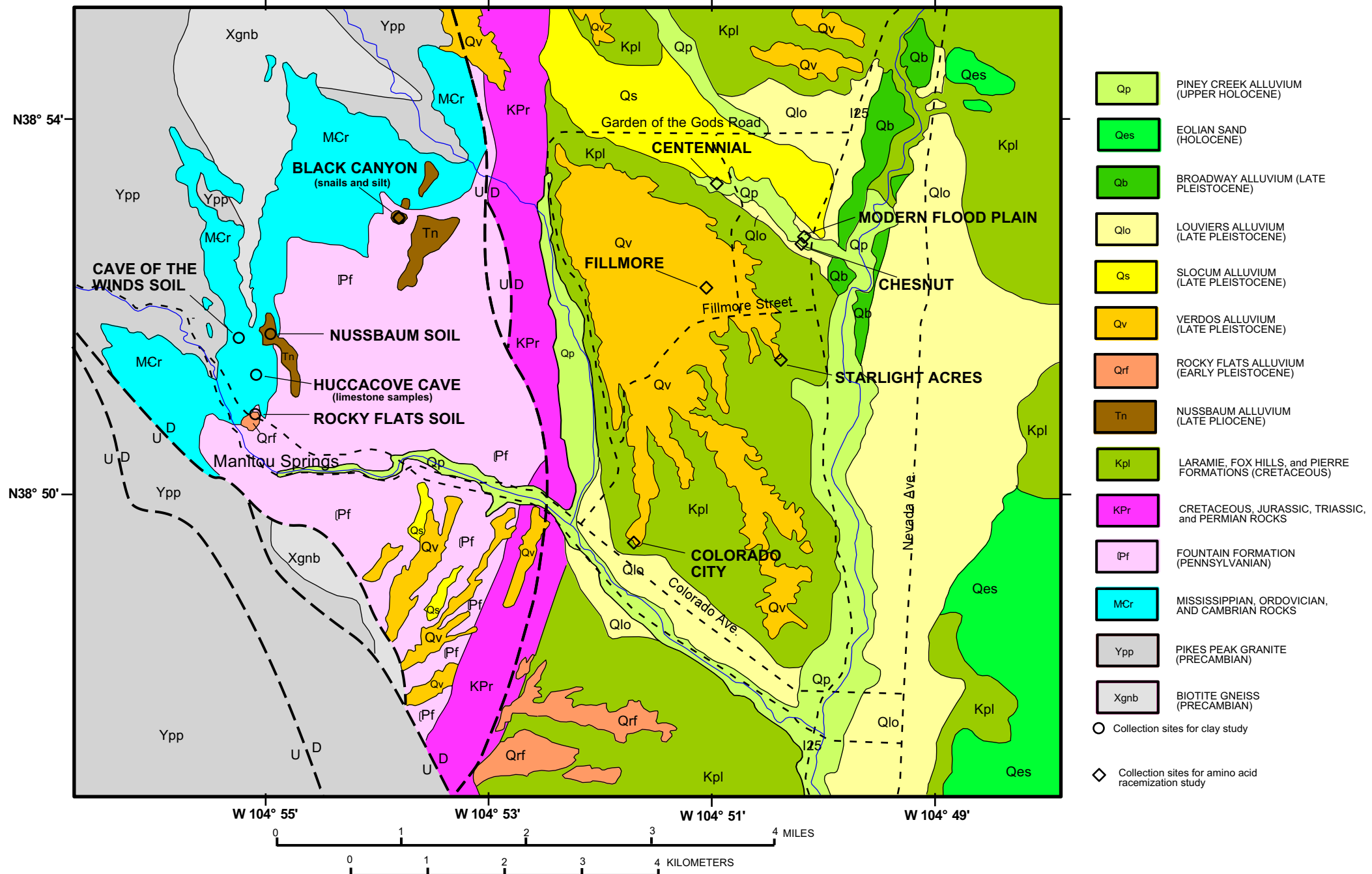


PLATE 3. GEOLOGY MAP OF COLORADO SPRINGS AND MANITOU SPRINGS AREA

with locations of snail and clay study collection sites.
Geology adapted from Trimble and Machette, (1979).



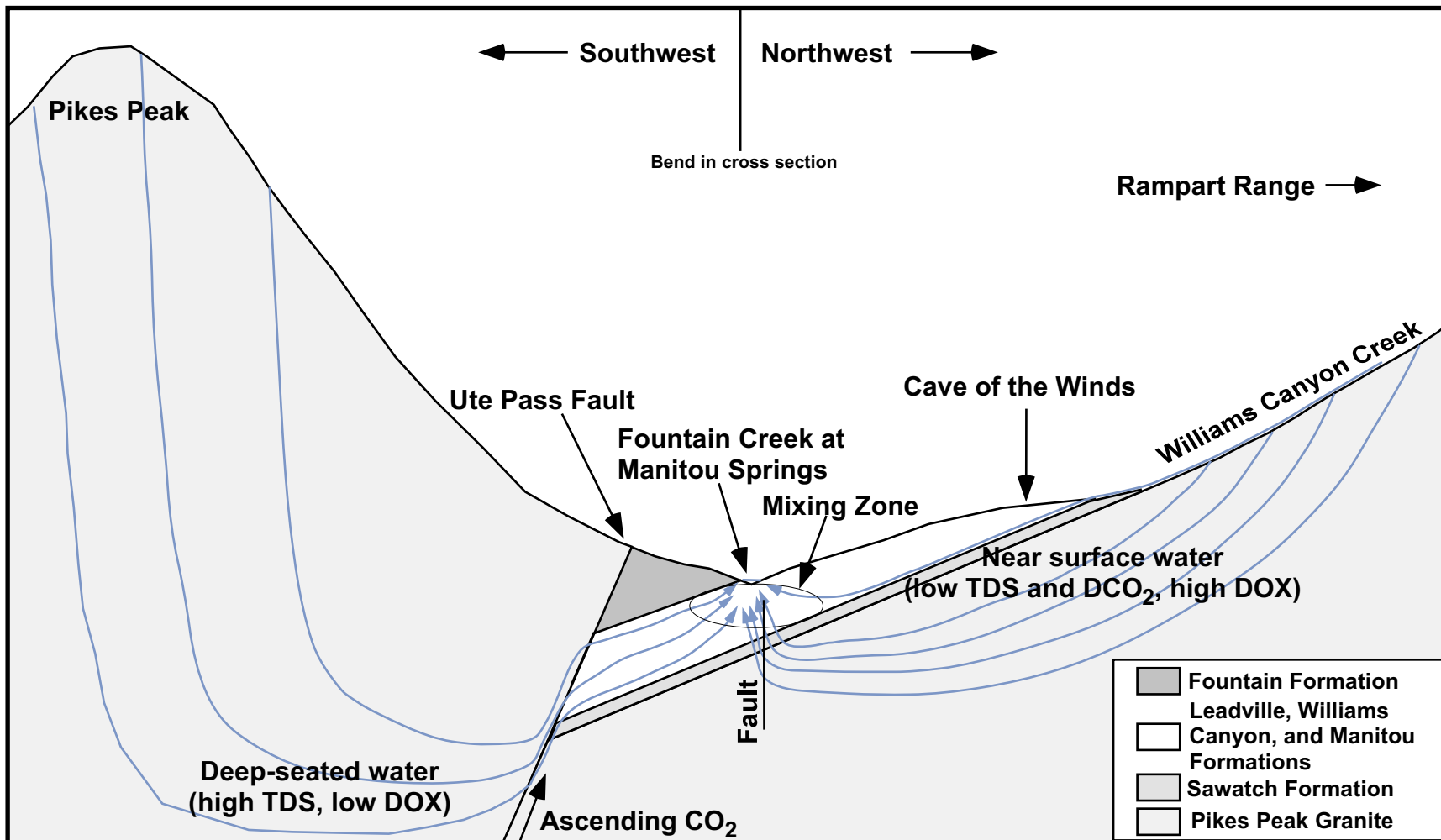


Figure 3. Schematic cross section showing conceptual model of the Manitou Springs system.

LEGEND

- | | |
|---------------------------|----------------------------------|
| Downtown Springs ○ | Miscellaneous |
| Shoshone | COW (Cave of the Winds Spring) △ |
| Cheyenne | Williams Canyon Creek □ |
| Soda | US (Upstream) |
| Navajo | BIS (Blue Ice Spring) |
| Wheeler | DS (Downstream) |
| Stratton | |
| Eastern Springs ■ | Iron Springs ▲ |
| 7-minute East | Iron Geyser |
| 7-minute West | Ouray |
| Western Springs ◇ | Chief |
| Ute Magnetic | |
| Twin | |
| Ute Chief | |
| Gusher | |
| Creighton | |

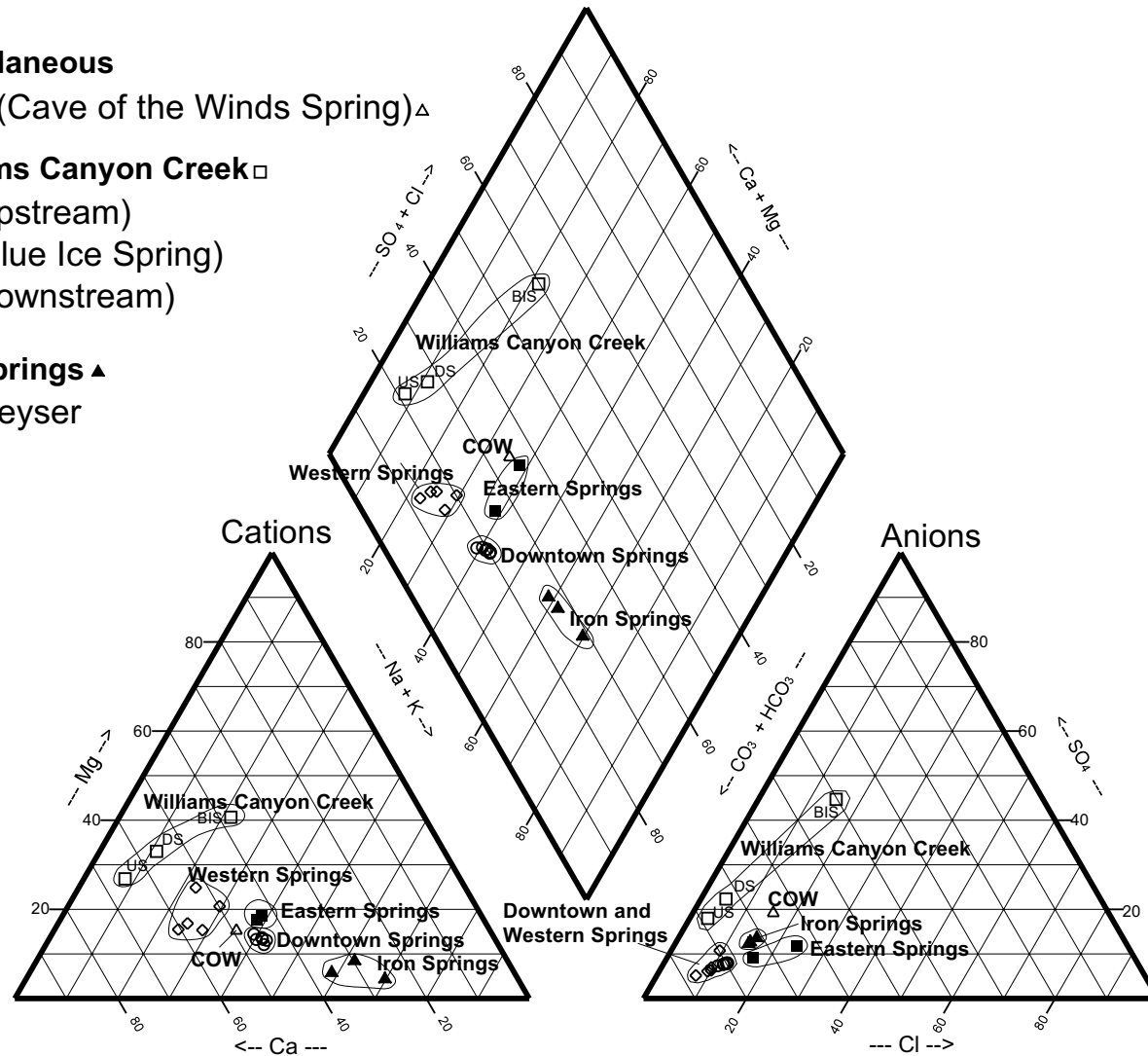


Figure 4. Piper diagram of selected springs and streams.

Table 2. Isotopic Data

	$^{87}\text{Sr}/^{86}\text{Sr}$	$\delta^{13}\text{C}$ PDB	$\delta^{18}\text{O}$ PDB
UTE MAGNETIC*	0.7196	-5.05	-9.12
CHEYENNE*	0.7210	-4.64	-10.53
7 MIN. EAST (WEST*)	0.7211	-4.39	-8.96
IRON GEYSER*	0.7229	-4.03	-8.94
MANITOU LIMESTONE	0.7099	-2.29	-6.06
PIKES PEAK H ₂ O	0.7132		
PIKES PEAK GRANITE			
WHOLE ROCK	0.8769		
PLAGIOCLASE	0.7189		
K-FELDSPAR	0.8767		
BIOTITE	11.3660		

Pikes Peak Granite data from Dan Unruh, U.S.G.S.

* = $\delta^{13}\text{C}$ and $\delta^{18}\text{O}$ of CO₂ gas

Table 3. Water Data *

	Downtown Springs						
	Shoshone	Cheyenne	Soda	Navajo	Wheeler	Stratton	Twin
Bicarbonate (HCO ₃)	2681	2562	2495	2508	2439	2236	1581
Fluoride (F)	7.7	7.0	6.8	6.6	6.3	5.5	3.9
Chloride (Cl)	242	229	220	211	208	171	80
Bromide (Br)	1.03	0.92	1.10	0.88	0.88	0.78	0.36
Nitrate (NO ₃)	0.08	0.90	0.53	0.62	0.86	0.98	1.00
Sulfate (SO ₄)	212	197	196	187	185	158	73
Nitrite (NO ₂)	N.D.	N.D.	N.D.	N.D.	N.D.	N.D.	N.D.
Phosphate (PO ₄)	N.D.	N.D.	N.D.	N.D.	N.D.	N.D.	N.D.
Boron (B)	1.0	0.8	0.9	0.9	1.4	0.7	2.0
Iron (Fe total)	0.04	0.05	0.23	0.02	0.10	1.07	0.08
Manganese (Mn)	3.80	2.50	2.40	2.80	2.70	0.44	0.22
Lithium (Li)	0.76	0.88	0.66	0.71	0.65	0.56	0.23
Sodium (Na)	491	529	459	475	451	345	147
Potassium (K)	75	79	68	71	65	50	20
Magnesium (Mg)	81	94	85	90	86	73	92
Calcium (Ca)	501	527	474	519	467	385	319
Lead (Pb)	0.015	<.001	<.01	N.M.	N.M.	N.M.	N.M.
Arsenic (As)	0.006	0.021	0.005	N.M.	N.M.	N.M.	N.M.
TDS	4297	4230	4010	4073	3914	3428	2320
Cond. (mS/cm)	4.38	4.00	4.29	4.16	4.12	3.50	2.49
Temp. °C	14.0	14.2	15.3	15.3	15.1	11.5	10.8
pH	6.50	6.18	6.32	6.30	6.35	6.20	6.19
Eh (volts)	0.543	0.515	0.481	0.503	0.513	0.443	0.566
DOX	0.50	0.20	N.D.	0.30	0.20	0.10	0.10
DCO ₂ -gr/l	2.20	2.38	2.43	N.M.	2.13	3.93	2.50
SiO ₂	51	47	48	47	44	37	18
Total alk.	2198	2100	2045	2056	1999	1833	1296
Sample Date	4/15/87	4/2/87	4/2/87	4/15/87	4/15/87	4/22/87	4/15/87
Flow l/min	1.5	1.4	2.0	8.6	2.4	2.0	6.7
Type	Spring	Spring	Spring	Spring	Well	Well	Well

	Eastern Springs		Iron Springs		
	7 min. East	7 min. West	Iron Geyser	Ouray	Chief
Bicarbonate (HCO ₃)	2538	2373	1726	1601	1345
Fluoride (F)	4.8	4.8	6.6	6.2	6.5
Chloride (Cl)	547	310	195	184	167
Bromide (Br)	2.10	1.30	0.96	0.80	0.85
Nitrate (NO ₃)	1.14	2.90	0.14	0.10	0.13
Sulfate (SO ₄)	366	231	227	219	202
Nitrite (NO ₂)	N.D.	N.D.	N.D.	N.D.	N.D.
Phosphate (PO ₄)	N.D.	N.D.	N.D.	N.D.	N.D.
Boron (B)	2.1	1.9	1.0	1.1	1.1
Iron (Fe total)	0.08	0.05	11.40	23.20	7.20
Manganese (Mn)	1.60	1.10	1.20	1.30	0.54
Lithium (Li)	0.77	0.81	0.98	1.11	0.85
Sodium (Na)	531	503	618	549	558
Potassium (K)	42	53	94	80	82
Magnesium (Mg)	135	136	35	43	20
Calcium (Ca)	559	516	355	250	196
Lead (Pb)	0.006	0.006	0.006	0.015	0.005
Arsenic (As)	0.022	0.022	0.122	0.114	0.019
TDS	4729	4135	3272	2961	2587
Cond. (mS/cm)	5.42	4.40	3.61	3.35	3.01
Temp. °C	11.6	11.1	7.8	9.2	9.8
pH	6.44	6.53	6.27	5.97	6.20
Eh (volts)	0.520	0.532	0.317	0.294	0.337
DOX	3.40	3.30	0.30	0.20	0.40
DCO ₂ -gr/l	2.68	1.77	2.82	3.02	2.67
SiO ₂	18	24	82	78	78
Total alk.	2080	1945	1415	1313	1103
Sample Date	4/2/87	4/2/87	4/6/87	4/6/87	4/6/87
Flow l/min	0.3	0.5	0.3	3.0	0.5
Type	Well	Well	Well	Spring	Well

	Western Springs				Creeks	
	Magnetic	Ute Chief	Gusher	Creighton	Fountain	Ruxton
Bicarbonate (HCO ₃)	2237	1362	1281	1004	104	60
Fluoride (F)	5.0	4.0	4.0	3.9	2.1	4.0
Chloride (Cl)	155	88	87	69	16	3.1
Bromide (Br)	0.70	0.38	0.39	0.27	0.06	0.02
Nitrate (NO ₃)	2.40	2.69	6.17	1.45	3.60	1.25
Sulfate (SO ₄)	132	77	84	106	11	8.6
Nitrite (NO ₂)	N.D.	N.D.	N.D.	N.D.	N.D.	N.D.
Phosphate (PO ₄)	N.D.	N.D.	N.D.	N.D.	N.D.	N.D.
Boron (B)	0.8	1.0	1.0	N.M.	0.4	0.3
Iron (Fe total)	0.08	0.04	0.05	0.02	0.10	0.04
Manganese (Mn)	0.32	0.12	0.13	0.08	0.03	0.01
Lithium (Li)	0.42	0.24	0.24	0.16	0.01	0.02
Sodium (Na)	295	146	136	118	18	10
Potassium (K)	38	22	19	15	1.6	1.9
Magnesium (Mg)	89	54	52	47	6.6	3.4
Calcium (Ca)	535	349	296	187	41	18
Lead (Pb)	N.M.	<.01	<.001	<.001	N.M.	N.M.
Arsenic (As)	N.M.	<.001	0.023	N.M.	N.M.	N.M.
TDS	3490	2107	1967	1550	205	111
Cond. (mS/cm)	3.58	2.25	2.08	1.68	0.28	0.16
Temp. °C	11.7	11.2	12.4	11.1	7.0	4.8
pH	6.29	6.12	6.13	5.97	8.54	7.10
Eh (volts)	0.542	0.553	0.559	0.571	0.506	0.583
DOX	0.10	0.35	1.20	2.00	9.50	8.25
DCO ₂ -gr/l	N.M.	2.83	2.56	1.30	N.M.	N.M.
SiO ₂	22	20	21	18	13	18
Total alk.	1834	1117	1050	823	85	49
Sample Date	4/27/87	4/22/87	4/22/87	9/17/87	4/22/87	4/6/87
Flow l/min	1.0	6.7	40	270	30000	100
Type	Well	Spring	Well	Well	Creek	Creek

	Williams Canyon Creek			Huccacove	Pikes	Cave of
	Up Stream	Blue Ice Spring	Down Stream	Cave	Peak Granite	the Winds Spring
Bicarbonate (HCO ₃)	233	269	232	188	198	225
Fluoride (F)	1.5	2.0	1.5	1.0	4.6	3.6
Chloride (Cl)	5.9	103	8.9	8.6	2.6	31
Bromide (Br)	0.03	0.61	0.05	0.14	0.05	0.18
Nitrate (NO ₃)	0.14	315.0	15.80	26.20	0.05	0.41
Sulfate (SO ₄)	42	413	56	126	21	52
Nitrite (NO ₂)	N.D.	N.D.	N.D.	0.01	N.D.	N.D.
Phosphate (PO ₄)	N.D.	N.D.	0.04	0.31	N.D.	N.D.
Boron (B)	0.1	1.6	0.2	0.6	N.M.	N.D.
Iron (Fe total)	0.02	0.02	0.01	0.03	0.27	0.09
Manganese (Mn)	0.02	0.06	0.03	0.03	0.04	0.07
Lithium (Li)	0.01	0.05	0.02	0.01	0.04	0.06
Sodium (Na)	9.0	106	14	5.5	34	39
Potassium (K)	0.5	15	2.0	3.3	1.3	1.1
Magnesium (Mg)	17	114	24	43	3.4	9.1
Calcium (Ca)	68	174	67	47	25	48
Lead (Pb)	N.M.	N.M.	N.M.	N.M.	0.006	N.M.
Arsenic (As)	N.M.	N.M.	N.M.	N.M.	N.M.	N.M.
TDS	377	1511	422	451	290	410
Cond. (mS/cm)	0.46	1.92	0.54	0.60	0.31	0.61
Temp. °C	5.4	2.1	5.6	10.3	13.2	11.4
pH	8.05	8.59	8.25	8.43	7.33	7.64
Eh (volts)	0.496	0.491	0.495	N.M.	N.M.	0.501
DOX	7.5	10.0	9.0	N.M.	2.3	0.1
DCO ₂ -gr/l	N.M.	N.M.	N.M.	N.M.	N.M.	N.M.
SiO ₂	21	18	19	11	31	28
Total alk.	191	220	191	155	162	185
Sample Date	4/27/87	4/27/87	5/3/87	4/26/87	9/17/87	4/26/87
Flow l/min	40	0.2	40	0.2	>500	15
Type	Creek	Spring	Creek	Stream	Spring	Spring

Milliequivalents per liter error (%) 0.4 5.7 1.0 4.3 1.8 4.0 0.9

Milliequivalents per liter error (%) 1.3 6.7 12.9 8.4 9.9

Milliequivalents per liter error (%) 4.1 3.8 0.1 5.5 14.8

Milliequivalents per liter error (%) 2.3 4.4 3.6 1.6 0.4 9.3

* Concentrations in mg/L except where noted. N.D. = Not Detectable (<0.01 mg/L) N.M. = Not Measured

Saturation Index (SI)** undersaturated<0 equilibrium=0 saturated>0

Albite(low)	NaAlSi ₃ O ₈	-1.53	-2.72	-2.13	-2.18	-2.04	-2.98	-3.91	Albite(low)	NaAlSi ₃ O ₈	-2.51	-1.82	-1.84	-3.03	-2.18	Albite(low)	NaAlSi ₃ O ₈	-3.2	-4.11	-4.01	-4.95	-0.18	-2.08	Albite(low)	NaAlSi ₃ O ₈	-0.33	0.95	-0.08	-0.97	0.07	0.51
Annite (biotite)	KFe ₃ AlSi ₃ O ₁₀ (OH)	-5.16	-7.98	-4.40	-7.76	-5.24	-4.38	-8.76	Annite (biotite)	KFe ₃ AlSi ₃ O ₁₀ (OH)	-6.26	-5.54	-0.26	-2.11	-1.27	Annite (biotite)	KFe ₃ AlSi ₃ O ₁₀ (OH)	-7.5	-10.17	-9.56	-12.8	0.01	-2.52	Annite (biotite)	KFe ₃ AlSi ₃ O ₁₀ (OH)	-0.56	-1.47	-1.52	-0.92	3.43	2.83
Anorthite	CaAl ₂ Si ₂ O ₈	-10.01	-12.26	-10.95	-11.03	-10.62	-12.38	-12.38	Anorthite	CaAl ₂ Si ₂ O ₈	-10.44	-9.58	-12.41	-14.60	-12.95	Anorthite	CaAl ₂ Si ₂ O ₈	-11.64	-12.84	-12.64	-14.43	-3.65	-8.08	Anorthite	CaAl ₂ Si ₂ O ₈	-4.16	-4.30	-3.86	-3.55	-4.83	-3.82
Calcite	CaCO ₃	0.54	0.10	0.27	0.50	0.29	-0.05	0.02	Calcite	CaCO ₃	0.60	0.64	0.08	-0.36	-0.28	Calcite	CaCO ₃	0.43	-0.39	-0.12	-0.99	0.47	-1.53	Calcite	CaCO ₃	0.49	-0.81	0.63	0.64	-0.89	0.00
CO2(g)	CO ₂	-0.41	-0.24	-0.31	-0.05	-0.34	-0.32	-0.17	CO2(g)	CO ₂	-0.23	-0.35	-0.25	0.04	-0.25	CO2(g)	CO ₂	-0.12	-0.49	-0.17	-0.56	-3.71	-2.5	CO2(g)	CO ₂	-2.88	-4.84	-3.12	-3.33	-2.46	-2.42
Dolomite	CaMg(CO ₃) ₂	0.43	-0.40	-0.05	0.40	0.01	-0.73	-0.42	Dolomite	CaMg(CO ₃) ₂	0.69	0.79	-0.81	-1.43	-1.49	Dolomite	CaMg(CO ₃) ₂	0.19	-1.48	-0.88	-2.47	0.19	-3.81	Dolomite	CaMg(CO ₃) ₂	0.37	-1.90	0.82	1.32	-2.51	-0.62
Fluorite	CaF ₂	1.38	1.30	1.23	1.22	1.17	1.08	0.74	Fluorite	CaF ₂	0.98	0.98	1.25	1.05	1.01	Fluorite	CaF ₂	1.08	0.83	0.75	0.62	-0.27	0.03	Fluorite	CaF ₂	-0.38	-4.70	-0.41	-1.02	0.12	0.15
Ferrihydrite	Fe(OH) ₃	-1.21	-2.08	-0.95	-2.08	-1.23	-0.72	-1.86	Ferrihydrite	Fe(OH) ₃	-1.18	-1.11	0.4	-0.14	0.07	Ferrihydrite	Fe(OH) ₃	-1.58	-2.36	-2.18	-3.07	2.26	-14.11	Ferrihydrite	Fe(OH) ₃	1.76	1.49	1.42	1.80	2.16	2.20
Goethite	FeOOH	2.77	1.92	3.08	1.96	2.80	3.17	2.00	Goethite	FeOOH	2.71	2.76	4.14	3.66	3.90	Goethite	FeOOH	2.31	1.52	1.74	0.8	5.97	4.19	Goethite	FeOOH	5.40	5.00	5.07	5.65	6.11	6.08
Magnetite	Fe ₃ O ₄	8.69	6.45	9.79	6.44	8.92	10.21	6.72	Magnetite	Fe ₃ O ₄	8.60	8.65	13.09	11.92	12.40	Magnetite															

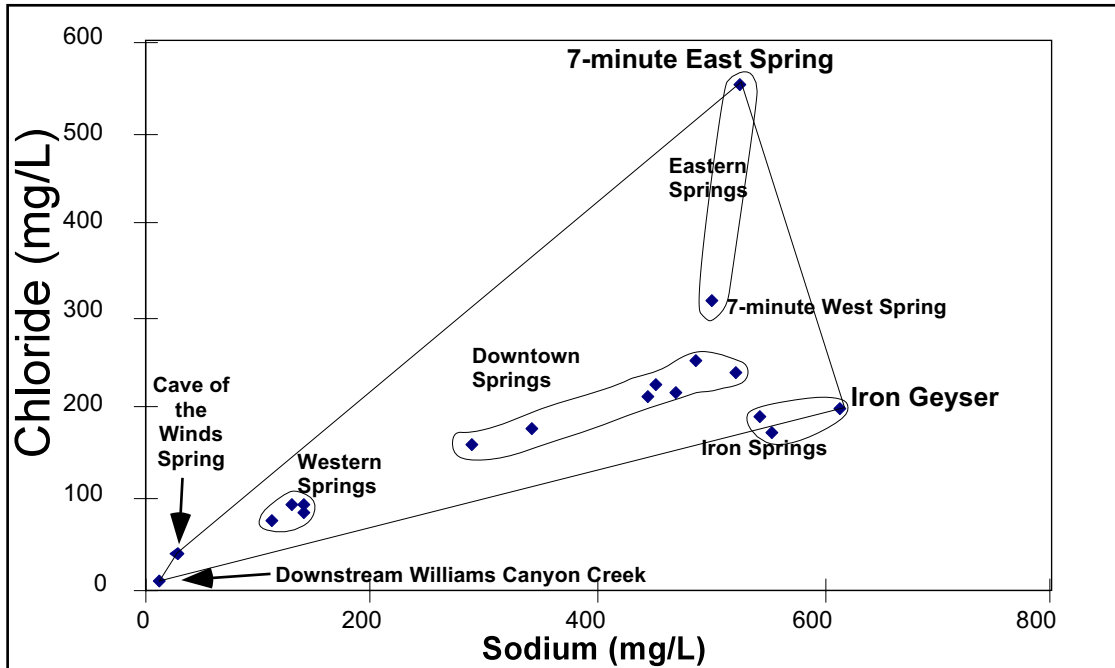


Figure 5. Plot of sodium versus chloride content of the springs of Manitou and low TDS waters. The polygon drawn on the plot contains almost all of the springs and streams in the Manitou Springs area. This suggests that the Western and Downtown Springs are a mixture of downstream Williams Canyon Creek and waters that have chemistry similar to the Iron Geyser, 7-minute East Spring, and Cave of the Winds Springs.

Table 4. Composition of the predominate rock types that react with the spring water at Manitou Springs.

	Pike Peak Granite*	Pike Peak Granite biotite*	Manitou Formation #1 (Base)	Manitou Formation #2	Manitou Formation #3	Manitou Formation #4	Manitou Formation #5 (Top)	Williams Canyon Formation	Leadville Formation (Base)
SiO ₂	73.00**	34.70	5.09	13.59	19.20	7.10	1.87	8.74	11.49
Al ₂ O ₃	13.37	18.34	0.63	2.01	0.95	0.42	0.20	0.82	1.98
Fe ₂ O ₃	0.55	3.27	0.29***	0.56	1.16	0.56	0.09	0.39	1.67
FeO	1.71	25.68	NM	NM	NM	NM	NM	NM	NM
MgO	0.09	0.97	4.13	5.21	17.54	7.36	0.53	0.72	19.74
CaO	1.05	0.46	48.63	39.62	24.58	44.06	54.86	51.55	24.89
Na ₂ O	3.41	0.68	0.13	0.04	0.09	0.01	0.20	0.15	0.06
K ₂ O	5.58	9.26	0.89	0.86	1.58	0.55	0.26	0.38	0.58
TiO ₂	0.22	2.15	0.01	0.04	0.07	0.02	0.01	0.04	0.06
P ₂ O ₅	0.02	0.03	0.29	0.38	0.21	0.29	0.36	0.27	0.20
MnO	0.05	0.55	0.02	0.06	0.09	0.10	0.02	0.02	0.05
F	0.46	2.75	NM	NM	NM	NM	NM	NM	NM
CO ₂ ****	NL	NL	42.67	36.77	38.44	42.62	43.63	41.24	41.09
Cl (ppm)	400	1700	147	198	454	339	130	45	332
S (ppm)	NL	NL	211	42	29	51	128	1016	588
Li (ppm)	48	2200	NM	NM	NM	NM	NM	NM	NM
Pb (ppm)	49	30	NM	NM	NM	NM	NM	NM	NM
Sr (ppm)	108	10	211	98	65	82	123	92	81
Total	99.53	99.06	102.76	99.12	103.91	103.09	102.02	104.32	101.81

*Average composition of the Pikes Peak Granite wholerock and biotite from Hawley and Wobus (1977).

**Values in Wt% except were noted.

*** Total iron in the limestones is reported as Fe₂O₃.

NM = Not Measured NL = Not Listed

**** Calculated by assuming that all the MgO and CaO are in dolomite and calcite.

Plate 5. Mass Balance Spreadsheet.

Table of Ion Concentrations of Springs, Modeled Inputs, and Downstream Input (units=mg/L)

	DISCHARGE												INPUT		
	MEASURED (Taken from Table 3)												Deep Source (Iron Geyser)	Marine Modified (7-minute East)	Low TDS (Cave of the Winds Spring)
	Shoshone	Cheyenne	Soda	Navajo	Wheeler	Stratton	Magnetic	Twin	Ute Chief	Gusher	Creighton	Downstream			
Potassium (K)	75	79	68	71	65	50	38	20	22	19	15	2	94	42	1
Sodium (Na)	491	529	459	475	451	345	295	147	146	136	118	14	618	531	39
Sulfate (SO ₄)	212	197	196	187	185	158	132	73	77	84	106	56	227	400	52
Chloride (Cl)	242	229	220	211	208	171	155	80	88	87	69	9	195	547	31
Fluoride (F)	7.7	7.0	6.8	6.6	6.3	5.5	5.0	3.9	4.0	4.0	3.9	1.5	6.6	4.8	3.6
Calcium (Ca)	501	527	474	519	467	385	535	319	349	296	187	67	355	559	47.9
Magnesium (Mg)	81	94	85	90	86	73	89	92	54	52	47	24	34.5	134.8	3.447
Iron (Fe total)	0.04	0.05	0.23	0.02	0.10	1.07	0.08	0.08	0.04	0.05	0.02	0.01	11.4	0.1	0.092
Manganese (Mn)	3.80	2.50	2.40	2.80	2.70	0.44	0.32	0.22	0.12	0.13	0.08	0.03	1.2	1.6	0.072
Nitrate (NO ₃)	0.08	0.90	0.53	0.62	0.86	0.98	2.40	1.00	2.69	6.17	1.45	15.80	0.1	1.1	0.41
Bromide (Br)	1.03	0.92	1.10	0.88	0.88	0.78	0.70	0.36	0.38	0.39	0.27	0.05	1.0	2.1	0.18
Lithium (Li)	0.76	0.88	0.66	0.71	0.65	0.56	0.42	0.23	0.24	0.16	0.02	0.98	0.77	0.06	
Flow Rate (L/min)	1.5	1.4	2.0	8.6	2.4	2.0	1.0	6.7	6.7	40	270	40	52	11	239

Table of Ion Flow Rates of Springs, Modeled Inputs, and Downstream Input (Concentrations multiplied by Flow Rate, units=mg/min)

	DISCHARGE												INPUT		
	MEASURED												Deep Source (Iron Geyser)	Marine Modified (7-minute East)	Low TDS (Cave of the Winds Spring)
	Shoshone	Cheyenne	Soda	Navajo	Wheeler	Stratton	Magnetic	Twin	Ute Chief	Gusher	Creighton	Downstream			
Potassium (K)	113	110	136	607	157	99	38	134	149	768	3958	81	4910	481	258
Sodium (Na)	736	741	919	4085	1083	691	295	979	970	5452	31801	552	32229	6083	9186
Sulfate (SO ₄)	318	276	392	1608	444	316	132	486	515	3372	28593	2240	11844	4584	12430
Chloride (Cl)	363	321	440	1815	499	342	155	533	587	3460	18592	356	10174	6268	7396
Fluoride (F)	12	10	14	57	15	11	5	26	27	158	1058	60	342	55	859
Calcium (Ca)	751	738	949	4460	1121	770	535	2126	2322	11832	50382	2684	18507	6404	11428
Magnesium (Mg)	122	132	170	770	205	146	89	613	362	2064	12571	956	1800	1545	822
Iron (Fe total)	0.06	0.07	0.47	0.18	0.23	2.14	0.08	0.50	0.26	1.84	6.21	0.52	595	0.9	22
Manganese (Mn)	5.7	3.5	4.8	24.1	6.5	0.9	0.3	1.5	0.8	5	22	1.2	63	18	17
Nitrate (NO ₃)	0.1	1.3	1.1	5.3	2.1	2.0	2.4	6.7	17.9	247	392	632	7	13	98
Bromide (Br)	1.5	1.3	2.2	7.6	2.1	1.6	0.7	2.4	2.5	16	72	2	50	24	43
Lithium (Li)	1.1	1.2	1.3	6.1	1.6	1.1	0.4	1.5	1.6	10	43	0.8	51	9	69

**Key for computing unknown inputs

Set #	Deep (X)	Marine Mod. (Y)	Low TDS (Z)
Set 1	195	547	31
Set 2	227	400	52
Set 3	94	42	1
Set 4	26750	547	31
Set 5	34212	400	52
Set 6	47199	531	39
Set 7	195	26750	31
Set 8	227	34212	52
Set 9	618	47199	39
Set 10	195	547	26750
Set 11	227	400	34212
Set 12	618	531	47199

Set #	Deep	Marine Mod.	Low TDS
Set 1	195	547	31
Set 2	227	400	52
Set 3	94	42	1
Set 4	26750	547	31
Set 5	34212	400	52
Set 6	47199	531	39
Set 7	195	26750	31
Set 8	227	34212	52
Set 9	618	47199	39
Set 10	195	547	26750
Set 11	227	400	34212
Set 12	618	531	47199

Set #	Deep	Marine Mod.	Low TDS
Set 1	195	547	31
Set 2	227	400	52
Set 3	94	42	1
Set 4	26750	547	31
Set 5	34212	400	52
Set 6	47199	531	39
Set 7	195	26750	31
Set 8	227	34212	52
Set 9	618	47199	39
Set 10	195	547	26750
Set 11	227	400	34212
Set 12	618	531	47199

Set #	Deep	Marine Mod.	Low TDS
Set 1	195	547	31
Set 2	227	400	52
Set 3	94	42	1
Set 4	26750	547	31
Set 5	34212	400	52
Set 6	47199	531	39
Set 7	195	26750	31
Set 8	227	34212	52
Set 9	618	47199	39
Set 10	195	547	26750
Set 11	227	400	34212
Set 12	618	531	47199

Set #	Deep	Marine Mod.	Low TDS
Set 1	195	547	31
Set 2	227	400	52
Set 3	94	42	1
Set 4	26750	547	31
Set 5	34212	400	52
Set 6	47199	531	39
Set 7	195	26750	31
Set 8	227	34212	52
Set 9	618	47199	39
Set 10	195	547	26750
Set 11	227	400	34212
Set 12	618	531	47199

Set #	Deep	Marine Mod.	Low TDS
Set 1	195	547	31
Set 2	227	400	52
Set 3	94	42	1
Set 4	26750	547	31
Set 5	34212	400	52
Set 6	47199	531	39
Set 7	195	26750	31
Set 8	227	34212	52
Set 9	618	47199	39
Set 10	195	547	26750
Set 11	227	400	34212
Set 12	618	531	47199

Set #	Deep	Marine Mod.	Low TDS
Set 1	195	547	31
Set 2	227	400	52
Set 3	94	42	1
Set 4	26750	547	31
Set 5	34212	400	52
Set 6	47199	531	39
Set 7	195	26750	31
Set 8	227	34212	52
Set 9	618	47199	39
Set 10	195	547	26750
Set 11	227	400	34212
Set 12	618	531	47199

	Average Calculated Input *	Ratio (Each input divided by total input)	Normalized Calculated Input (Ratio multiplied by Adjusted Discharge, units=L/min)
Deep Source	58.7	0.173	52.2
Marine Modified	12.9	0.038	11.5
Low TDS Source	268.3	0.789	238.6
Total calculated input =	339.9		
Adjusted Discharge (see above)			302.2

Set #	Deep	Marine Mod.	Low TDS
Set 1	195	547	31
Set 2	227	400	52
Set 3	94	42	1
Set 4	26750	547	31
Set 5	34212	400	52
Set 6	47199	531	39
Set 7	195	26750	31
Set 8	227	34212	52
Set 9	618	47199	39
Set 10	195	547	26750
Set 11	227	400	34212
Set 12	618	531	47199

Set #	Deep	Marine Mod.	Low TDS
Set 1	195	547	31
Set 2	227	400	52
Set 3	94	42	1
Set 4	26750	547	31
Set 5	34212	400	52
Set 6	47199	531	39
Set 7	195	26750	31
Set 8	227	34212	52
Set 9	618	47199	39
Set 10	195	547	26750
Set 11	227	400	34212
Set 12	618	531	47199

Set #	Deep	Marine Mod.	Low TDS
Set 1	195	547	31
Set 2	227	400	52
Set 3	94	42	1
Set 4	26750	547	31
Set 5	34212	400	52
Set 6	47199	531	39
Set 7	195	26750	31
Set 8	227	34212	52
Set 9	618	47199	39
Set 10	195	547	26750
Set 11	227	400	34212
Set 12	618	531	47199

Set #	Deep	Marine Mod.	Low TDS
Set 1	195	547	31
Set 2	227	400	52
Set 3	94	42	1
Set 4	26750	547	31
Set 5	34212	400	52
Set 6	47199	531	39
Set 7	195	26750	31
Set 8	227	34212	52
Set 9	618	47199	39
Set 10	195	547	26750
Set 11	227	400	34212
Set 12	618	531	47199

Set #	Deep	Marine Mod.	Low TDS
Set 1	195	547	31
Set 2	227	400	52
Set 3	94	42	1
Set 4	26750	547	31
Set 5	34212	400	52
Set 6	47199	531	39
Set 7	195	26750	31
Set 8	227	34212	52
Set 9	618	47199	39
Set 10	195	547	26750
Set 11	227	400	34212
Set 12	618		

Table 5A. Analyses of sediments being deposited by modern springs.

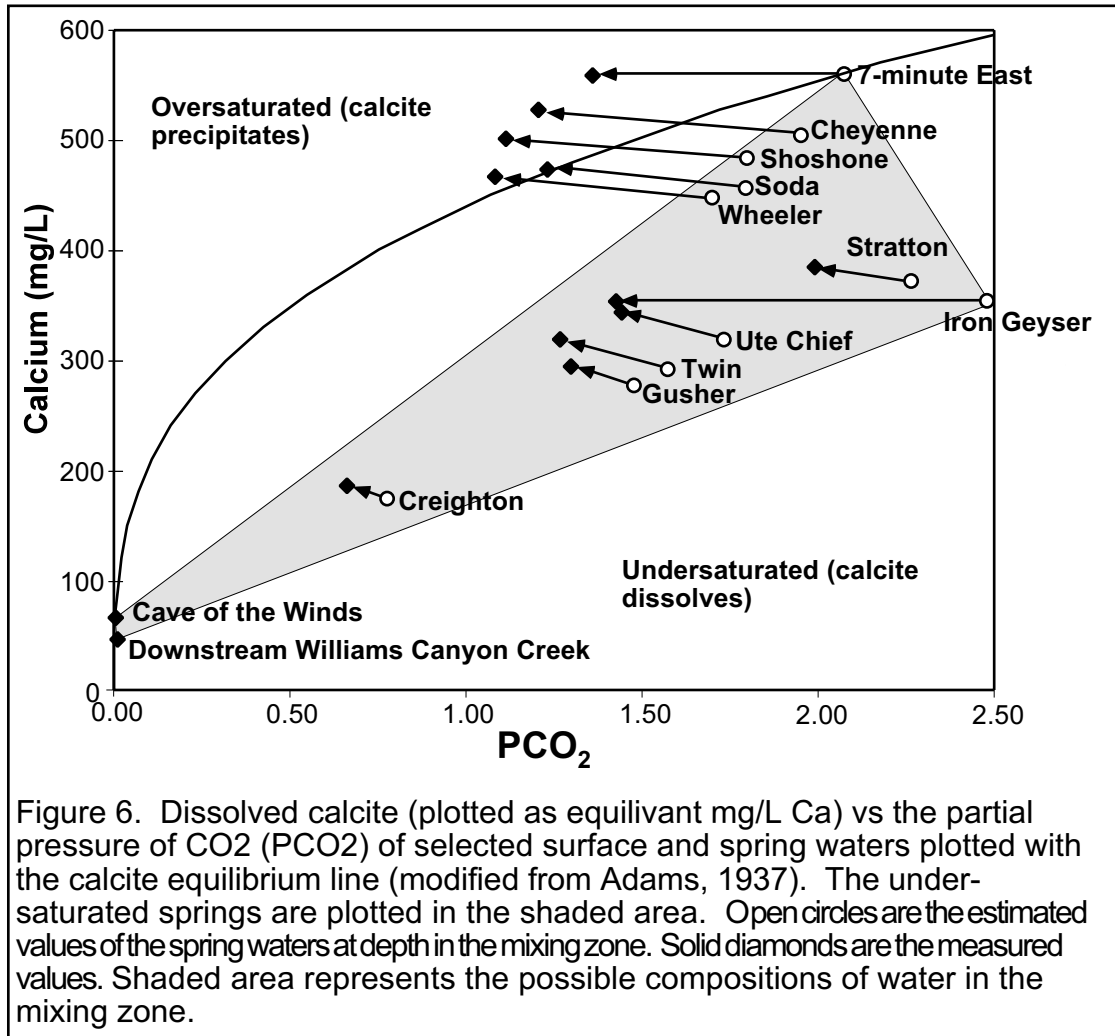
	As	Pb	Mn	Fe	Sediment Type
	ppm	ppm	Wt%	Wt%	
Ouray Spring	4200	181	0.12	58.02	Fe-oxide
Chief Spring	3200	225	N.M.	N.M.	Fe-oxide
Iron Geyser	3400	170	N.M.	N.M.	Fe-oxide

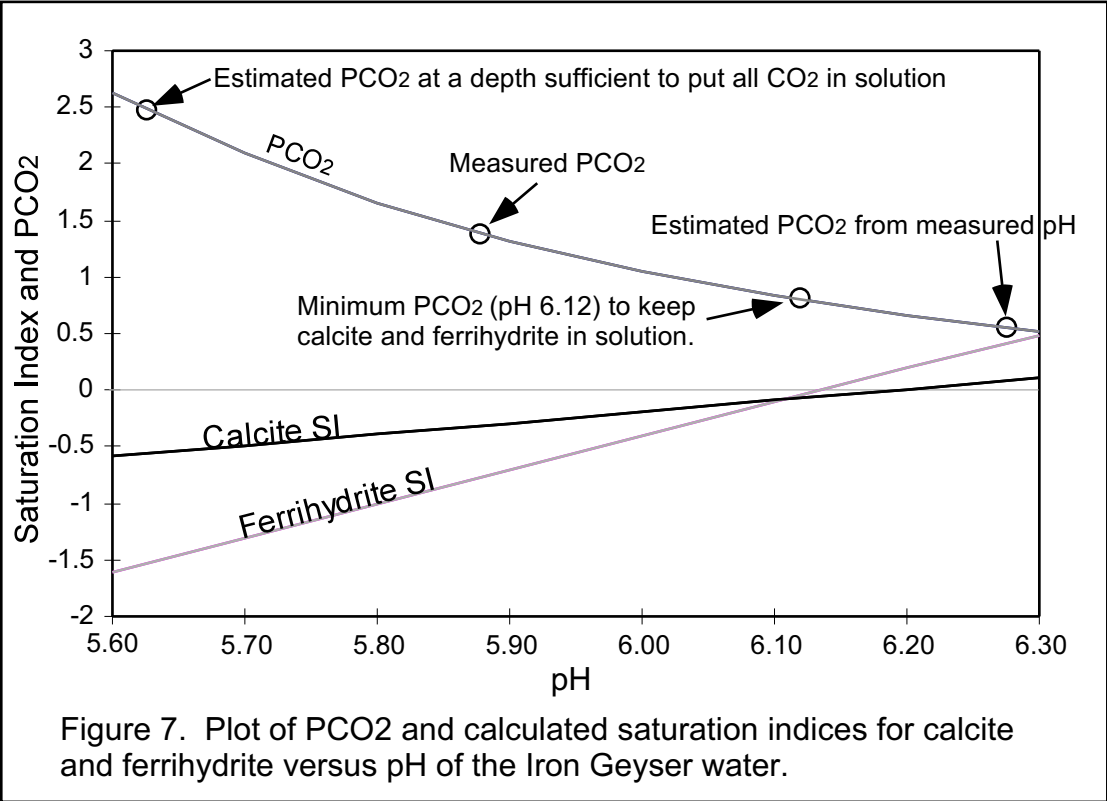
Table 5B. Analyses of stratigraphic column at south end of Thieves Canyon.

Depth (cm)	As ppm	Pb ppm	Mn Wt%	Fe Wt%	Ni ppm	Zn ppm	Sr ppm	Sb ppm	Ba ppm	Sediment Type
0.00	734	456	0.94	6.97	57	378	223	53	2100	Clay + Silt
2.38	694	497	0.93	7.29	44	348	214	54	2000	Clay + Silt
4.38	240	133	1.06	7.82	67	385	228	49	1900	Clay + Silt
6.75	611	397	5.31	6.34	93	628	494	45	5900	Clay + Silt
8.75	544	338	0.44	3.82	40	367	180	14	1700	Clay + Silt
10.50	593	430	1.26	5.51	62	376	328	40	3100	Clay + Silt
12.50	614	433	2.59	6.07	84	460	636	44	5600	Clay + Silt
14.25	520	411	5.54	5.16	124	628	1600	52	11200	Clay + Silt
16.50	781	70	34.92	1.32	375	1300	6500	31	57000	Hollandite
19.00	39	22	39.01	0.80	294	1500	2300	32	63500	Hollandite
21.50	806	37	38.33	1.09	450	1400	5400	29	57200	Hollandite
24.00	825	237	0.05	6.72	47	290	136	58	252	Clay + Silt
26.50	2200	748	0.13	22.59	108	504	137	131	133	Goe*+Hem
27.00	5800	3600	0.87	42.87	278	679	79	353	1400	Goe+Hem
27.50	7400	3300	0.96	48.87	194	834	73	454	1100	Goe+Hem
29.38	5200	2700	0.72	63.45	146	722	58	618	465	Goe+Hem
31.50	7400	3900	1.14	72.87	247	806	87	547	558	Goe+Hem
32.50	1500	497	0.09	7.62	78	392	159	102	171	Goe+Hem
35.00	21	835	0.18	11.53	65	486	131	176	365	Res.**+Silt
36.50	8900	4500	1.56	56.88	248	1657	127	543	1700	Goe+Hem
39.00	8800	6200	1.50	73.23	197	1472	120	499	777	Goe+Hem
41.00	627	177	0.06	2.33	30	187	64	17	411	Res.**
44.50	438	83	0.06	2.22	39	185	76	7	360	Res.
46.50	596	163	0.05	2.40	37	180	64	13	346	Res.
										Bedrock

N.M.=Not Measured * Goe = Goethite Hem = Hematite

** Residual remaining after limestone dissolution.





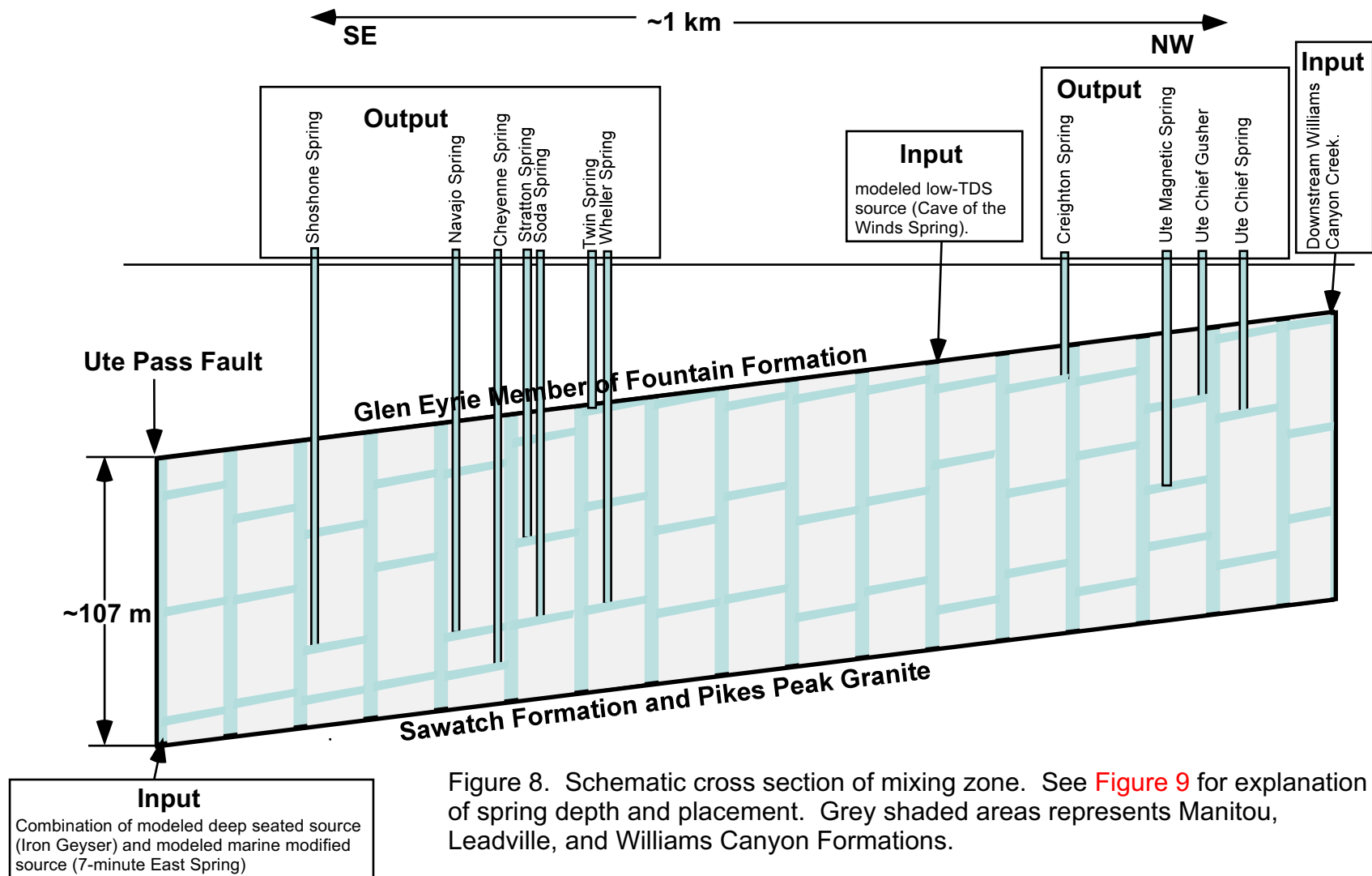


Figure 8. Schematic cross section of mixing zone. See Figure 9 for explanation of spring depth and placement. Grey shaded areas represents Manitou, Leadville, and Williams Canyon Formations.

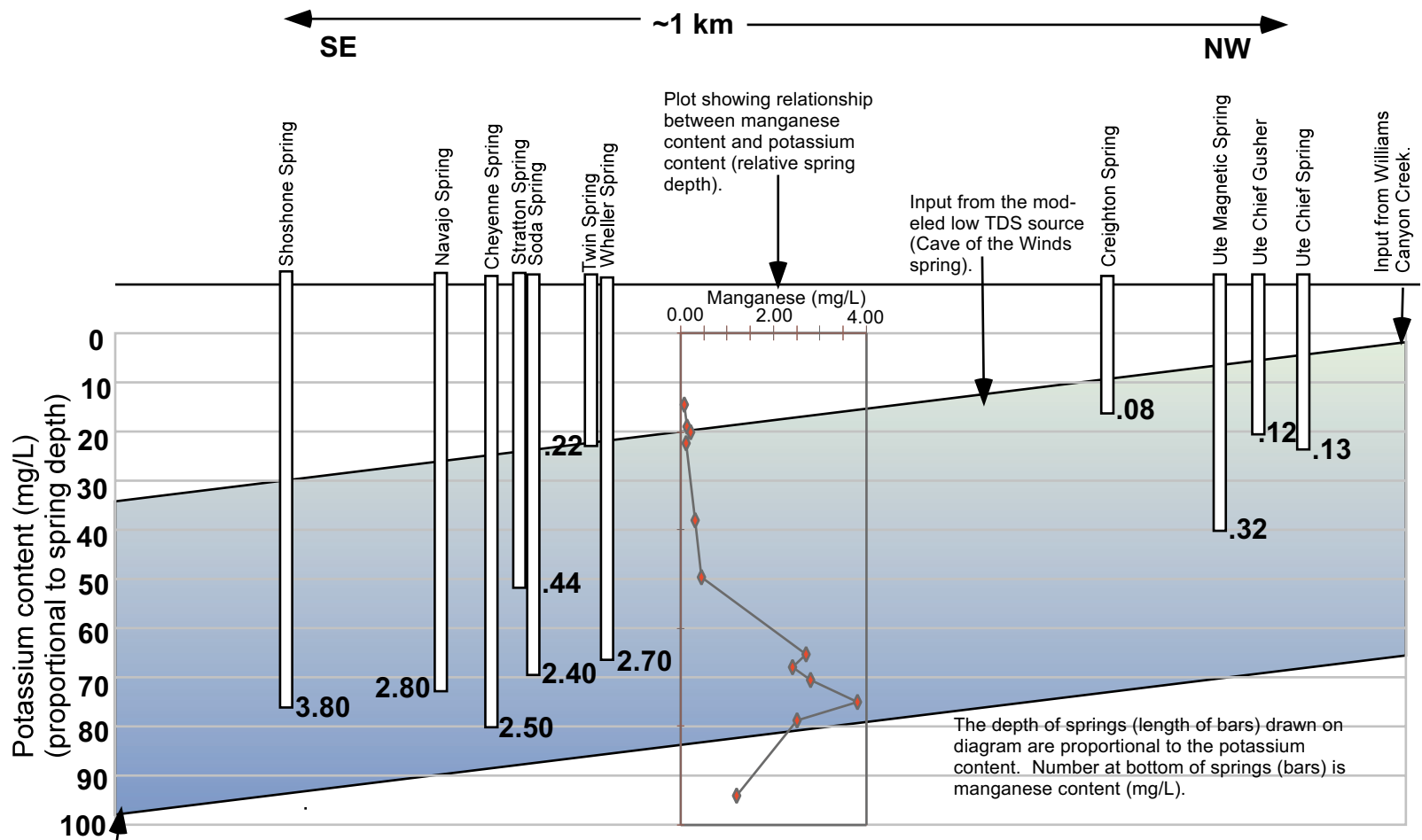


Figure 9. Plot of potassium content (relative depth of springs) versus relative distance between springs along a NW-SE trend. Shaded area represents the mixing zone (Manitou, Leadville, and Williams Canyon Formations).

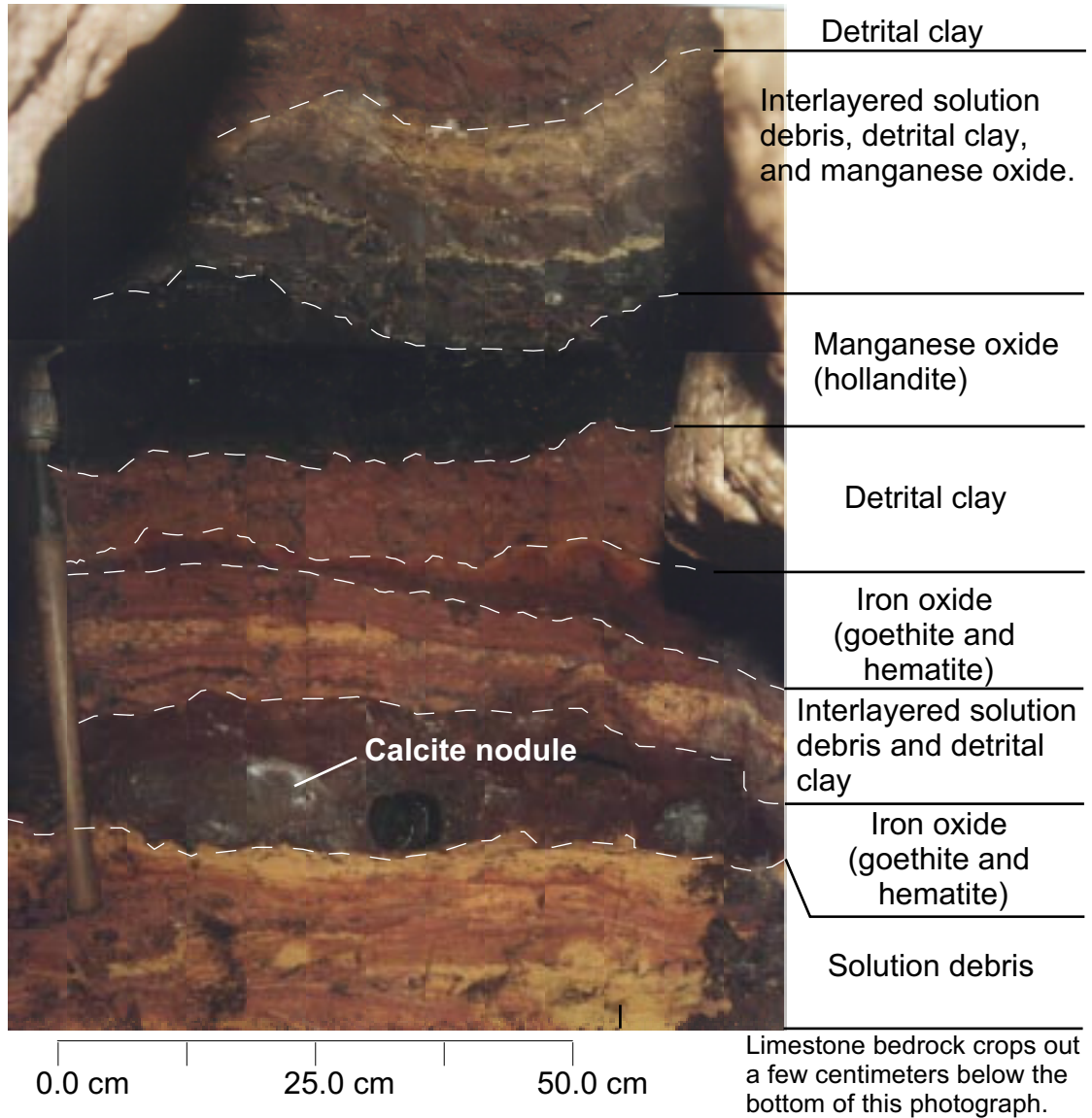
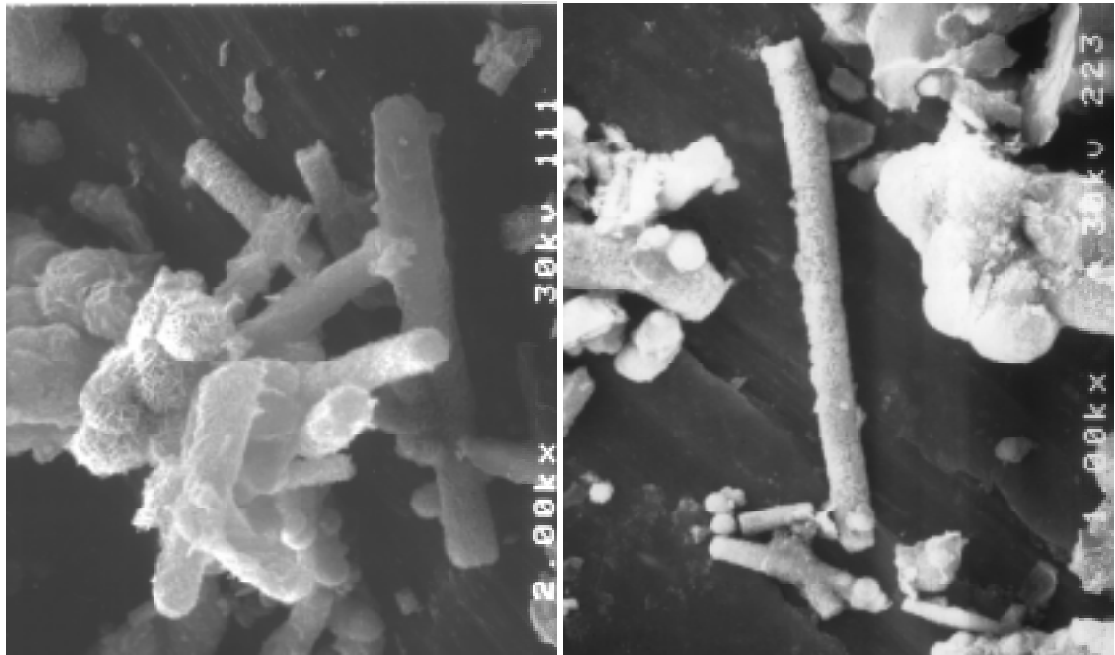
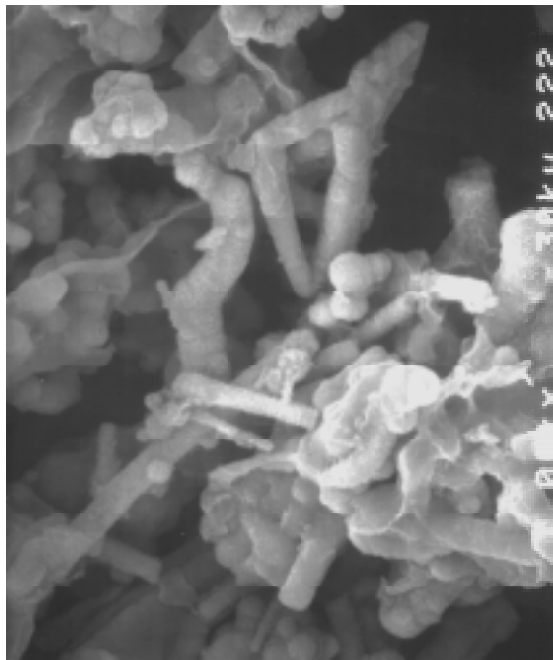


Figure 10. Photograph of outcrop at Electric Coolaid Acid Test Alcove, which is located at south end of Thieves Canyon (Plate 2). Dashed lines are drawn on contacts of sediment units.

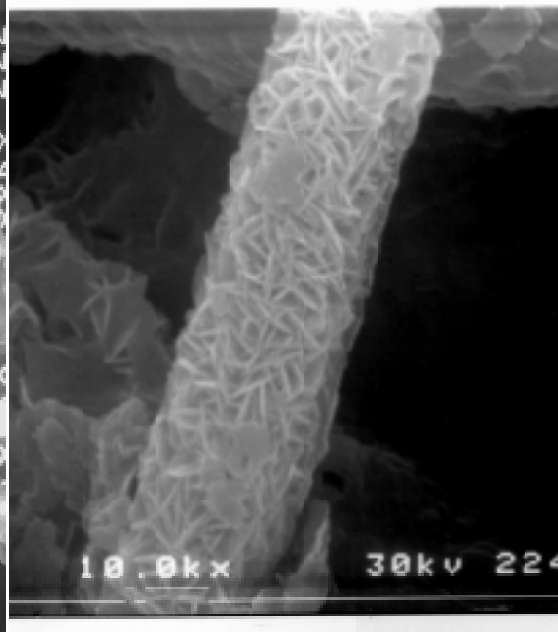


A

B



C



D

Scale for A, B, and C 10 μm

Scale for D 1 μm

Figure 11. Photomicrographs of hematite in the iron oxide beds at south end of Thieves Canyon. All photomicrographs show rods that may be fossilized bacteria. Photomicrograph D shows blades of hematite crystals that make up rods.

Fig. 12A-Calcite, clay, silt, and sand content of limestone.

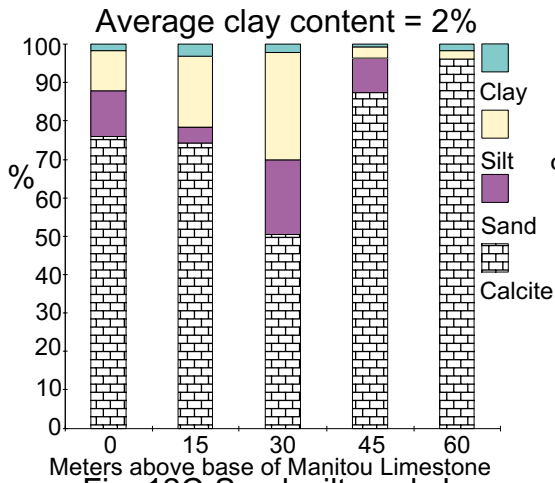


Fig. 12B-Mineralogy of clay in limestone.

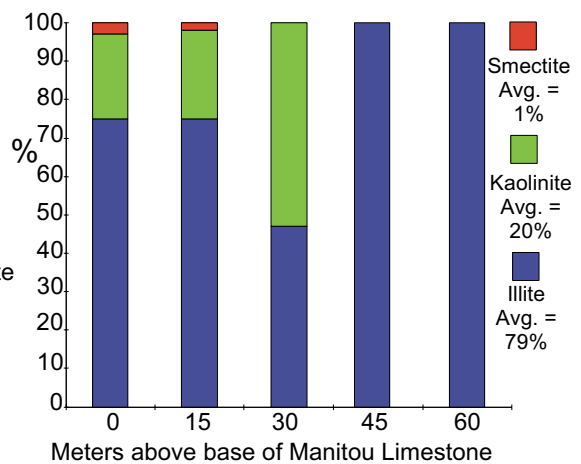


Fig. 12C-Sand, silt, and clay content of cave sediment.

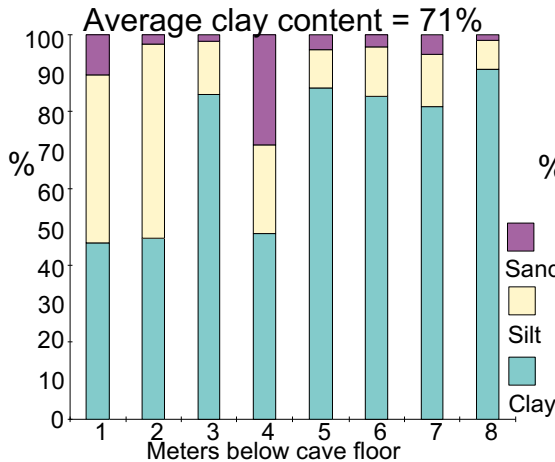


Fig. 12D-Mineralogy of cave clay.

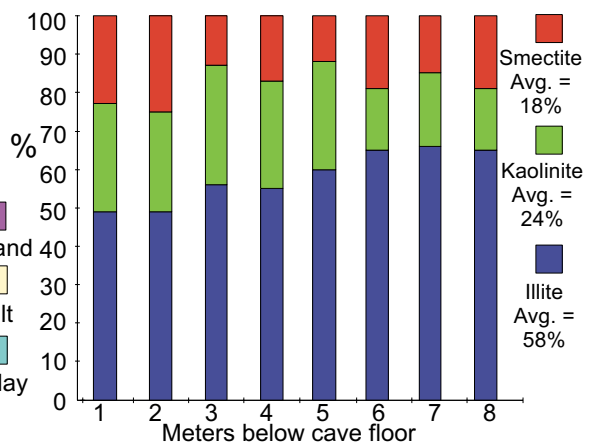


Fig. 12E-Sand, silt, and clay content of soils and sediment.

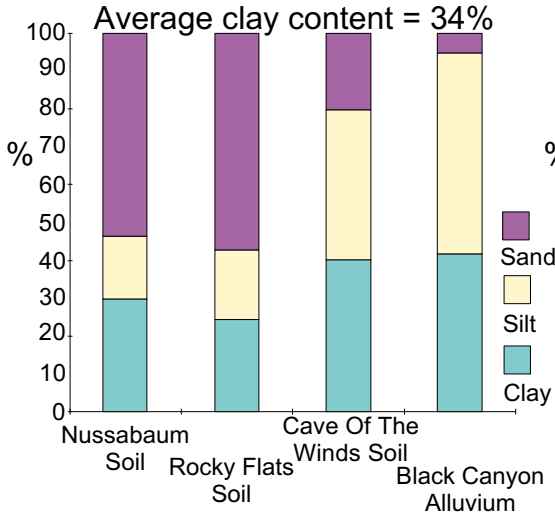


Fig. 12F-Mineralogy of soil and sediment clay.

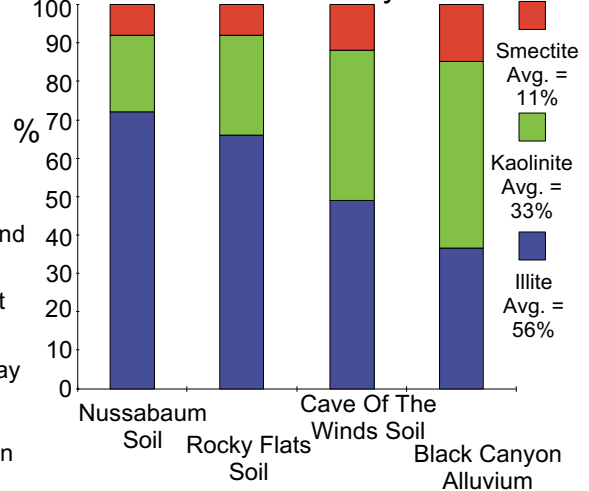


Figure 12. Grain size distribution and clay mineralogy.

TABLE 6 Species identified, their location, and amount of shells counted.

	Modern Flood Plain		Centennial		Manitou Cave		Chesnut		Filmore		Starlight		Colorado City				Black Canyon			
													East		West					
Carychium exiguum (Say)													8	3	105	35	18	5		
Cionella lubrica (Muller)					20	3	1	0					2	1						
Columella alticola (ingersoll)									4	0					1	0				
Derocerus spp.													1	0			4	1		
Discus whitneyi					4	1	4	0												
Euconulus fulvus (Muller)					16	2	20	2							2	1				
Fossaria parva (Lea)							19	2			3	1	8	3	10	3				
Gastrocopta armifera (Say)	1	0	1	0	47	7	5	1	38	6	17	7	5	2						
Gastrocopta cristata Pilsbry	1	0							1	0	15	6	19	6	10	3				
Gastrocopta holzingeri (Sterki)	6	2					6	1			96	39	37	12	3	1				
Gastrocopta pellucida (Pfeiffer)	1	0			193	27			3	1			6	2	3	1	136	28		
Gastrocopta procera (Gould)	6	2			5	1			35	6	5	2	14	5	3	1				
Gyraulus parvus (Say)													2	1	53	13				
Hawaiiia minuscula (Binney)	23	6	43	5	82	12	134	14	84	14	12	5	20	7	12	3	26	5		
Oreohelix spp.					28	4														
Oxyloma spp.							20	2			6	2	5	2						
Physa spp.													1	0	10	3				
Pisidium casertanum (Poli)													13	4	200	50				
Pupilla muscorum (Linne)	70	18	174	22	20	3	4	0	2	0	9	4	12	4	2	1	52	11		
Pupoides albilabris (C.B. Adams)									7	1	4	2	8	3						
Pupoides hordaceous (Gabb)																	133	28		
Pupoides inornata Vanatta	35	9	7	1	1	0			130	22	3	1	6	2	9	2	7	1		
Stagnicola spp.															10	3				
Succinea spp.			4	0					45	8					3	1				
Vallonia cyclophorella (Sterki)	250	63	579	72	197	28	381	39	240	41	60	24	20	7	32	8	123	25		
Vertigo gouldi and ovata			1	0	4	1	390	39												
Zonitoides arboreus (Say)	1	0			96	13	1	0			7	3	20	7	15	4	6	1		
TOTAL	394	100	809	100	713	100	989	100	585	100	248	100	304	100	397	100	483	100		

Numbers in green are the count of identified species. Numbers in red are the percentage of total.

Table 7A Alloisoleucine and isoleucine (A/I) ratios of snails.

Sample Location	Species	Lab Number	Results			Average	Standard Deviation
Modern	P	AAL-5990	0.020	0.022		0.021	0.0010
Modern	V	AAL-5989	0.021	0.020		0.021	0.0005
Centennial	P	AAL-5970	0.023	0.021		0.022	0.0010
Centennial	V	AAL-5969	0.024	0.032		0.028	0.0040
Manitou Cave	G	AAL-5993	0.042	0.056	0.051	0.050	0.0058
Manitou Cave	P	AAL-5992	0.039	0.044	0.041	0.041	0.0021
Manitou Cave	V	AAL-5991	0.043	0.069		0.056	0.0130
Chesnut	GO	AAL-5972	0.106	0.124		0.115	0.0090
Chesnut	V	AAL-5971	0.106	0.103		0.105	0.0015
Colorado City	G	AAL-5986	0.154	0.210	0.163	0.176	0.0246
Colorado City	V	AAL-5985	0.076	0.083		0.080	0.0035
Fillmore 1	G	AAL-5976	0.279	0.274		0.277	0.0025
Fillmore 1	V	AAL-5975	0.298	0.275		0.287	0.0115
Fillmore 2	G	AAL-5988	0.239	0.233		0.236	0.0030
Fillmore 2	V	AAL-5987	0.283	0.270		0.277	0.0065
Starlight	P	AAL-5768	0.423	0.414	0.420	0.419	0.0037
Starlight	V	AAL-5767	0.276	0.317	0.296	0.296	0.0167
Starlight 1	G	AAL-5974	0.302	0.322		0.312	0.0100
Starlight 1	V	AAL-5973	0.307	0.231	0.224	0.254	0.0376
Starlight 2	G	AAL-5978	0.292	0.298		0.295	0.0030
Starlight 2	V	AAL-5977	0.246	0.244		0.245	0.0010
Black Canyon	P	AAL-5766	0.502	0.531	0.543		
					0.529	0.526	0.0150
Black Canyon	V	AAL-5765	0.545	0.545	0.546		
			0.544	0.515	0.576	0.545	0.0176

V = Vallonia cyclophorella P = Pupilla muscorum G = Gastrocopta armifera
 GO = Vertigo gouldii and Vertigo ovata

Table 7B. Average values and standard deviation of A/I ratios of selected snails from each site.

	Average - standard deviation	Average	Average + standard deviation
Modern Flood Plain	0.020	0.021	0.022
Centennial	0.021	0.025	0.029
Chesnut	0.103	0.110	0.117
Filmore and Starlight	0.249	0.275	0.301
Black Canyon	0.523	0.536	0.549

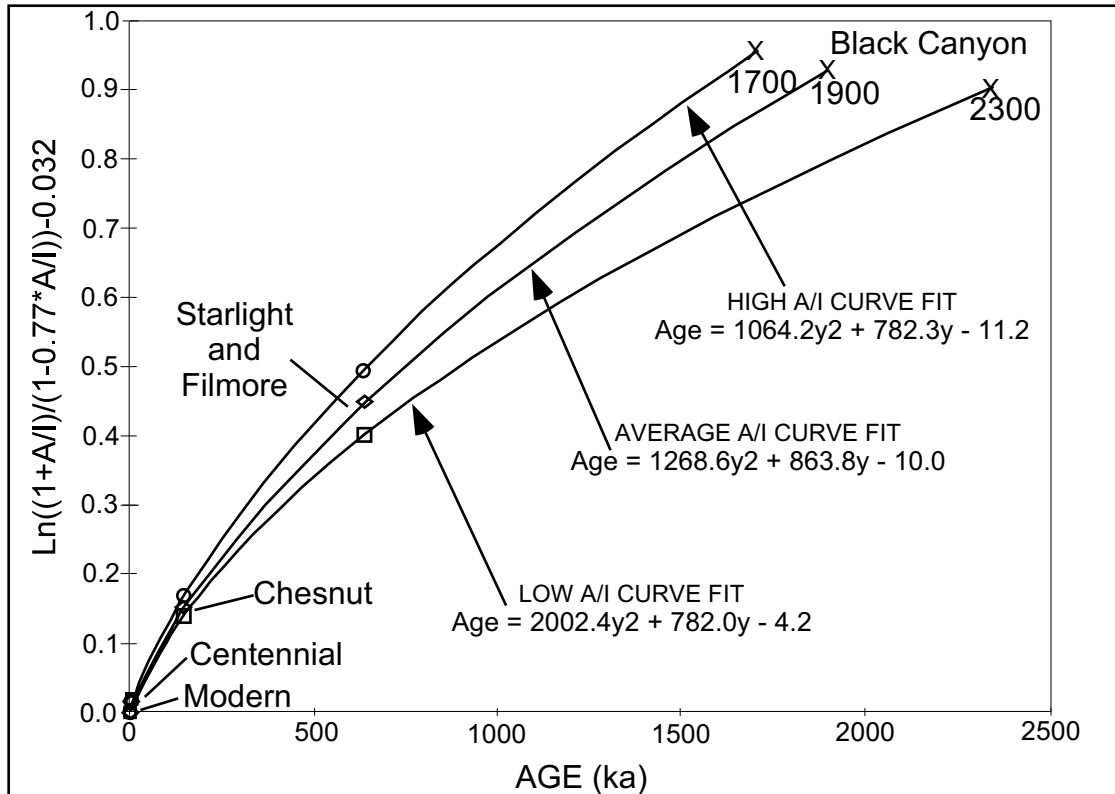


Figure 13. The A/I of snails from the Starlight and Filmore (Verdos Alluvium), Chesnut (Louviere Alluvium), Centennial (Piney Creek), and Modern Flood Plain sites are used for curve fitting. The diamonds represent the curve fit of the average A/I. The circles and squares represent the curve fits of +/- one standard deviation of the A/I. The A/I of the snails from the Black Canyon site with the appropriate equations are used to extrapolate the age of the Nussbaum Alluvium (1.9+0.4/-0.2 Ma).

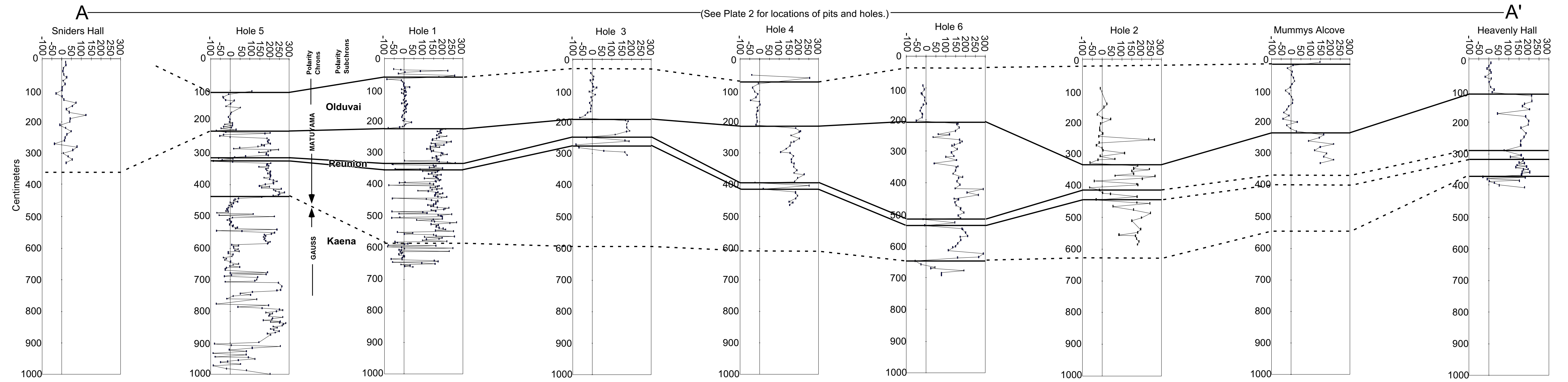
Table 8. Uranium-thorium and ¹⁴C dates.

	¹⁴ C Age (years B.P.)	Lab. Number*
Centennial site	1495 ± 130	GX-15992
Manitou Cave	1505 ± 75	GX-15993
*Krueger Enterprises Inc.		
	Uranium-thorium Age** (years B.P.)	
Narrows Cave	32,000 ± 2,000	
**Dan Muhs, U.S.G.S., 1990, per. comm.		

Table 9. Complete Paleomagnetic results of Hole 6, Grand Concert Hall

Sample Number	Depth cm	Natural			10 mT			15 mT		
		Dec.	Inc.	Int.	Dec.	Inc.	Int.	Dec.	Inc.	Int.
11	80	-9	62	1.2E-04	-21	55	5.4E-05	-13	57	4.7E-05
12	93	-30	45	1.5E-04	-7	54	6.8E-05	-16	52	5.0E-05
13	105	-11	52	2.0E-04	-4	52	1.2E-04	-9	60	1.1E-04
14	118	-23	27	1.5E-04	-23	26	1.1E-04	-24	24	9.7E-05
21	121	-14	44	1.8E-04	-21	40	1.2E-04	-20	39	9.6E-05
22	131	-11	46	2.7E-04	-7	39	1.7E-04	-6	40	1.5E-04
23	141	0	41	1.4E-04	-13	34	7.2E-05	-7	37	6.6E-05
24	151	4	42	3.2E-04	3	38	2.1E-04	2	38	1.8E-04
31	154	-11	40	3.8E-04	-15	31	2.1E-04	-14	34	1.9E-04
32	163	-27	40	2.2E-04	-21	38	1.4E-04	-24	36	1.3E-04
33	172	-24	41	2.6E-04	-29	36	1.8E-04	-30	35	1.6E-04
34	182	-17	40	2.5E-04	-19	38	1.7E-04	-20	37	1.6E-04
41	184	-18	38	4.4E-04	-17	40	3.1E-04	-18	39	2.9E-04
42	194	-15	41	1.8E-04	-24	42	1.1E-04	-20	36	9.6E-05
43	204	-17	58	1.4E-04	-45	62	4.7E-05	-50	64	3.4E-05
44	213	164	-32	1.1E-04	162	-27	9.9E-05	162	-29	9.1E-05
51	216	115	11	7.0E-05	149	-9	6.1E-05	155	-11	5.7E-05
52	226	155	-29	9.5E-05	165	-36	1.0E-04	168	-35	9.2E-05
53	236	-14	52	7.4E-05	144	75	1.4E-05	149	59	1.1E-05
54	246	30	50	1.3E-04	54	30	5.5E-05	62	30	5.0E-05
61	249	81	47	6.7E-05	114	13	4.6E-05	119	3	3.7E-05
62	257	-2	51	1.2E-04	34	41	2.3E-05	35	16	1.0E-05
63	264	176	58	2.7E-05	164	-7	2.3E-05	170	-16	2.3E-05
64	271	177	-17	5.0E-05	184	3	6.4E-05	183	3	6.2E-05
71	273	-12	88	6.7E-04	169	-9	4.7E-05	172	-8	4.5E-05
72	281	202	14	3.9E-05	142	12	7.4E-05	144	8	7.0E-05
81	283	127	-11	1.2E-04	131	-19	9.6E-05	131	-18	8.6E-05
82	294	150	-17	6.4E-05	156	-21	6.2E-05	158	-24	5.2E-05
83	305	93	16	5.4E-05	130	-16	5.2E-05	128	-17	4.5E-05
84	316	59	30	2.2E-05	140	-34	2.2E-05	142	-38	2.0E-05
91	319	28	62	7.2E-05	82	47	2.2E-05	100	29	1.7E-05
92	329	85	67	4.5E-05	148	5	3.8E-05	154	-2	3.5E-05
93	339	-2	53	5.5E-05	41	61	1.4E-05	41	56	1.3E-05
94	349	17	75	6.3E-05	140	34	2.5E-05	162	26	2.2E-05
101	352	101	-26	5.4E-05	159	15	4.5E-05	153	3	4.1E-05
102	362	81	76	5.2E-05	131	33	2.0E-05	150	17	1.5E-05
103	372	67	79	7.7E-05	139	0	2.6E-05	137	-6	3.2E-05
104	382	178	11	4.7E-05	179	-16	4.7E-05	186	-21	4.7E-05
111	385	170	24	5.5E-05	165	-3	4.9E-05	165	-2	4.5E-05
112	396	159	-12	3.7E-05	156	-30	3.5E-05	157	-29	3.3E-05
113	407	184	-10	3.9E-05	174	-32	4.8E-05	172	-32	4.5E-05
114	418	186	9	3.4E-05	145	-47	5.2E-05	148	-50	4.5E-05
121	420	-37	-30	2.4E-05	-70	-57	1.2E-05	-49	-54	1.0E-05
122	431	228	52	2.5E-05	214	25	1.4E-05	208	18	1.1E-05
123	439	-44	55	3.1E-05	249	16	1.1E-05	266	16	1.1E-05
124	451	126	3	2.1E-05	145	-32	2.2E-05	142	-36	1.9E-05
131	453	211	7	1.6E-05	136	-38	9.8E-06	164	-55	9.8E-06
132	463	172	37	1.5E-05	144	-43	2.4E-05	147	-40	1.9E-05
133	472	69	-21	9.3E-06	149	-46	1.6E-05	152	-50	1.6E-05
134	481	263	19	5.4E-06	167	-32	1.3E-05	176	-28	1.2E-05
141	484	115	8	1.9E-05	183	-35	1.4E-05	174	-40	1.1E-05
142	493	189	-6	7.2E-05	188	-19	5.8E-05	192	-22	5.1E-05
143	502	176	62	2.1E-05	157	23	9.6E-06	163	20	8.2E-06
144	512	68	35	1.3E-05	186	-36	6.3E-06	175	-36	6.6E-06
151	514	-19	40	3.4E-05	-39	15	8.3E-06	-15	15	5.9E-06
152	525	41	70	4.7E-05	139	66	1.8E-05	146	60	1.6E-05
153	535	-6	46	8.1E-05	-4	33	3.3E-05	-7	36	2.6E-05
154	545	189	33	1.2E-04	185	21	1.1E-04	182	21	1.0E-04
161	547	173	57	2.8E-05	186	2	2.4E-05	187	0	2.4E-05
162	558	208	7	2.6E-05	200	-28	3.8E-05	201	-28	3.2E-05
163	568	10	68	1.7E-05	206	-25	9.1E-06	211	-33	1.1E-05
171	570	146	73	4.4E-05	175	27	2.9E-05	173	31	2.7E-05
172	580	255	54	1.0E-05	190	-46	1.5E-05	176	-43	1.6E-05
173	591	131	63	4.3E-05	161	14	2.1E-05	160	10	2.2E-05
174	601	39	67	2.2E-05	148	14	6.4E-06	150	2	7.4E-06
181	603	92	52	7.9E-06	163	-18	6.4E-06	135	-31	4.9E-06
182	613	2	69	2.6E-05	152	87	1.2E-05	113	78	8.2E-06
183	624	-44	19	2.1E-05	-69	-45	1.7E-05	-67	-53	1.4E-05
184	634	-16	5	1.6E-05	267	-55	1.1E-05	-86	-59	8.6E-06
191	636	106	60	2.0E-06	112	-37	3.0E-06	160	1	1.4E-06
192	646	-38	7	2.3E-05	-54	-26	1.8E-05	-55	-40	1.2E-05
193	657	2	47	2.6E-05	-4	19	5.7E-06	-26	-27	3.0E-06
194	667	14	64	4.3E-05	42	63	1.6E-05	45	61	1.0E-05
201	669	8	45	4.5E-05	25	43	2.5E-05	24	45	1.6E-05
202	677	22	84	5.0E-05	183	84	2.6E-05	192	79	1.8E-05
203	685	48	52	3.3E-05	74	50	1.7E-05	78	44	1.2E-05
204	692	25	48	1.9E-05	56	25	6.3E-06	78	-17	1.6E-06

Plate 6. Cross-section and correlation of the magnetic declination of sampled pits and cored holes from the Grand Concert Hall and Heavenly Hall.



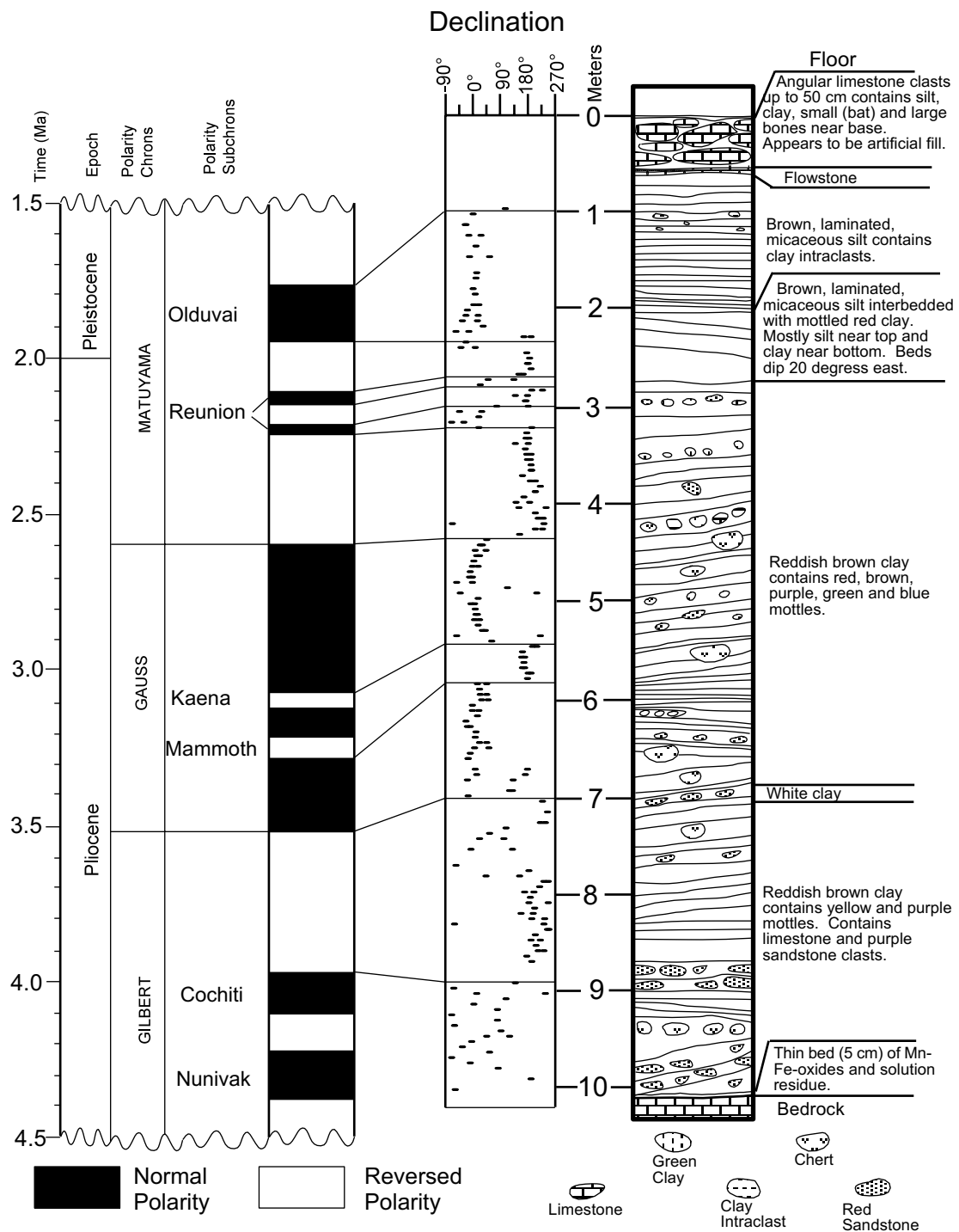
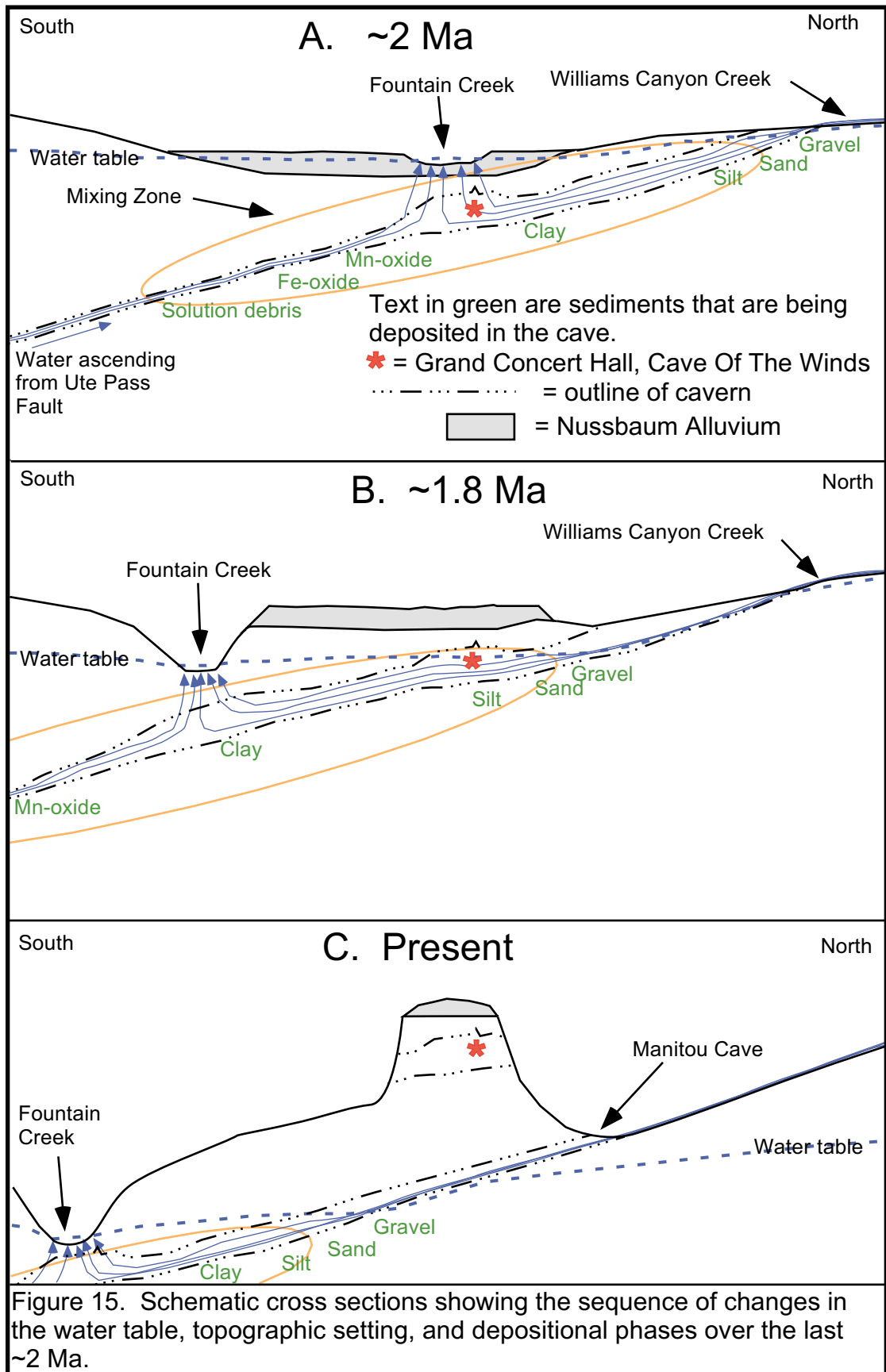


Figure 14. Paleomagnetic correlation and stratigraphy of Grand Concert Hall Hole 5. Paleomagnetic time scale adapted from Harland and others (1982).

Table 10. Chemical analysis of the magnetic grains from cave sediments and rock samples.

NAME	MgO	Al ₂ O ₃	SiO ₂	TiO ₂	MnO	FeO	Total cations
Pikes Peak Migmatite	0.00	0.65	0.18	0.20	0.34	91.89	93.26
Pikes Peak Granite	0.00	2.33	0.39	0.22	0.36	90.20	93.49
Narrows Cave	0.00	0.45	0.55	0.18	0.29	91.84	93.30
Cave of the Winds	0.32	1.99	1.79	0.22	0.82	88.63	93.77
comparison)						93.09	93.09



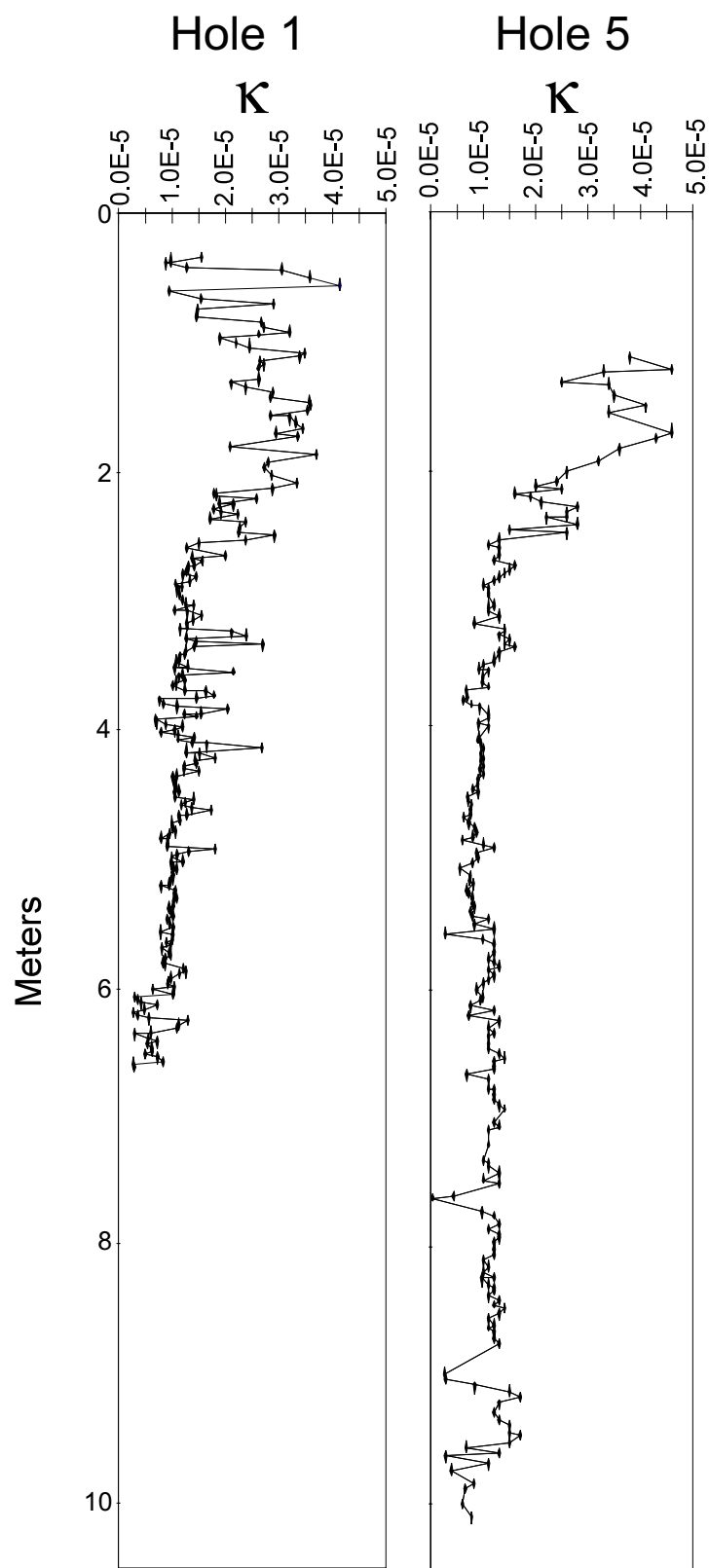


Figure 16. Volume magnetic susceptibility (κ) of samples from Holes 1 and 5, Grand Concert Hall.

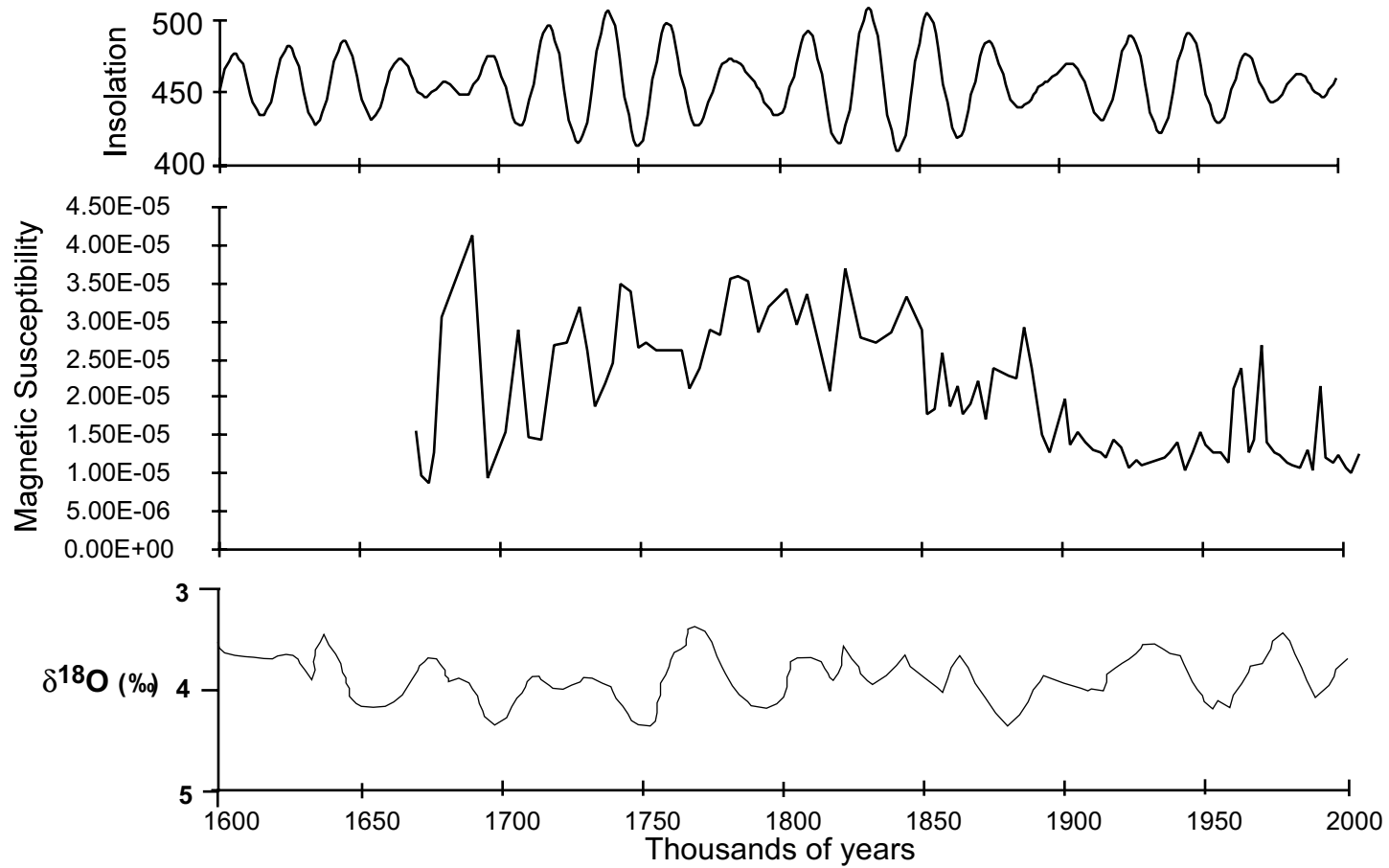


Figure 17. Comparison of insolation, magnetic susceptibility, and ocean record. Top curve represents predicted insolation values for 15° N latitude in July (Berger and Loutre, 1991). The $\delta^{18}\text{O}$ curve is benthonic data taken from ODP677 (Shackleton and others, 1990). The magnetic susceptibility curve is from Hole 1, Grand Concert Hall.

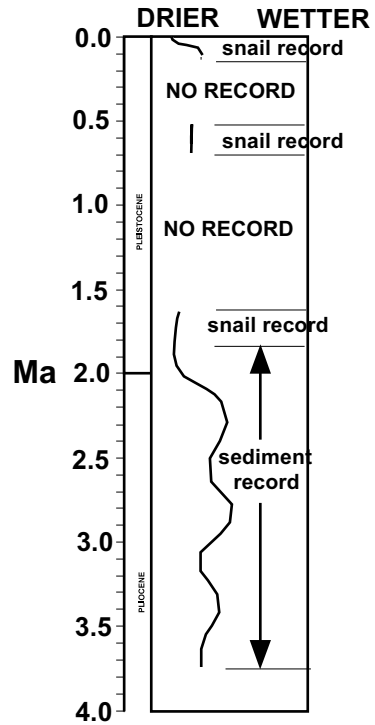


Figure 18. Hypothesized partial climate record of the Manitou Springs area.